

# **Mouse RGMs: A Three Protein Family with Diverse Function and Localization**

**Inauguraldissertation**

zur Erlangung der Würde eines Doktors der Philosophie vorgelegt der  
Philosophisch-Naturwissenschaftlichen Fakultät der Universität Basel  
von

**Rishard Salie**

aus Oakville, Ontario, Canada

Basel, 2005

Genehmigt von der Philosophisch-Naturwissenschaftlichen Fakultät  
Auf Antrag von

Prof. Dr. Silvia Arber  
(Dissertationsleiterin)

Dr. Nicole Schaeren-Wiemers  
(Koreferentin)

Prof. Dr. Heinrich Reichert  
(Vorsitzender)

Basel, 20/09/05

Prof. Dr. Hans-Jakob Wirz  
(Dekan)



## Abstract

### Identification and Functional Characterization of the Mouse RGM Family

In the developing chick visual system, axons project from the retina to the optic tectum in a stereotypical manner to produce a topographic map. This topography conserves spatial information registered by the retina by preserving nearest neighbour relationships among the termination zones of projecting retinal ganglion cells (RGCs). Thus, two RGCs which lie next to each other in the retina will have axonal projections terminating very near each other within the optic tectum, while RGCs which are at opposite sides of the retina will have diametrically opposed termination zones. The establishment of the retinotectal topographic map relies on tight spatial and temporal control of molecules which control axon guidance, branching and termination. One such molecule, proposed to inhibit axonal growth into the tectum, Repulsive Guidance Molecule (RGM), has been implicated in control of RGC axon termination along the anterior-posterior axis of the chick optic tectum.

We discovered three mouse genes homologous to chick RGM, the protein products of which share similarities in structure, proteolytic cleavage and putative GPI-anchoring, but which differ in spatio-temporal expression, cell surface targeting and most importantly function. Two members of this gene family (*mRGMa* and *mRGMb*) are expressed in the nervous system. In the visual system, *mRGMa* is prominently expressed in the superior colliculus, the mouse equivalent of the chick optic tectum, and *mRGMb* in the retinal ganglion cell layer at the time of anterior-posterior targeting of RGC axons. The third member of the family, *mRGMc*

(independently identified as *hemojuvelin* (*hju*)), is expressed most strongly in skeletal muscles, but also in liver and heart.

Surprisingly, neither *mRGMa* nor *mRGMb* are expressed in a gradient in the superior colliculus. Moreover, disruption of either *mRGMa* or *mRGMb* does not affect the anterior-posterior targeting of the topographic map. Instead, half of *mRGMa* mutant mice show a severe defect in cephalic neural tube closure, known as exencephaly, while the remaining animals appear phenotypically normal. All *mRGMb* mutant mice die at approximately three weeks of age for unknown reasons, indicating an essential requirement for *RGMb*, however its specific function remains a mystery.

Mice deficient in *mRGMc* suffer from severe iron overload. This condition is similar to juvenile hemochromatosis, a human disease resulting from mutations in the gene *HFE2*, the human homologue of *mRGMc*. At a molecular level, the severity of the disease state in *Hju* mutant mice can be explained by dramatic decrease in *hepcidin*, a negative regulator of iron absorption produced by the liver in response to ingested iron. Interestingly, these mice retain the ability to produce *hepcidin* in response to inflammatory stimuli. Furthermore, induction of inflammatory response causes a rapid downregulation of *Hju* in wildtype mice. Our findings define a key role for *Hju* in dietary iron-sensing and reveal how *Hju* acts a switch during inflammation, to prevent conflict between the pathway controlling dietary iron homeostasis and that controlling inflammatory iron sequestration as a defense mechanism against infection.

## Table of Contents

<b><u>Chapter 1:</u> Introduction: Early Development of the Vertebrate CNS</b>	<b>13</b>
<b>1.1 Neural Induction</b>	<b>14</b>
<b>1.2 Neurulation</b>	<b>19</b>
<b>1.3 Patterning Molecules: Multitasking in the Nervous System</b>	<b>26</b>
1.3.1 Abstract	26
1.3.2 Multitasking Molecules	27
1.3.3 Exploiting Shh and BMP Activities in the Spinal Cord to Function in Axon Guidance	28
1.3.4 Evolutionary and Cell Type Specific Divergence in Wnt Signalling	32
1.3.5 FGFs Determine Rostro-Caudal Identity and Act as Presynaptic Organizers	35
1.3.6 Outlook	37
<b>1.4 Axon Guidance</b>	<b>38</b>
1.4.1 Netrins and Their Receptors	39
1.4.2 Slits and Robos	40
1.4.3 Semaphorins and Their Receptors	41
1.4.4 Ephrins and Eph Receptors	42
1.4.5 RGMs and Neogenin	44
<b>1.5 References</b>	<b>46</b>

<b><u>Chapter 2:</u> RGM Gene Function Is Required for Neural Tube Closure but not Retinal Topography in the Mouse Visual System</b>	60
<b>2.1 Abstract</b>	61
<b>2.2 Introduction</b>	62
<b>2.3 Results</b>	65
2.3.1 Isolation of Three Genes in the Mouse Genome Homologous to <i>cRGM</i>	65
2.3.2 Differential Expression of <i>mRGM</i> Family Members During Development	70
2.3.3 Expression Analysis of Mouse <i>RGMs</i> in the Visual System	72
2.3.4 Generation of <i>mRGMa</i> Mutant Mice	74
2.3.5 Mutation in <i>mRGMa</i> Results in an Exencephalic Phenotype <i>in Utero</i>	74
2.3.6 Exencephalic <i>mRGMa</i> Mutants Show no Defects in Early Brain Patterning	78
2.3.7 Viable <i>mRGMa</i> Mutants Show no Defects in Retinocollicular Projections	80
<b>2.4 Discussion</b>	83
2.4.1 Identification of a Novel Family of GPI-Anchored Proteins Homologous to <i>cRGMa</i>	83
2.4.2 <i>In Vivo</i> Function of <i>mRGMa</i> in the Developing Nervous System	86

<b>2.5 Materials and Methods</b>	88
2.5.1 Characterization of <i>mRGM</i> Gene Family and Histology	88
2.5.2 Generation and Analysis of <i>mRGMa</i> Mutant Mice	89
<b>2.6 References</b>	91
<b><u>Chapter 3: mRGMb is Essential for Survival Until Adulthood, but its Function Remains Unknown</u></b>	95
<b>3.1 A Potential Role for <i>mRGMb</i> in Axon Guidance and Establishment of Cutaneous Afferent Projections</b>	96
3.1.1 Introduction	96
<b>3.2 Results and Discussion</b>	97
3.2.1 <i>mRGMb</i> Mutant Mice Do Not Exhibit Defects in Retinocollicular Topography	97
<b>3.3 <i>mRGMb</i> Mutant Mice Do Not Exhibit Defects in Establishment of Cutaneous Afferent Projections</b>	101
3.3.1 Introduction	101
<b>3.4 Results and Discussion</b>	102
3.4.1 Projection Pattern of Primary Sensory Afferents in the Dorsal Horn	102
3.4.2 Dorsal Horn Morphogenesis	106
<b>3.5 Material and Methods</b>	108
3.5.1 Generation of <i>mRGMb</i> Mutant Mice	108
3.5.2 Analysis of Retinocollicular Projections	108
3.5.3 Histology	109
<b>3.6 References</b>	110



<b><u>Chapter 4: mRGMc Plays Role in Iron Metabolism</u></b>	113
<b>4.1 Iron Homeostasis</b>	113
4.1.1 The Role of Iron in the Body	113
4.1.2 Regulation of Iron Absorption	115
4.1.3 IREs and IRPs: Translational Regulators of Iron Metabolism Proteins	117
4.1.4 Iron Homeostasis: Regulation in Response to Multiple Factors	118
4.1.5 Hepcidin, the Iron Regulatory Hormone	119
4.1.6 Hereditary Hemochromatosis: A Disease of Iron Overload	121
<b>4.2 Aim of the Following Study</b>	123
<b>4.3 Hemojuvelin Is Essential For Dietary Iron-Sensing and Its Mutation Leads to Severe Iron Overload</b>	125
4.3.1 Abstract	125
4.3.2 Introduction	126
4.3.3 <i>Results</i>	128
4.3.3.1 <i>Generation of HJV Mutant Mice and         Expression of HJV in Periportal Hepatocytes</i>	128
4.3.3.2 <i>HJV Mutation in Mice Causes Severe Iron Overload</i>	130
4.3.3.3 <i>Lack of Hepcidin Expression in HJV Mutant Mice</i>	134
4.3.3.4 <i>Acute Inflammation Can Induce Hepcidin         Expression in HJV Mutant Mice</i>	136
4.3.3.5 <i>Inflammation Induces Selective Downregulation</i>	

<i>of H<sub>1v</sub> in Liver but not Muscle</i>	138
4.3.4 Discussion	139
4.3.5 Methods	144
<i>4.3.5.1 Generation, Maintenance and Analysis of H<sub>1v</sub> Mutant Mice</i>	144
<i>4.3.5.2 Northern Blot Analysis and Histology</i>	144
<i>4.3.5.3 Iron Quantification, Blood Glucose Measurement and Statistical Analysis</i>	145
<i>4.3.5.4 LPS, Cytokine and Iron Injection</i>	145
4.3.6 References	147
<b><u>Chapter 5: General Discussion and Perspectives</u></b>	155
<b>5.1 Chick RGM</b>	155
<b>5.2 mRGMa</b>	156
<b>5.3 mRGMb</b>	158
<b>5.4 mRGMc</b>	158
<b>5.5 References</b>	159
<b><u>Appendices:</u></b>	162
<b>A: Acknowledgments</b>	163
<b>B: Curriculum Vitae</b>	164



## **Chapter 1:**

### **Introduction: Early Development of the Vertebrate CNS**

## **Chapter 1: Introduction**

The early development of the vertebrate nervous system is a complex and continuous process which requires a high degree of organization. It proceeds through multiple events, each precisely ordered both spatially and temporally. While these events are often interdependent upon each other, they can be subdivided into separate categories. This introductory chapter will review neural induction, neurulation and its defects, as well as patterning of the nervous system and axon guidance.

### **1.1 Neural Induction**

Neural induction is the process by which ectodermal tissue of the developing embryo is further specified to become the neural plate. Induction of the ectoderm into neural tissue requires a series of molecular signals that arise from organizer tissue (Spemann's organizer in amphibians, or Hensen's Node in avians and mammals) (Spemann, 1924). Spemann's organizer was discovered through embryonic tissue grafting experiments in which a portion of a donor embryo, the blastopore lip, was transplanted to a second embryo. This donor tissue generated a second neural axis on the recipient embryo, from what would normally have become epidermal precursor tissue.

The search for the inducer was clouded by the fact that a large number of molecules, both biological and chemical, could induce neural tissue from the

ectoderm (reviewed by Stern, 2004). For decades the 'neural inducer' remained a mystery, until experiments by various laboratories revealed several interesting observations. First, the dissociation and reaggregation of *Xenopus* animal caps (Grunz and Tacke, 1989) resulted in a complete neuralization of all ectodermal tissue in the absence of any chemical inducer. In addition, expression of a dominant-negative activin receptor generated ectopic neural tissue (Hemmati-Brivanlou and Melton, 1992). When it was discovered that the misexpressed dominant-negative activin receptor functioned as a TGF $\beta$  inhibitor (Wilson and Hemmati-Brivanlou, 1995), the idea of neuralization by removal of an inhibitory source was presented. Three molecules expressed by the organizer were found to have neuralizing activity: Noggin (Smith and Harland, 1992), Chordin (Sasai et al., 1994) and Follistatin (Hemmati-Brivanlou et al., 1994). All were found to bind Bone Morphogenetic Proteins (BMPs), a subclass of the TGF $\beta$ -related family, and to antagonize BMP signalling (Piccolo et al., 1996; Zimmerman et al., 1996; Fainsod et al., 1997). Use of morpholino oligonucleotides to knock down these three BMP antagonists produced a near total loss of the neural plate (Khokha et al., 2005). Moreover, when animal cap cells are treated with RNA of downstream products of BMP signalling, they lose the ability to take on neural cell fate (Suzuki et al., 1997b; Suzuki et al., 1997a). The prime candidate for the factor that inhibits neuralization is BMP-4, which is not only expressed in an appropriate spatiotemporal manner (Fainsod et al., 1994), but also acts as a potent inducer of epidermal differentiation from the ectoderm (Wilson and Hemmati-Brivanlou, 1995).

These results culminated in the 'default theory' of neural differentiation in which ectodermal tissue has the natural predisposition to take on a neural cell fate,

unless this is inhibited by BMPs, in which case it takes on epidermal fate (Figure 1A). The antagonization of the inhibitory effects of the BMPs by Noggin, Chordin and Follistatin causes neuralization of ectodermal precursor tissue. Ectodermal tissue that continues to be inhibited by BMPs has the potential to become epidermal tissue.

The story, however, is not quite as simple as that. The question of the sufficiency of BMP inhibition to specify fate has not been fully answered. Ectodermal tissue must have had prior exposure to the organizer (for at least five hours) before it becomes competent to respond to BMP antagonists (Streit et al., 1998). This implies that the ectoderm has to be primed by other factors before it attains the potential to become neural. Interestingly, neither Chordin nor Noggin has the ability to neuralize ectodermal tissue that has been treated with dominant negative Fibroblast Growth factor (FGF) receptor (Launay et al., 1996; Sasai et al., 1996). In fact, inhibition of FGF signalling appears to completely eliminate neural cell fates *in vitro* (Streit et al., 2000; Wilson et al., 2000). What are the roles of the FGFs in determining neural cell fate? This question has generated controversial results in the field of neural induction.

There is evidence that FGFs can induce neural characteristics from ectodermal cells in *Xenopus* (Strong et al., 2000) and in chick (Storey et al., 1998), independent of BMP inhibition. In addition, the urochordates, the simplest members of the chordate family, do not rely on BMP inhibition in the generation of their nervous tissue. Instead, this event is mediated entirely by FGFs (Bertrand et al., 2003). Other studies describe FGF effects on neuralization of ectodermal tissue but in conjunction with the inhibition of BMPs (Linker and Stern, 2004; Delaune et al., 2005). It has also

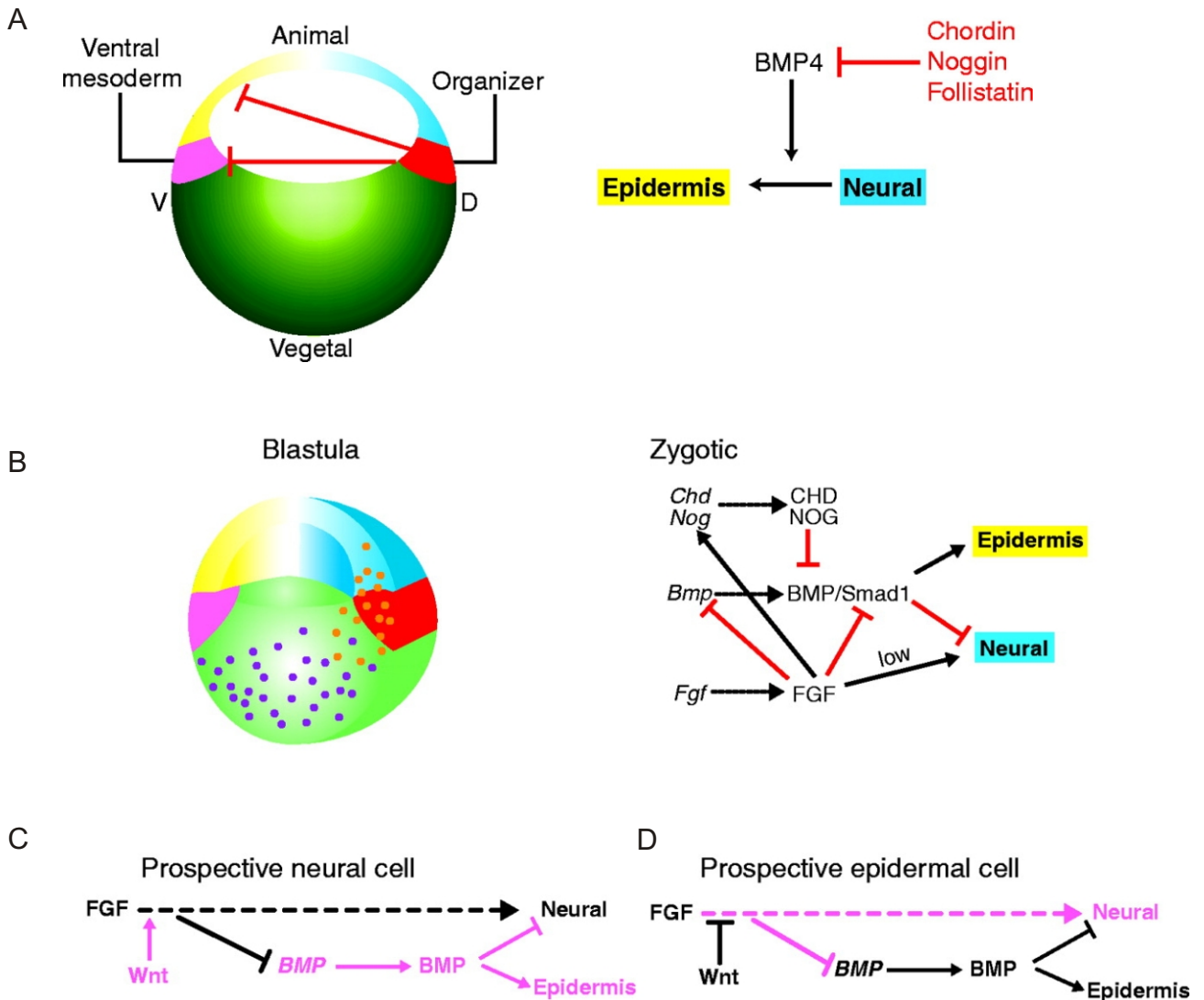


**Figure 1. Models of Neural Induction.** A) The default model. Ectodermal tissue will take on neural fate unless inhibited by BMPs. BMP inhibition is lifted by BMP antagonists produced by the organizer (Spemann's Organizer in *Xenopus*, Hensen's Node in chick and mammals). B) An alternative model includes FGFs as inhibitors of BMP signalling. C,D) The most recent model postulates a requirement for FGF's to induce neural competency, and places early Wnt expression as an inhibitor of FGF signalling, inducing an epidermal cell fate. Adapted from Stern, 2005.



been argued that FGFs do not affect neural differentiation at all. Evidence for this was provided by experiments in which dominant negative FGFR1 was found to disrupt mesodermal formation, but not neural induction in *Xenopus* (Amaya et al., 1991; Holowacz and Sokol, 1999). This was challenged with other studies pointing at FGFR4 as the receptor mediating neural induction (Hongo et al., 1999; Hardcastle et al., 2000). The potential for FGFs to be primary neural inducers is still under discussion, but what is clear is that FGFs are major players in neural induction. Receptor inhibition experiments using a pan-FGFR inhibitor indicate a definitive requirement of FGF signalling in *Xenopus* neural induction (Delaune et al., 2005) and similar results have come to light in the chick (Streit et al., 2000; Linker and Stern, 2004), and mouse (Kuschel et al., 2003; Wright et al., 2004; Ladher et al., 2005).

The mechanism of FGF action in neural induction is believed to be partially reliant on its ability to inhibit BMP downstream targets. FGFs activate the MAP Kinase pathway leading to phosphorylation of the BMP effector Smad1, inhibiting it (Pera et al., 2003) (Figure 1B). BMP signalling acts in part by phosphorylating Smad1 at an alternative site, stimulating transcriptional activity (De Robertis and Kuroda, 2004). Although FGF signalling can inhibit BMP repression of neural fate, many recent studies show that FGF effects are at least in part independent of this BMP inhibitory effect (Linker and Stern, 2004; Rentzsch et al., 2004; Delaune et al., 2005). A model has been proposed which successfully integrates the activities of BMPs and FGFs in neural induction, along with a third family of proteins, the Wnts (Wilson et al., 2001; Shimogori et al., 2004) and Wnt antagonists (De Robertis and Kuroda, 2004) (Figure 1C,D). In this model, prospective neural cells are exposed to FGFs but not Wnts early in development (pre gastrulation). FGF alone promotes

neurulation in two ways. Firstly, independent of BMP signalling (but not necessarily directly), FGFs induce neural character and secondly by impeding BMPs epidermalizing signal (Figure 1C). A cell bound for the epidermal cell fate would have been exposed to both FGF and Wnts early in development. Wnts interfere with FGF signalling preventing neural promotion and disinhibiting BMP signalling (Shimogori et al., 2004; Dailey et al., 2005) (Figure 1D). This allows the cell to proceed to an epidermal cell fate. While this is the currently accepted model, a recent publication which elegantly manipulated FGFs, BMP and Wnt antagonists failed to induce neural markers in the developing chick implying the system is more complex than we realize (Linker and Stern, 2004).

## **1.2 Neurulation**

During neurulation, the neural plate, a two dimensional structure becomes the neural tube, the three dimensional anlage of the CNS. This is achieved by a process known as neurulation in which the neural plate undergoes a series of morphological changes, bending, folding and finally fusing to form a cylindrical shape, the precursor of the brain and spinal cord.

Bending of the neural plate ('furling') occurs all the way down the rostrocaudal neuraxis at the Median Hinge Point (MHP), which is induced by unknown secreted factors released by the notochord (Ybot-Gonzalez et al., 2002) (Figure 2B,C). Furling also occurs along two discontinuous Dorsolateral Hinge Points (DLHP) which run parallel to the MHP (Shum and Copp, 1996). It is believed that the DLHPs, which are present in the cephalic regions as well as the lower spinal cord, but absent from future upper spinal cord levels, are negatively regulated by

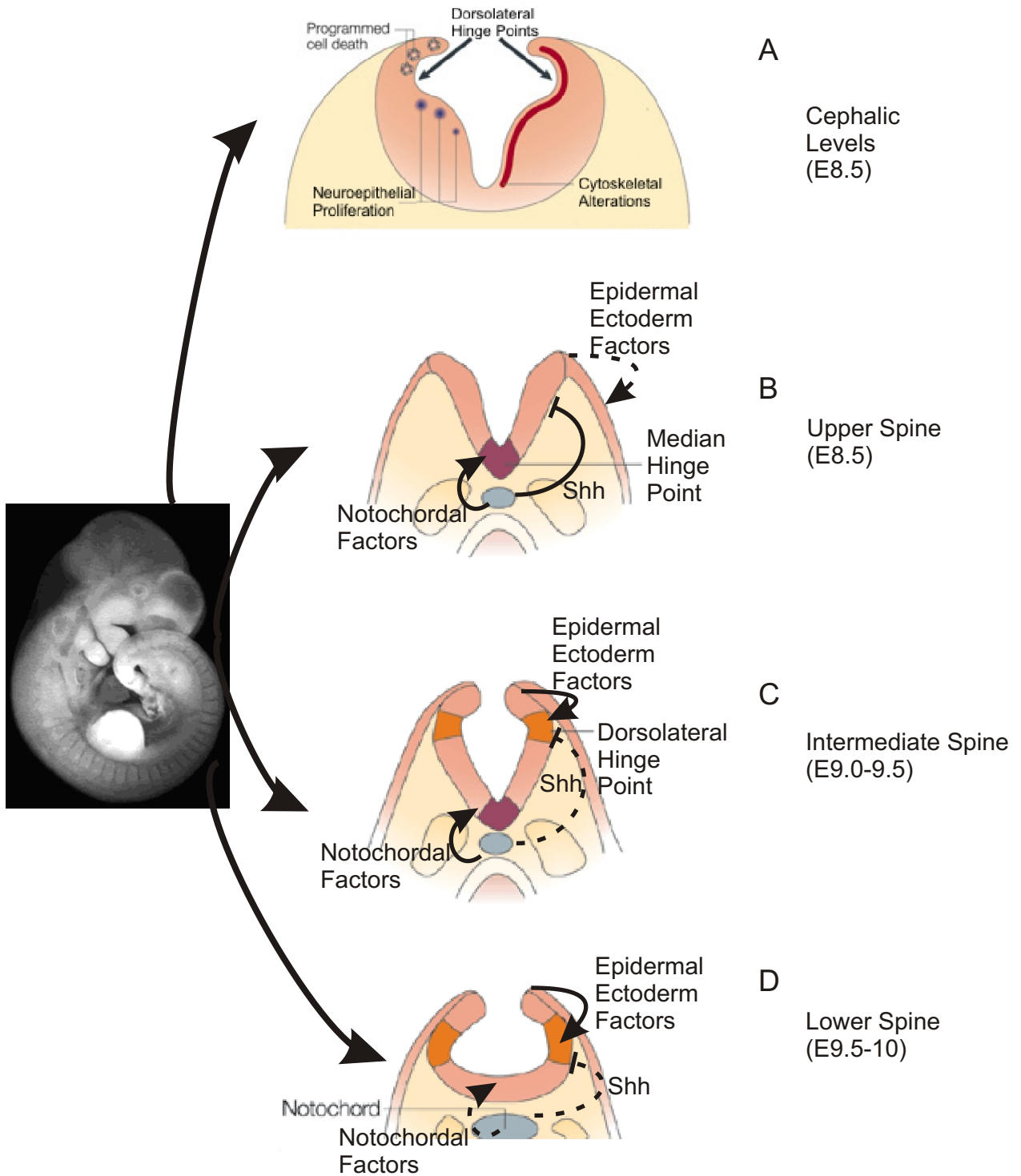


**Figure 2. Interactions Regulating Neural Tube Closure.** A) At cephalic levels programmed cell death, neuroepithelial cell proliferation, and cytoskeletal changes shape the developing neural tube. B, C, D) At various levels, unknown notochord produced factors induce MHP furrowing. Unknown factors from the epidermal ectoderm induce DLHPs, which are blocked by Shh signalling in the upper spine. Solid lines indicate active signalling influences, while dotted lines show inactive or blocked signalling. Adapted from Stern, 2005 and Ybot-Gonzalez et al., 2002.

Sonic Hedgehog (Shh) produced by the notocord (Smith and Schoenwolf, 1989; Ybot-Gonzalez et al., 2002) (Figure 2B). Induction of the DHLPs appears to be the result of an unknown factor produced by the surface ectoderm at the dorsal lip of the neural tube or perhaps by mechanical force produced by the epidermal ectoderm at the border of the neural plate (Ybot-Gonzalez et al., 2002) (Figure 2C,D). Rostrally, the unknown DHLP inducing factor is presumed to be stronger than the DHLP suppressive effects of Shh. Alternatively, the rostral aspect of the neural tube may contain a Shh inhibitor preventing the elimination of the DHLPs. These questions have yet to be explored in the cranial neural folds.

In upper spinal regions a high level of Shh inhibits the formation of the DHLPs (Figure 2B). More caudally, as Shh signalling becomes less potent, it lacks the strength to suppress the DHLPs at lower levels of the spinal cord. Support for the idea of Shh repression of the DHLP comes from several studies. In *Shh* mutant mice, DHLPs are found at all levels of the spinal cord, including upper spinal levels, and neural tube closure occurs normally (Ybot-Gonzalez et al., 2002). In contrast, ectopic expression of Shh produces severe neural tube defects (NTDs), likely due to disturbance of the DHLPs, (Kirillova et al., 2000) and disruption of negative regulators of Shh signalling produce similar defects (Hui and Joyner, 1993; Nakata et al., 1998; Eggenschwiler et al., 2001; Koyabu et al., 2001).

Furrowing of neural folds occurs by rotation of the neural plate along the MHP, due to morphological changes in the neuroepithelial cells. Neuroepithelial cells at the MHP undergo an apical narrowing and basal spreading, a process that is thought to be mediated by cytoskeletal rearrangement, changes in the cell cycle and nuclear

migration (Smith and Schoenwolf, 1987, 1988, 1989; Schoenwolf and Smith, 2000; Colas and Schoenwolf, 2001, 2003). The dorsal lips of the neural folds are brought together by the bending of the DLHPs. While furrowing at the MHP is the result of changes in the neuroepithelium, folding along the DLHPs is mediated by forces generated by the associated epidermal ectoderm layer. Folding at the DLHPs is mediated by molecular factors yet to be discerned. Physically, the tissue undergoes changes that can be divided into five steps: Epithelial ridging, kinking, delamination, apposition and finally fusion (Lawson et al., 2001) (Figure 3).

Epithelial ridging, is the elongation of neuroepithelial cells along their apicobasal axis and the apicobasal shortening of neighbouring epidermal ectodermal cells (Figure 3A). Kinking is a change in shape involving both the neuroepithelium and the epidermal ectodermal cells. In contrast to the cells at the MHP, cells at the junction of the neural plate and the epidermal ectoderm narrow basally and widen apically, resulting in an angled bend at the border of the two cell types that are connected by the extracellular matrix (ECM) at the basal surface (Figure 3B).

During the delamination phase, the basal surfaces of the neuroepithelial and epidermal ectodermal cells line up against each other creating the neural fold interface (Fernandez Caso et al., 1992) (Figure 3C). Epithelial apposition, only occurring at future cranial levels, is a combination of expansion of the neural folds and cell division resulting in an increase surface area (Sausedo et al., 1997; Lawson et al., 2001) (Figure 3D).

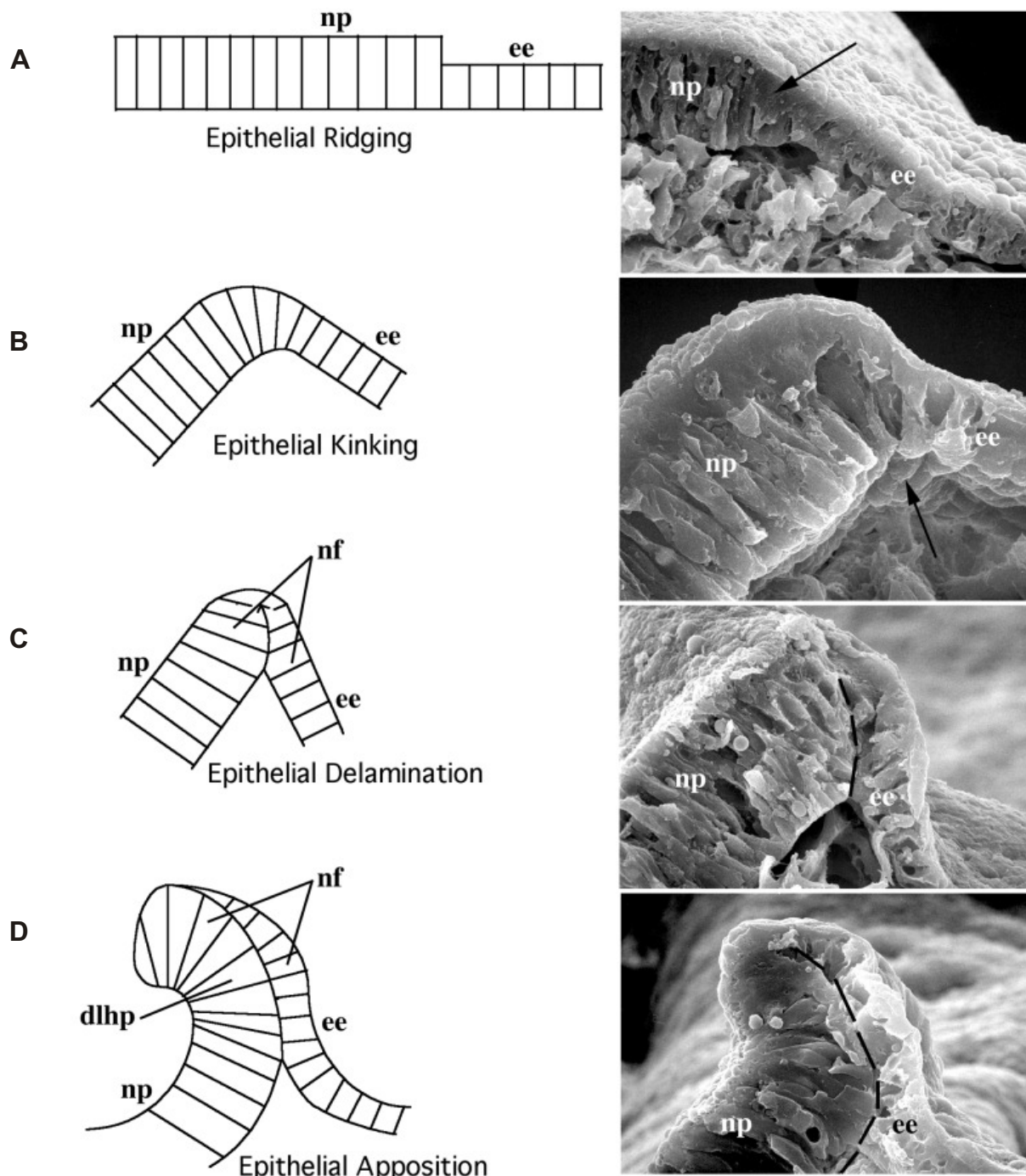


**Figure 3. Epithelial Changes in Neurulation.** A) Epithelial Ridging involves the elongation of neuroepithelial cells and shortening of neighbouring epidermal ectodermal cells. B) During Epithelial Kinking, cells at the junction of the neural plate and the epidermal ectoderm narrow basally and widen apically. C) Epithelial delamination consists of the basal surfaces of the neuroepithelial and epidermal ectodermal cells lining up against each other creating the neural fold interface. D) Epithelial apposition is characterized by expansion of the neural folds and cell division. From Colas and Schoenwolf, 2001.

After the morphological changes that shape and align the neural folds, the opposing lips adhere and then fuse. As the folds approach each other the tips extrude lamellipodia which interlace (Sadler, 1978; Geelen and Langman, 1979). This adhesion is sensitive to phosphoinositidyl phospholipase C treatment (Geelen and Langman, 1979), suggesting a role for GPI-anchored proteins in fusion of the neural tube. In support of this idea, it has been shown that, that mice mutant in *Ephrin-A5*, a GPI-anchored protein with known axon guidance functions, have partially penetrant defects in neural tube closure (Holmberg et al., 2000). Apoptotic cell death, which occurs in the neural folds during normal neural tube fusion (Lawson et al., 1999), also plays an important role in closure (Figure 2A). Either decrease of apoptosis in the neural folds by disruption of caspase 9 (Haydar et al., 1999) or p53 (Sah et al., 1995), or increase in apoptosis by mutation of Tulp3 (Ikeda et al., 2001) or Tcof1 (Dixon et al., 2000) results in neural tube closure defects.

Murine neural tube fusion is independently initiated at three separate sites along the neural groove. The first of these sites to close lies at the caudal edge of the developing hindbrain (Figure 4A). Closure also occurs slightly later at the future midbrain/forebrain junction, and again at the most rostral part of the neural tube. These closures proceed in a zipperlike manner both rostrally and caudally from the first and second closure sites, and in the caudal direction only from the third (Figure 4A). Failure to fuse along any of these three location results in a variety of neural tube defects (NTDs). Lack of fusion at closure site one, early in gestation, results in the fatal defect craniorachischisis, in which the majority of the spinal cord and part of the brain remains open. Failure of this closure later in development as the neural tube seals in a caudal direction results in spina bifida, a milder defect in which only a

small portion of the spinal cord remains open. Lack of fusion at the second closure site results in exencephaly (Figure 4B), in which the cranial neural folds exvaginate and fail to induce skull tissue, while a defect in closure site three causes severe facial deformities as well as potential exencephaly.

Interestingly, many of the molecules that are involved in neural induction and formation of the neural tube reappear with astonishing variance in function, often playing completely different instructive roles in accordance with the time and location of their expression. The involvement of BMPs, FGFs, Wnts and Shh, all major players in neural induction, will be discussed with respect to their role in patterning and axon guidance in the next section.



### 1.3 Patterning Molecules: Multitasking in the Nervous System

Rishard Salie\*, Vera Niederkofler\* & Silvia Arber *Neuron* **45**, 189-192. (2005).

\*indicates equal contribution

#### 1.3.1 Abstract

Classical patterning molecules previously implicated in controlling cell fate choices in the nervous system have recently been shown to play additional roles in axon guidance and synaptogenesis. Bone morphogenetic proteins (BMPs), Sonic hedgehog (Shh), Wnts and fibroblast growth factors (FGFs) all participate in multiple acts of controlling neuronal circuit assembly. Depending on the cellular context, they can provide instructive signals at the growth cone or synapse, or alternatively can elicit responses in the nucleus initiating transcriptional changes. Differences in signal transduction pathways may contribute to the diversity of the functional repertoire of these versatile molecules.

### 1.3.2 Multitasking Molecules

Precise spatiotemporal gene regulation governs nervous system development by controlling cell proliferation, migration and patterning as well as later events such as neuronal circuit formation and specificity in synaptogenesis. Gene families with evolutionarily conserved roles in patterning embryonic tissue such as Hedgehogs, bone morphogenetic proteins (BMPs), Wnts and fibroblast growth factors (FGFs) act by assigning cell fates through transcriptional control of gene expression (Anderson et al., 1997; Jessell, 2000; Patapoutian and Reichardt, 2000; Altmann and Brivanlou, 2001). Within the nervous system, they were long believed to play exclusive roles in regulating patterning processes. In contrast, many molecules involved in regulating axon guidance and synaptogenesis act preferentially at the growth cone or synapse (Tessier-Lavigne and Goodman, 1996; Yu and Bargmann, 2001; Scheiffele, 2003). Work from recent years however, has revealed several well-documented examples of molecular multitasking forcing us to reconsider this division.

When elucidating mechanisms by which multifunctional molecules exhibit their activities, two important aspects need to be considered. First, because of their inductive properties, determination of whether patterning molecules also control axonal outgrowth and neuronal circuit formation is inherently challenging. Consequently, direct and potential indirect activities are difficult to distinguish and need to be evaluated carefully. Second, the transduction mechanisms by which multifunctional molecules transmit their signals to result in appropriate cellular responses might depend significantly on whether they are acting in assigning cell fate or in controlling axonal targeting and synaptogenesis. In particular, it is well

established that patterning molecules often result in the induction of transcriptional changes, whereas rapid integration of signals directly by the growth cone or synapse is a prerequisite for activity of molecules involved in axon guidance and synaptogenesis (Jessell, 2000; Yu and Bargmann, 2001; Scheiffele, 2003). This minireview focuses on recent studies of several families of classical patterning molecules and how their roles in cell fate assignment compare to their function in axon guidance and synaptogenesis. Particular emphasis will be given to the question of how signals are being transduced to elicit cellular responses.

### **1.3.3 Exploiting Shh and BMP Activities in the Spinal Cord to Function in Axon Guidance**

Two main signalling sources within the developing vertebrate spinal cord coordinately control the generation of distinct progenitor cell domains along the dorso-ventral axis. While the graded action of Shh released from the floor plate is a major determinant for the generation of cell types in the ventral spinal cord, BMP signals produced by the roof plate act to pattern the dorsal spinal cord (Figure 5; Jessell, 2000; Altmann and Brivanlou, 2001). BMPs are also involved in the generation of neural crest cells and act to determine autonomic cell lineages (Anderson et al., 1997). Once generated, commissural neurons in the dorsal spinal cord extend axons towards and across the floor plate. The molecular mechanisms involved in these guidance decisions are well understood and classical guidance molecules such as Netrins and Slits play major roles in this process (Tessier-Lavigne and Goodman, 1996; Yu and Bargmann, 2001). Interestingly, recent studies have shown that members of the BMP and Hedgehog gene families also contribute to guidance of commissural axons towards the floor plate (Figure 5).

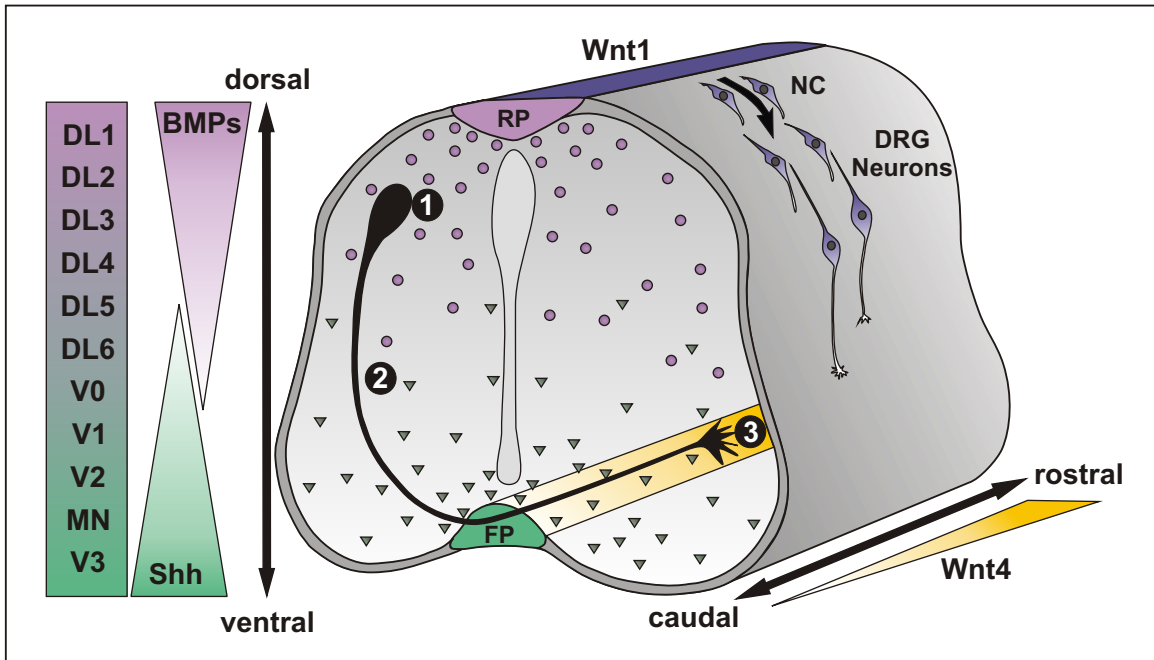


**Figure 5. Control of Commissural Axon Guidance by Patterning Molecules.**

(Left) At early stages, BMPs (purple) from the roof plate (RP) control the generation of distinct neuronal subtypes in the dorsal spinal cord (DL1-DL6) whereas Shh (green) from the floor plate (FP) acts to pattern the ventral spinal cord (V0-V3, MN). (Right) At later stages, commissural axon guidance is influenced sequentially by (1) BMPs (purple) from the RP to direct axons ventrally, (2) combinatorial activities of Netrin-1 and Shh (green) to attract axons to the FP and (3) Wnt4 (yellow) expression in a caudal-low rostral-high gradient to control rostral turning towards the brain. BMP and Shh signals are shown only on the cross sectional face of the three-dimensional schematic drawing of the spinal cord but are expressed along the entire rostro-caudal length of the spinal cord. Wnt1 signals (blue) derived from the roof plate act to instruct neural crest (NC) cells to acquire DRG sensory neuron identity. Dorsal-ventral and rostro-caudal axes are indicated by black arrows.

Experiments from the Dodd lab have provided evidence that the roof plate and select members of the BMP family possess repulsive activity capable of directing axons ventrally (Augsburger et al., 1999; Butler and Dodd, 2003). Analysis of roof plate activity from mice mutant in *BMP6*, *BMP7* or *GDF7* showed that only BMP7 and GDF7 contribute to this activity (Butler and Dodd, 2003). This result was somewhat surprising since GDF7 lacked deflecting activity *in vitro* (Augsburger et al., 1999). Interestingly, roof plates from *BMP7/GDF7* double mutant mice showed no further reduction in repulsive activity in this assay when compared to roof plates from either the *BMP7* or *GDF7* single mutants (Butler and Dodd, 2003). These results pointed to the formation of active heterodimers of BMP7 and GDF7 functioning in repulsion *in vivo*. Indeed, co-culture experiments showed that BMP7/GDF7 heterodimers exhibit stronger repulsive activity than BMP7 homodimers and immunoprecipitation experiments confirmed physical interaction between BMP7 and GDF7 under these conditions (Butler and Dodd, 2003). It remains to be determined through which receptor complexes this repulsive signalling activity is mediated. At least part of the signal transduction machinery is likely to be distinct from that involved in controlling neuronal fate in the dorsal spinal cord since BMP6 exhibits patterning activity but fails to guide commissural axons. It is also known that BMP7 and GDF7 influence axon guidance at concentrations below that required for neuronal specification (Augsburger et al., 1999). Moreover, the ability of BMP7 to induce growth cone collapse in dissociated spinal cord neurons *in vitro* occurs over a time scale that excludes transcriptional mechanisms, implying a direct effect of BMPs at the growth cone. Together, these findings suggest that BMP7/GDF7 heterodimers act at the growth cone in a repulsive manner to direct commissural axons away from the roof plate.

The establishment of the further trajectory of commissural axons towards the ventral midline is influenced by attractive cues derived from the floor plate (Figure 5). While the role of Netrin-1 in this process is well established (Tessier-Lavigne and Goodman, 1996), the fact that floor plates from *Netrin-1* mutant mice still show some residual ability to attract commissural axons *in vitro* suggested that other floor plate derived factors might collaborate with Netrin-1. Moreover, while most commissural axons do not reach the ventral midline in mice mutant in either *Netrin-1* or its receptor *DCC*, some axons still arrive at the floor plate. Indeed, a recent study suggests that Shh acts in concert with Netrin-1 as a chemoattractant in a manner independent of its initial role in patterning to draw commissural axons toward the midline (Charron et al., 2003). Using collagen gel co-culture assays, this study shows that commissural axons reorient towards a source of Shh, establishing the sufficiency of Shh in this process. The action of Shh in patterning cell types in the ventral spinal cord is mediated through Smoothed (Smo), the activity of which can be blocked efficiently by application of cyclopamine. Since the remaining attractive activity of *Netrin-1* mutant floor plates is diminished upon application of cyclopamine, at least part of the signalling cascade responsible for interacting with the cytoskeleton to mediate chemoattraction is most likely conserved between patterning and guidance activities downstream of Shh.

What effects do BMPs and Shh have on commissural axon outgrowth *in vivo*? Both *BMP7* and *GDF7* mutant commissural neurons exhibit transient defects in axonal polarization at early stages of axon extension, but at later stages their axons revert to a normal ventral trajectory (Butler and Dodd, 2003). The *in vivo* impact of

Shh on guidance of commissural axons towards the midline was assessed in mice with conditional inactivation of *Smo* in the dorsal spinal cord including commissural neurons. While axons in these mice reach the midline, axonal trajectories towards the floor plate appear more widespread and irregular than in wild-type (Charron et al., 2003). Together, these findings suggest that rather than being primary axon outgrowth and guidance forces for commissural axons, BMPs and Shh might act to fine tune trajectories of commissural axons growing towards the floor plate in response to Netrin-1 (Figure 5).

#### **1.3.4 Evolutionary and Cell Type Specific Divergence in Wnt Signalling**

Apart from their well-characterized roles in influencing cell proliferation, Wnts were recently also shown to be involved in specification of dorsal root ganglia (DRG) sensory neurons at early developmental stages (Figure 5; Lee et al., 2004). Moreover, several studies have addressed the role of Wnt signalling in axon guidance, neurite outgrowth (see below) and synaptogenesis (Packard et al., 2003). Wnts are not only versatile in regards to their biological functions, but also with respect to the mechanisms by which Wnt signals are transduced and integrated. Interestingly, phylogenetically distant species appear to use distinct signalling strategies to do so.

Commissural neurons in the *Drosophila* embryonic ventral nerve cord project their axons towards and across the midline. Axon guidance towards the midline also involves chemoattraction by Netrins, but there is currently no evidence that either BMP homologues or Hh proteins are involved in these events in *Drosophila*. Axons crossing the midline in *Drosophila* have to choose between two alternative routes: the

anterior or the posterior commissure. Initial details regarding the mechanism responsible for this choice were revealed when Derailed (Drl; an atypical receptor tyrosine kinase with homology to vertebrate Ryk) was discovered to be both necessary and sufficient to direct axons through the anterior commissure (Bonkowsky et al., 1999). Drl is selectively expressed on axons choosing the anterior commissure and ectopic expression of Drl in neurons normally choosing the posterior commissure forces them to the anterior path. An elegant genetic screen identified Wnt5 as a ligand for Drl (Yoshikawa et al., 2003). *Wnt5* is expressed by neurons adjacent to the posterior commissure and in *wnt5* mutants, as in *drl* mutants, anterior commissural axons project abnormally through the posterior commissure. Furthermore, Wnt5 misexpression in midline glia leads to a marked reduction or complete loss of the anterior commissure. Since no genetic interaction between Drl and the well-established Wnt receptor component Frizzled could be detected in control of midline guidance in *Drosophila*, Drl seems to transduce the chemorepellant Wnt5 signal in a Frizzled independent manner (Yoshikawa et al., 2003). Despite the fact that the intracellular region of Drl is not predicted to possess catalytic activity, this domain appears to be functionally essential in *Drosophila* (Yoshikawa et al., 2003). In contrast, the *C.elegans* Ryk ortholog LIN-18 functions in parallel to Frizzled/LIN-17 signalling during vulval cell fate specification, and the kinase domain of LIN-18 is dispensable for its function (Inoue et al., 2004).

In vertebrates, commissural axons turn rostrally after crossing the floor plate, projecting toward their targets in the brain. Wnt signalling has been implicated in controlling this decision (Lyuksytava et al., 2003; Figure 5). *Wnt4* is expressed in a high-anterior to low-posterior gradient along the spinal cord in the floor plate



throughout the time window when commissural neurons make the decision to turn towards the brain. Wnt4 expressed from COS cell aggregates can induce postcrossing commissural axons to turn either anteriorly or posteriorly, depending on the position these cells are placed. Interestingly, the observed activity of Wnt4 selectively affects postcrossing but not precrossing commissural axons. While it is currently not known how sensitivity to Wnts is induced after midline crossing, commissural neurons have also been shown to switch their responsiveness to Netrin-1 and Slit after crossing the midline (Stein and Tessier-Lavigne, 2001). In functional experiments *in vitro*, the addition of secreted Frizzled-related proteins (sFRPs) to block Wnt binding to its receptor is able to randomize the turning event of commissural axons after crossing the midline. *In vivo*, commissural axons from mice mutant in *Frizzled3* lose anterior preference in turning after midline crossing. Since mammalian Ryk is not expressed by dorsal commissural neurons, it does not appear to be involved in transduction of the Wnt4 signal in this system. These findings suggest that an anterior-posterior gradient of *Wnt4* expression is read by *Frizzled3* on commissural axons and converted into an instructive, attractive guidance cue to efficiently steer these axons towards the brain (Figure 5; Lyuksytava et al., 2003). A recent study from the Baltimore lab shows that mammalian Ryk forms a complex with *Frizzled-8* and binds directly to Wnt-1 and Wnt3a (Lu et al., 2004). Furthermore, it provides evidence for direct binding of the intracellular domain of mammalian Ryk to Dishevelled, thus activating the canonical Wnt pathway downstream of the receptor complex.

Many interesting questions remain in resolving how Wnts act in different cellular contexts and/or species to transduce Wnt signals into appropriate cellular

responses. Mammalian Wnt signals have been shown to influence axon growth positively for both commissural axons signalling through Frizzled-3 (Lyuksytava et al., 2003) and cultured DRG neurons signalling through Ryk (Lu et al., 2004). It can be anticipated that other neuronal populations might respond to Wnt signals in a repulsive manner, analogous to the *Drosophila* Wnt5 signal read by Drl (Yoshikawa et al., 2003). In support of this, the activity of several classes of axon guidance molecules depends both on the complement of receptors expressed by a neuron as well as on the intracellular state of active signalling molecules such as cyclic nucleotides (Yu and Bargmann, 2001). For example, Netrin-1 acts as a chemoattractant for commissural axons in the spinal cord whereas it repels trochlear motor axons at hindbrain levels (Tessier-Lavigne and Goodman, 1996). Exactly how Wnts, and in particular gradients of Wnts, are transduced at different stages of neuronal differentiation will be of great interest in future studies. Interspecies comparison of Wnt signalling cascades and their activities within distinct classes of neurons will certainly help to reveal the full breadth of effects mediated by Wnt signalling.

### **1.3.5 FGFs Determine Rostro-Caudal Identity and Act as Presynaptic**

#### **Organizers**

Recent evidence implicates FGFs as important upstream signalling molecules in assigning anterior-posterior identity to spinal motor neurons (Dasen et al., 2003). This study demonstrates that spinal progenitors can read graded FGF signals resulting in the expression of defined Hox-c proteins at distinct rostro-caudal levels of the spinal cord. In turn, Hox-c proteins impose columnar fate upon spinal motor neurons, acting upstream in the determination of motor neuron fate, which specifies

the expression of downstream genes involved in execution of axon pathfinding decisions. Whereas *Hoxc6* expression determines lateral motor column fate at forelimb levels, *Hoxc9* acts at thoracic levels to determine the fate of column of terni motor neurons (Dasen et al., 2003). In future experiments, it will be interesting to define whether not only motor neurons are responsive to FGF signalling to generate rostro-caudal diversity, but whether interneurons and DRG neurons also use the same strategy.

Acting at the growth cone and synapse, members of the FGF family of proteins have not only been implicated in the establishment of trochlear motor neuron trajectories (Irving et al., 2002), but have also recently been isolated as important players in presynaptic organization during synaptogenesis (Umemori et al., 2004). To identify target-derived molecules influencing differentiation of presynaptic nerve terminals, extracts derived from forebrain of postnatal mice were added to cultured chick embryonic motor neurons. Such cultures showed a significant increase in presynaptic differentiation when compared to control cultures. This assay was subsequently used for the purification of active components derived from postnatal forebrain extracts, resulting in the identification of FGF22 as one active component. In a survey of 12 different purified FGFs, not only FGF22, but also the two closely related family members FGF10 and FGF7, had very similar activities in inducing vesicle aggregation and neurite branching. The findings were extended to study the role of FGF signalling in controlling presynaptic neuronal differentiation of cerebellar mossy fibers *in vivo*. In support of the *in vitro* experiments, conditional elimination of FGFR2 postnatally resulted in a significant reduction in presynaptic mossy fiber specializations within the cerebellum. While the current study mainly focuses on

vesicle aggregation and neurite branching, other members of the FGF family appear to have distinct and diverse combinations of activities, at least when added to motor neurons in culture (Umemori et al., 2004). It will be interesting to characterize these activities as well as the types of neurons responsive to these factors in future studies.

### **1.3.6 Outlook**

The use of patterning molecules for multiple, important tasks during nervous system formation is a prominent, recurring theme. The recycling of signalling sources established at early developmental stages to independently direct later steps of development represents a wonderful way to further exploit complex signalling systems. Much attention in the future must be given to define distinctions and similarities of signalling pathways involved in the translation of extracellular signals into downstream cellular responses. It will be of particular interest to identify which actions permanently change cellular identity by initiating transcriptional responses and which events act at defined subcellular sites without altering permanently neuronal identity. Finally, given the recent exciting discoveries of molecular multitasking it seems unlikely that patterning molecules retire at the end of development and it will be intriguing to determine their functions in mature neuronal circuits.

## 1.4 Axon Guidance

As the nervous system develops, projecting axons sense their environment via the growth cone, an expanded, membranous edge at the tip of the elongating axon with numerous filopodia and lamellipodia studded with receptor proteins (Tanaka and Sabry, 1995). By sampling the surrounding environment, the growth cone senses attractive or repulsive guidance cues, which can either be secreted from a distance (long-range) or lie in the path of extending axon (short-range) (reviewed by Song and Poo, 2001). Binding of an attractive ligand to its receptor on the growth cone triggers changes in the cytoskeleton, leading to filopodial extension in the direction of the source. Repulsive guidance cues trigger retraction and collapse of the growth cone causing it to turn away from the signal (Cooper, 2002). Interpretation of these molecular cues is complex and depends not only on the ligand binding receptor expressed, but also upon co-receptors (Hong et al., 1999), the level of cyclic nucleotides present in the growth cone (Ming et al., 1997; Song et al., 1997) and cross talk between intracellular signalling cascades (Guan and Rao, 2003). Differences in these factors can allow a single axon guidance molecule to be interpreted by a growth cone as either attractive or repulsive.

While molecules involved in neural induction and patterning have recently been implicated in axon guidance, they are not traditionally considered as axon guidance molecules. The best studied molecular cues involved in the wiring of the nervous system belong to four families of molecules: Netrins, Semaphorins, Slits and Ephrins. All of these ligands and their receptors are evolutionarily conserved to some extent with regards to both structure and their roles in organizing the nervous system (Chisholm and Tessier-Lavigne, 1999).

### 1.4.1 Netrins and Their Receptors

Originally discovered as homologues of *C. elegans* proteins required for the circumferential migration of cells and axons in *C. elegans*, the netrin family of proteins have been shown to play a crucial role in guidance of commissural axons toward the ventral midline of the developing embryo. Netrin-1 has been shown to bind Deleted in Colon Cancer (DCC), mediating a chemoattractive effect (Hedgecock et al., 1990). Mice with defects in either Netrin-1 or DCC show severe defects in ventral extension of commissural axons as well as absence of the corpus callosum and other forebrain commissures (Serafini et al., 1996; Fazeli et al., 1997). In the presence of the Unc-5 receptor group Netrin-1 is chemorepulsive for subpopulations of circumferential axons in *C. elegans* (Hedgecock et al., 1990; Leonardo et al., 1997; Hong et al., 1999). This ability of axon guidance molecules to switch between chemoattraction and repulsion is common to many molecular cues and adds to the complexity and economy of the developing nervous system.

Of the four known mammalian Unc-5 proteins, Unc5h1, Unc5h2, Unc5h3 and Unc5h4 (Engelkamp, 2002), only two are confined to the nervous system. Unc5h1, found in cranial motor neuron subpopulations, is believed to induce apoptotic cell death via interactions with the melanoma antigen gene (MAGE) protein NRAGE (Barrett and Guthrie, 2001; Williams et al., 2003a), while disruption of Unc5h3 results in rostral cerebellar malformation (RCM) (Kuramoto et al., 2004). Unc5h3 has also

been shown to play a role in neuronal migration (Przyborski et al., 1998), which may be responsible for the laminar defects found in RCM.

Neogenin, a member of the DCC family, also binds netrins (Gad et al., 1997; Keeling et al., 1997; Wang et al., 1999). While mice mutant in *neogenin* lack an obvious axon guidance phenotype (Leighton et al., 2001), Neogenin mediates Netrin-1 dependent cell clustering during mammary gland development (Srinivasan et al., 2003) and is also involved in myotube formation (Kang et al., 2004). As discussed in in section 1.5.5, Neogenin has also been described as a receptor for cRGM and mRGMa.

#### **1.4.2 Slits and Robos**

The Slit family of secreted proteins, initially discovered in a *Drosophila* screen for genes controlling midline axon guidance, derive their name from the nerve cord phenotype of these flies, in which growth cones enter the midline but fail to leave it (Rothberg et al., 1988). This produces an aggregation of axons at the midline that resembles a 'slit'. Slits act as repulsive ligands for Roundabout (Robo) receptors, a function conserved in both vertebrates and invertebrates (Brose et al., 1999; Kidd et al., 1999; Li et al., 1999). In the fruit fly, Slit is expressed at a high level along the midline glia (Rothberg et al., 1990). Robo receptor expression is always high on axons that never cross the midline, while it is low on axons fated for crossing before they reach the midline, but quickly upregulated on these neurons post-crossing (Kidd et al., 1998). Additionally, a third molecule Commissureless (Comm) has been shown to regulate Slit/Robo interaction by sorting Robo to the late endosomal pathway preventing its expression at the cell surface (Keleman et al., 2002; Keleman

et al., 2005). In mammals, three Slit orthologues have been characterized (Itoh et al., 1998) with repulsive activity in various systems such as the hippocampus (Nguyen Ba-Charvet et al., 1999), retina (Ringstedt et al., 2000; Plump et al., 2002) and olfactory bulb (Li et al., 1999) (reviewed in (Brose and Tessier-Lavigne, 2000)). Additionally, Slits have been shown to direct neuroblast migration towards the olfactory bulb (Nguyen-Ba-Charvet et al., 2002; Nguyen-Ba-Charvet et al., 2004), as well as being identified as stimulators of axonal branching (Wang et al., 1999).

### **1.4.3 Semaphorins and Their Receptors**

The Semaphorin family, initially discovered in the insect nervous system (Kolodkin et al., 1992; Kolodkin et al., 1993) is the largest family of axon guidance molecules, with at least 20 separate genes encoding its members. Defined by a conserved ~420-amino acid Sema domain at their NH<sub>2</sub>-termini, Semaphorins are divided into eight classes. Classes 1 and 2 are found in invertebrates, classes 3 to 7 are found in vertebrates, and class V Semaphorins are viral (reviewed in (Raper, 2000)). Semaphorins can be transmembrane (classes 4-6), GPI-anchored (class 7) or secreted (class 3). As with many guidance molecules, Semaphorins function both in attraction and repulsion of growing axons. Repellent activity has been demonstrated in the hippocampus (Chedotal et al., 1998; Steup et al., 1999) and olfactory system (Kobayashi et al., 1997; Pasterkamp et al., 1999) as well as the peripheral nervous system (Kitsukawa et al., 1997; Taniguchi et al., 1997). Attractive Semaphorin function has been observed in the olfactory system (de Castro et al., 1999) as well as in the cortex (Bagnard et al., 1998).



Multiple receptor complexes mediate Semaphorin signalling. Neuropilins (NP-1 and 2) are transmembrane proteins that exclusively bind class 3 secreted Semaphorins. The small cytoplasmic domain of the Neuropilins contains no known signalling sequence and is believed not to play a role in Semaphorin signalling. In fact, mice mutants lacking the cytoplasmic tail of NP-1 still transduce Semaphorin function, suggesting that these receptors are not involved in direct signalling (Nakamura et al., 1998). Plexins, another family of molecules, are transmembrane proteins that bind certain Semaphorin classes directly, and also complex with Neuropilins to mediate class 3 Semaphorin effects (Winberg et al., 1998; Tamagnone et al., 1999). Interestingly, Semaphorin 3E, has recently been shown to signal directly through PlexinD1, independent of the Neuropilins (Gu et al., 2005). Semaphorin signalling is further increased in complexity by several other moderators including L1, a neuronal cell adhesion molecule, which is necessary for repulsion of cortical axons by Semaphorin 3A (Castellani et al., 2000), and B1 integrin subunits which mediate growth promotion of olfactory bulb axons (Pasterkamp et al., 2003).

#### **1.4.4 Ephrins and Eph Receptors**

Ephrins, originally discovered as ligands for the Eph family of orphan receptors (Cheng and Flanagan, 1994), are divided into two classes: Ephrin-As, GPI-anchored to the membrane and Ephrin-Bs which are transmembrane proteins. Similarly, the Eph receptors are also divided into two classes: A and B depending on which Ephrin type they preferentially bind. Ephrins are promiscuous, often binding several Eph receptor subtypes within the same class. The primary exception is the EphA4 receptor, which has been shown to interact with members of both class A and class B Ephrins (Orioli and Klein, 1997; Kullander et al., 2001).

Ephrin/Ephs, can signal bidirectionally, activating signal transduction pathways in both ligand and receptor expressing cells (Cowan et al., 2004), reviewed in (Davy and Soriano, 2005). Interestingly, this ability extends to the GPI-anchored Ephrin-As, which have been shown to inhibit neurogenesis and neural progenitor cell proliferation via reverse signalling (Davy et al., 1999; Holmberg et al., 2005). The major role described for the Ephrin-As is in topographic mapping of the anterior-posterior axis of the tectum/superior colliculus an activity dependent upon graded expression patterns of Ephrin-As/EphAs in both the colliculus and the retina ((Cheng et al., 1995; Drescher et al., 1995; Feldheim et al., 2000), reviewed in McLaughlin et al., 2003)).

The Ephrin-Bs have been implicated in dorso-ventral mapping of the retina to the lateral-medial axis of the superior colliculus (Hindges et al., 2002). Correct mapping requires both forward signalling via EphB receptors and reverse signalling, in which EphBs serve as ligands to signal back through the transmembrane EphrinBs (Hindges et al., 2002; Mann et al., 2002). In addition to their function in retinotopic map formation Ephrin-Bs have also been assigned roles in formation of the optic chiasm (Williams et al., 2003b), commissural axon pathfinding (Imondi and Kaprielian, 2001), prevention of corticospinal tract projections from recrossing the midline (Kullander et al., 2001) as well as non-neuronal processes such as cardiac valve formation (Cowan et al., 2004).

### 1.4.5 RGMs and Neogenin

Another axon guidance factor, Repulsive Guidance Molecule (RGM), was discovered in the chick during a screen for molecules involved in retinotectal guidance (Stahl et al., 1990). Based on work in previous studies, the screen operated under several premises. The first was that axon guidance molecules in the optic tectum would be developmentally regulated in such a way that they would have a low concentration in the anterior optic tectum, and a high concentration at the posterior end (Sperry, 1963; Bonhoeffer and Huf, 1982). The second was that the repellent activity of the posterior part of the tectum could be eliminated by treatment with phosphatidylinositol-specific phospholipase C (PI-PLC), which selectively cleaves GPI-anchored proteins (Walter et al., 1990). Finally, it was believed that this protein would be labelled by antisera generated against a posterior tectal membrane preparation, that disrupted its repellent activity. A 33 kDa protein fulfilling these criteria was discovered and protein fractions containing this molecule were capable of inducing repellent activity in both the collapse and stripe assays (Stahl et al., 1990). This molecule, RGM, was later purified, sequenced and then cloned from the chick optic tectum and its activity confirmed (Monnier et al., 2002).

In order to identify the receptor for RGM, a recent study used a fusion protein of chick RGM (cRGM) with a C-terminal alkaline phosphatase tag (cRGM-AP) to screen a mouse brain cDNA library (Rajagopalan et al., 2004). Neogenin, a DCC-like family member (Vielmetter et al., 1994) was discovered to bind cRGMa and, like Eph receptors known to mediate Ephrin effects in retinotectal guidance, is expressed in a gradient across the chick retina. Function blocking antibodies to Neogenin reduced the repellent effect of cRGM on RGC axons, and DRG neurons, normally

unresponsive to cRGM repellent effects, are sensitized to its repulsive activity by ectopic expression (Rajagopalan et al., 2004).

We identified three murine homologs of the 33kDa cRGM: mRGMa, mRGMb, and mRGMc (Niederkofler et al., 2004). The remainder of this work will be devoted to characterizing these molecules with regards to expression, cellular localization, and function.

## 1.5 References:

- Altmann CR, Brivanlou AH (2001) Neural patterning in the vertebrate embryo. *Int. Rev Cytol* 203:447-482.
- Amaya E, Musci TJ, Kirschner MW (1991) Expression of a dominant negative mutant of the FGF receptor disrupts mesoderm formation in *Xenopus* embryos. *Cell* 66:257-270.
- Anderson DJ, Groves A, Lo L, Ma Q, Rao M, Shah NM, Sommer L (1997) Cell lineage determination and the control of neuronal identity in the neural crest. *Cold Spring Harb Symp Quant Biol* 62:493-504.
- Augsburger A, Schuchardt A, Hoskins S, Dodd J, Butler S (1999) BMPs as mediators of roof plate repulsion of commissural neurons. *Neuron* 24:127-141.
- Bagnard D, Lohrum M, Uziel D, Puschel AW, Bolz J (1998) Semaphorins act as attractive and repulsive guidance signals during the development of cortical projections. *Development* 125:5043-5053.
- Barrett C, Guthrie S (2001) Expression patterns of the netrin receptor UNC5H1 among developing motor neurons in the embryonic rat hindbrain. *Mech Dev* 106:163-166.
- Bertrand V, Hudson C, Caillol D, Popovici C, Lemaire P (2003) Neural tissue in ascidian embryos is induced by FGF9/16/20, acting via a combination of maternal GATA and Ets transcription factors. *Cell* 115:615-627.
- Bonhoeffer F, Huf J (1982) In vitro experiments on axon guidance demonstrating an anterior-posterior gradient on the tectum. *Embo J* 1:427-431.
- Bonkowsky JL, Yoshikawa S, O'Keefe DD, Scully AL, Thomas JB (1999) Axon routing across the midline controlled by the *Drosophila* Derailed receptor. *Nature* 402:540-544.
- Brose K, Tessier-Lavigne M (2000) Slit proteins: key regulators of axon guidance, axonal branching, and cell migration. *Curr Opin Neurobiol* 10:95-102.
- Brose K, Bland KS, Wang KH, Arnott D, Henzel W, Goodman CS, Tessier-Lavigne M, Kidd T (1999) Slit proteins bind Robo receptors and have an evolutionarily conserved role in repulsive axon guidance. *Cell* 96:795-806.
- Butler SJ, Dodd J (2003) A role for BMP heterodimers in roof plate-mediated repulsion of commissural axons. *Neuron* 38:389-401.
- Castellani V, Chedotal A, Schachner M, Faivre-Sarrailh C, Rougon G (2000) Analysis of the L1-deficient mouse phenotype reveals cross-talk between Sema3A and L1 signalling pathways in axonal guidance. *Neuron* 27:237-249.

- Charron F, Stein E, Jeong J, McMahon AP, Tessier-Lavigne M (2003) The morphogen sonic hedgehog is an axonal chemoattractant that collaborates with netrin-1 in midline axon guidance. *Cell* 113:11-23.
- Chedotal A, Del Rio JA, Ruiz M, He Z, Borrell V, de Castro F, Ezan F, Goodman CS, Tessier-Lavigne M, Sotelo C, Soriano E (1998) Semaphorins III and IV repel hippocampal axons via two distinct receptors. *Development* 125:4313-4323.
- Cheng HJ, Flanagan JG (1994) Identification and cloning of ELF-1, a developmentally expressed ligand for the Mek4 and Sek receptor tyrosine kinases. *Cell* 79:157-168.
- Cheng HJ, Nakamoto M, Bergemann AD, Flanagan JG (1995) Complementary gradients in expression and binding of ELF-1 and Mek4 in development of the topographic retinotectal projection map. *Cell* 82:371-381.
- Chisholm A, Tessier-Lavigne M (1999) Conservation and divergence of axon guidance mechanisms. *Curr Opin Neurobiol* 9:603-615.
- Colas JF, Schoenwolf GC (2001) Towards a cellular and molecular understanding of neurulation. *Dev Dyn* 221:117-145.
- Colas JF, Schoenwolf GC (2003) Assessing the contributions of gene products to the form-shaping events of neurulation: a transgenic approach in chick. *Genesis* 37:64-75.
- Cooper HM (2002) Axon guidance receptors direct growth cone pathfinding: rivalry at the leading edge. *Int J Dev Biol* 46:621-631.
- Cowan CA, Yokoyama N, Saxena A, Chumley MJ, Silvany RE, Baker LA, Srivastava D, Henkemeyer M (2004) Ephrin-B2 reverse signalling is required for axon pathfinding and cardiac valve formation but not early vascular development. *Dev Biol* 271:263-271.
- Dailey L, Ambrosetti D, Mansukhani A, Basilico C (2005) Mechanisms underlying differential responses to FGF signalling. *Cytokine Growth Factor Rev* 16:233-247.
- Dasen JS, Liu JP, Jessell TM (2003) Motor neuron columnar fate imposed by sequential phases of Hox-c activity. *Nature* 425:926-933.
- Davy A, Soriano P (2005) Ephrin signalling in vivo: look both ways. *Dev Dyn* 232:1-10.
- Davy A, Gale NW, Murray EW, Klinghoffer RA, Soriano P, Feuerstein C, Robbins SM (1999) Compartmentalized signalling by GPI-anchored ephrin-A5 requires the Fyn tyrosine kinase to regulate cellular adhesion. *Genes Dev* 13:3125-3135.

- de Castro F, Hu L, Drabkin H, Sotelo C, Chedotal A (1999) Chemoattraction and chemorepulsion of olfactory bulb axons by different secreted semaphorins. *J Neurosci* 19:4428-4436.
- De Robertis EM, Kuroda H (2004) Dorsal-ventral patterning and neural induction in *Xenopus* embryos. *Annu Rev Cell Dev Biol* 20:285-308.
- Delaune E, Lemaire P, Kodjabachian L (2005) Neural induction in *Xenopus* requires early FGF signalling in addition to BMP inhibition. *Development* 132:299-310.
- Dixon J, Brakebusch C, Fassler R, Dixon MJ (2000) Increased levels of apoptosis in the pre-fusion neural folds underlie the craniofacial disorder, Treacher Collins syndrome. *Hum Mol Genet* 9:1473-1480.
- Drescher U, Kremoser C, Handwerker C, Loschinger J, Noda M, Bonhoeffer F (1995) In vitro guidance of retinal ganglion cell axons by RAGS, a 25 kDa tectal protein related to ligands for Eph receptor tyrosine kinases. *Cell* 82:359-370.
- Eggenchwiler JT, Espinoza E, Anderson KV (2001) Rab23 is an essential negative regulator of the mouse Sonic hedgehog signalling pathway. *Nature* 412:194-198.
- Engelkamp D (2002) Cloning of three mouse *Unc5* genes and their expression patterns at mid-gestation. *Mech Dev* 118:191-197.
- Fainsod A, Steinbeisser H, De Robertis EM (1994) On the function of BMP-4 in patterning the marginal zone of the *Xenopus* embryo. *Embo J* 13:5015-5025.
- Fainsod A, Deissler K, Yelin R, Marom K, Epstein M, Pillemer G, Steinbeisser H, Blum M (1997) The dorsalizing and neural inducing gene *follistatin* is an antagonist of BMP-4. *Mech Dev* 63:39-50.
- Fazeli A, Dickinson SL, Hermiston ML, Tighe RV, Steen RG, Small CG, Stoeckli ET, Keino-Masu K, Masu M, Rayburn H, Simons J, Bronson RT, Gordon JI, Tessier-Lavigne M, Weinberg RA (1997) Phenotype of mice lacking functional Deleted in colorectal cancer (*Dcc*) gene. *Nature* 386:796-804.
- Feldheim DA, Kim YI, Bergemann AD, Frisen J, Barbacid M, Flanagan JG (2000) Genetic analysis of ephrin-A2 and ephrin-A5 shows their requirement in multiple aspects of retinocollicular mapping. *Neuron* 25:563-574.
- Fernandez Caso M, De Paz P, Fernandez Alvarez JG, Chamorro C, Villar JM (1992) Delamination of neuroepithelium and nonneural ectoderm and its relation to the convergence step in chick neurulation. *J Anat* 180 ( Pt 1):143-153.
- Gad JM, Keeling SL, Wilks AF, Tan SS, Cooper HM (1997) The expression patterns of guidance receptors, DCC and Neogenin, are spatially and temporally distinct throughout mouse embryogenesis. *Dev Biol* 192:258-273.

- Geelen JA, Langman J (1979) Ultrastructural observations on closure of the neural tube in the mouse. *Anat Embryol (Berl)* 156:73-88.
- Grunz H, Tacke L (1989) Neural differentiation of *Xenopus laevis* ectoderm takes place after disaggregation and delayed reaggregation without inducer. *Cell Differ Dev* 28:211-217.
- Gu C, Yoshida Y, Livet J, Reimert DV, Mann F, Merte J, Henderson CE, Jessell TM, Kolodkin AL, Ginty DD (2005) Semaphorin 3E and plexin-D1 control vascular pattern independently of neuropilins. *Science* 307:265-268.
- Guan KL, Rao Y (2003) Signalling mechanisms mediating neuronal responses to guidance cues. *Nat Rev Neurosci* 4:941-956.
- Hardcastle Z, Chalmers AD, Papalopulu N (2000) FGF-8 stimulates neuronal differentiation through FGFR-4a and interferes with mesoderm induction in *Xenopus* embryos. *Curr Biol* 10:1511-1514.
- Haydar TF, Kuan CY, Flavell RA, Rakic P (1999) The role of cell death in regulating the size and shape of the mammalian forebrain. *Cereb Cortex* 9:621-626.
- Hedgecock EM, Culotti JG, Hall DH (1990) The *unc-5*, *unc-6*, and *unc-40* genes guide circumferential migrations of pioneer axons and mesodermal cells on the epidermis in *C. elegans*. *Neuron* 4:61-85.
- Hemmati-Brivanlou A, Melton DA (1992) A truncated activin receptor inhibits mesoderm induction and formation of axial structures in *Xenopus* embryos. *Nature* 359:609-614.
- Hemmati-Brivanlou A, Kelly OG, Melton DA (1994) Follistatin, an antagonist of activin, is expressed in the Spemann organizer and displays direct neuralizing activity. *Cell* 77:283-295.
- Hindges R, McLaughlin T, Genoud N, Henkemeyer M, O'Leary DD (2002) EphB forward signalling controls directional branch extension and arborization required for dorsal-ventral retinotopic mapping. *Neuron* 35:475-487.
- Holmberg J, Clarke DL, Frisen J (2000) Regulation of repulsion versus adhesion by different splice forms of an Eph receptor. *Nature* 408:203-206.
- Holmberg J, Armulik A, Senti KA, Edoff K, Spalding K, Momma S, Cassidy R, Flanagan JG, Frisen J (2005) Ephrin-A2 reverse signalling negatively regulates neural progenitor proliferation and neurogenesis. *Genes Dev* 19:462-471.
- Holowacz T, Sokol S (1999) FGF is required for posterior neural patterning but not for neural induction. *Dev Biol* 205:296-308.
- Hong K, Hinck L, Nishiyama M, Poo MM, Tessier-Lavigne M, Stein E (1999) A ligand-gated association between cytoplasmic domains of UNC5 and DCC family



- receptors converts netrin-induced growth cone attraction to repulsion. *Cell* 97:927-941.
- Hongo I, Kengaku M, Okamoto H (1999) FGF signalling and the anterior neural induction in *Xenopus*. *Dev Biol* 216:561-581.
- Hui CC, Joyner AL (1993) A mouse model of greig cephalopolysyndactyly syndrome: the extra-toesJ mutation contains an intragenic deletion of the *Gli3* gene. *Nat Genet* 3:241-246.
- Ikeda A, Ikeda S, Gridley T, Nishina PM, Naggert JK (2001) Neural tube defects and neuroepithelial cell death in *Tulp3* knockout mice. *Hum Mol Genet* 10:1325-1334.
- Imondi R, Kaprielian Z (2001) Commissural axon pathfinding on the contralateral side of the floor plate: a role for B-class ephrins in specifying the dorsoventral position of longitudinally projecting commissural axons. *Development* 128:4859-4871.
- Inoue T, Oz HS, Wiland D, Gharib S, Deshpande R, Hill RJ, Katz WS, Sternberg PW (2004) *C. elegans* LIN-18 is a Ryk ortholog and functions in parallel to LIN-17/Frizzled in Wnt signalling. *Cell* 118:795-806.
- Irving C, Malhas A, Guthrie S, Mason I (2002) Establishing the trochlear motor axon trajectory: role of the isthmic organiser and *Fgf8*. *Development* 129:5389-5398.
- Itoh A, Miyabayashi T, Ohno M, Sakano S (1998) Cloning and expressions of three mammalian homologues of *Drosophila* slit suggest possible roles for Slit in the formation and maintenance of the nervous system. *Brain Res Mol Brain Res* 62:175-186.
- Jessell TM (2000) Neuronal specification in the spinal cord: inductive signals and transcriptional codes. *Nat Rev Genet* 1:20-29.
- Kang JS, Yi MJ, Zhang W, Feinleib JL, Cole F, Krauss RS (2004) Netrins and neogenin promote myotube formation. *J Cell Biol* 167:493-504.
- Keeling SL, Gad JM, Cooper HM (1997) Mouse Neogenin, a DCC-like molecule, has four splice variants and is expressed widely in the adult mouse and during embryogenesis. *Oncogene* 15:691-700.
- Keleman K, Ribeiro C, Dickson BJ (2005) Comm function in commissural axon guidance: cell-autonomous sorting of Robo in vivo. *Nat Neurosci* 8:156-163.
- Keleman K, Rajagopalan S, Cleppien D, Teis D, Paiha K, Huber LA, Technau GM, Dickson BJ (2002) Comm sorts robo to control axon guidance at the *Drosophila* midline. *Cell* 110:415-427.

- Khokha MK, Yeh J, Grammer TC, Harland RM (2005) Depletion of three BMP antagonists from Spemann's organizer leads to a catastrophic loss of dorsal structures. *Dev Cell* 8:401-411.
- Kidd T, Bland KS, Goodman CS (1999) Slit is the midline repellent for the robo receptor in *Drosophila*. *Cell* 96:785-794.
- Kidd T, Brose K, Mitchell KJ, Fetter RD, Tessier-Lavigne M, Goodman CS, Tear G (1998) Roundabout controls axon crossing of the CNS midline and defines a novel subfamily of evolutionarily conserved guidance receptors. *Cell* 92:205-215.
- Kirilova I, Novikova I, Auge J, Audollent S, Esnault D, Encha-Razavi F, Lazjuk G, Attie-Bitach T, Vekemans M (2000) Expression of the sonic hedgehog gene in human embryos with neural tube defects. *Teratology* 61:347-354.
- Kitsukawa T, Shimizu M, Sanbo M, Hirata T, Taniguchi M, Bekku Y, Yagi T, Fujisawa H (1997) Neuropilin-semaphorin III/D-mediated chemorepulsive signals play a crucial role in peripheral nerve projection in mice. *Neuron* 19:995-1005.
- Kobayashi H, Koppel AM, Luo Y, Raper JA (1997) A role for collapsin-1 in olfactory and cranial sensory axon guidance. *J Neurosci* 17:8339-8352.
- Kolodkin AL, Matthes DJ, Goodman CS (1993) The semaphorin genes encode a family of transmembrane and secreted growth cone guidance molecules. *Cell* 75:1389-1399.
- Kolodkin AL, Matthes DJ, O'Connor TP, Patel NH, Admon A, Bentley D, Goodman CS (1992) Fasciclin IV: sequence, expression, and function during growth cone guidance in the grasshopper embryo. *Neuron* 9:831-845.
- Koyabu Y, Nakata K, Mizugishi K, Aruga J, Mikoshiba K (2001) Physical and functional interactions between Zic and Gli proteins. *J Biol Chem* 276:6889-6892.
- Kullander K, Croll SD, Zimmer M, Pan L, McClain J, Hughes V, Zabski S, DeChiara TM, Klein R, Yancopoulos GD, Gale NW (2001) Ephrin-B3 is the midline barrier that prevents corticospinal tract axons from recrossing, allowing for unilateral motor control. *Genes Dev* 15:877-888.
- Kuramoto T, Kuwamura M, Serikawa T (2004) Rat neurological mutations cerebellar vermis defect and hobble are caused by mutations in the netrin-1 receptor gene *Unc5h3*. *Brain Res Mol Brain Res* 122:103-108.
- Kuschel S, Ruther U, Theil T (2003) A disrupted balance between Bmp/Wnt and Fgf signalling underlies the ventralization of the *Gli3* mutant telencephalon. *Dev Biol* 260:484-495.
- Ladher RK, Wright TJ, Moon AM, Mansour SL, Schoenwolf GC (2005) FGF8 initiates inner ear induction in chick and mouse. *Genes Dev* 19:603-613.

- Launay C, Fromentoux V, Shi DL, Boucaut JC (1996) A truncated FGF receptor blocks neural induction by endogenous *Xenopus* inducers. *Development* 122:869-880.
- Lawson A, Anderson H, Schoenwolf GC (2001) Cellular mechanisms of neural fold formation and morphogenesis in the chick embryo. *Anat Rec* 262:153-168.
- Lawson A, Schoenwolf GC, England MA, Addai FK, Ahima RS (1999) Programmed cell death and the morphogenesis of the hindbrain roof plate in the chick embryo. *Anat Embryol (Berl)* 200:509-519.
- Lee HY, Kleber M, Hari L, Brault V, Suter U, Taketo MM, Kemler R, Sommer L (2004) Instructive role of Wnt/beta-catenin in sensory fate specification in neural crest stem cells. *Science* 303:1020-1023.
- Leighton PA, Mitchell KJ, Goodrich LV, Lu X, Pinson K, Scherz P, Skarnes WC, Tessier-Lavigne M (2001) Defining brain wiring patterns and mechanisms through gene trapping in mice. *Nature* 410:174-179.
- Leonardo ED, Hinck L, Masu M, Keino-Masu K, Ackerman SL, Tessier-Lavigne M (1997) Vertebrate homologues of *C. elegans* UNC-5 are candidate netrin receptors. *Nature* 386:833-838.
- Li HS, Chen JH, Wu W, Fagaly T, Zhou L, Yuan W, Dupuis S, Jiang ZH, Nash W, Gick C, Ornitz DM, Wu JY, Rao Y (1999) Vertebrate slit, a secreted ligand for the transmembrane protein roundabout, is a repellent for olfactory bulb axons. *Cell* 96:807-818.
- Linker C, Stern CD (2004) Neural induction requires BMP inhibition only as a late step, and involves signals other than FGF and Wnt antagonists. *Development* 131:5671-5681.
- Lu W, Yamamoto V, Ortega B, Baltimore D (2004) Mammalian Ryk is a Wnt coreceptor required for stimulation of neurite outgrowth. *Cell* 119:97-108.
- Lyuksyutova AI, Lu CC, Milanesio N, King LA, Guo N, Wang Y, Nathans J, Tessier-Lavigne M, Zou Y (2003) Anterior-posterior guidance of commissural axons by Wnt-frizzled signalling. *Science* 302:1984-1988.
- Mann F, Ray S, Harris W, Holt C (2002) Topographic mapping in dorsoventral axis of the *Xenopus* retinotectal system depends on signalling through ephrin-B ligands. *Neuron* 35:461-473.
- McLaughlin T, Hindges R, O'Leary DD (2003) Regulation of axial patterning of the retina and its topographic mapping in the brain. *Curr Opin Neurobiol* 13:57-69.
- Ming GL, Song HJ, Berninger B, Holt CE, Tessier-Lavigne M, Poo MM (1997) cAMP-dependent growth cone guidance by netrin-1. *Neuron* 19:1225-1235.

- Monnier PP, Sierra A, Macchi P, Deitinghoff L, Andersen JS, Mann M, Flad M, Hornberger MR, Stahl B, Bonhoeffer F, Mueller BK (2002) RGM is a repulsive guidance molecule for retinal axons. *Nature* 419:392-395.
- Nakamura F, Tanaka M, Takahashi T, Kalb RG, Strittmatter SM (1998) Neuropilin-1 extracellular domains mediate semaphorin D/III-induced growth cone collapse. *Neuron* 21:1093-1100.
- Nakata K, Nagai T, Aruga J, Mikoshiba K (1998) Xenopus Zic family and its role in neural and neural crest development. *Mech Dev* 75:43-51.
- Nguyen Ba-Charvet KT, Brose K, Marillat V, Kidd T, Goodman CS, Tessier-Lavigne M, Sotelo C, Chedotal A (1999) Slit2-Mediated chemorepulsion and collapse of developing forebrain axons. *Neuron* 22:463-473.
- Nguyen-Ba-Charvet KT, Plump AS, Tessier-Lavigne M, Chedotal A (2002) Slit1 and slit2 proteins control the development of the lateral olfactory tract. *J Neurosci* 22:5473-5480.
- Nguyen-Ba-Charvet KT, Picard-Riera N, Tessier-Lavigne M, Baron-Van Evercooren A, Sotelo C, Chedotal A (2004) Multiple roles for slits in the control of cell migration in the rostral migratory stream. *J Neurosci* 24:1497-1506.
- Niederkofler V, Salie R, Sigrist M, Arber S (2004) Repulsive guidance molecule (RGM) gene function is required for neural tube closure but not retinal topography in the mouse visual system. *J Neurosci* 24:808-818.
- Orioli D, Klein R (1997) The Eph receptor family: axonal guidance by contact repulsion. *Trends Genet* 13:354-359.
- Packard M, Mathew D, Budnik V (2003) Wnts and TGF beta in synaptogenesis: old friends signalling at new places. *Nat Rev Neurosci* 4:113-120.
- Pasterkamp RJ, Ruitenber MJ, Verhaagen J (1999) Semaphorins and their receptors in olfactory axon guidance. *Cell Mol Biol (Noisy-le-grand)* 45:763-779.
- Pasterkamp RJ, Peschon JJ, Spriggs MK, Kolodkin AL (2003) Semaphorin 7A promotes axon outgrowth through integrins and MAPKs. *Nature* 424:398-405.
- Patapoutian A, Reichardt LF (2000) Roles of Wnt proteins in neural development and maintenance. *Curr Opin Neurobiol* 10:392-399.
- Pera EM, Ikeda A, Eivers E, De Robertis EM (2003) Integration of IGF, FGF, and anti-BMP signals via Smad1 phosphorylation in neural induction. *Genes Dev* 17:3023-3028.
- Piccolo S, Sasai Y, Lu B, De Robertis EM (1996) Dorsoventral patterning in Xenopus: inhibition of ventral signals by direct binding of chordin to BMP-4. *Cell* 86:589-598.

- Plump AS, Erskine L, Sabatier C, Brose K, Epstein CJ, Goodman CS, Mason CA, Tessier-Lavigne M (2002) Slit1 and Slit2 cooperate to prevent premature midline crossing of retinal axons in the mouse visual system. *Neuron* 33:219-232.
- Przyborski SA, Knowles BB, Ackerman SL (1998) Embryonic phenotype of *Unc5h3* mutant mice suggests chemorepulsion during the formation of the rostral cerebellar boundary. *Development* 125:41-50.
- Rajagopalan S, Deitinghoff L, Davis D, Conrad S, Skutella T, Chedotal A, Mueller BK, Strittmatter SM (2004) Neogenin mediates the action of repulsive guidance molecule. *Nat Cell Biol* 6:756-762.
- Raper JA (2000) Semaphorins and their receptors in vertebrates and invertebrates. *Curr Opin Neurobiol* 10:88-94.
- Rentzsch F, Bakkers J, Kramer C, Hammerschmidt M (2004) Fgf signalling induces posterior neuroectoderm independently of Bmp signalling inhibition. *Dev Dyn* 231:750-757.
- Ringstedt T, Braisted JE, Brose K, Kidd T, Goodman C, Tessier-Lavigne M, O'Leary DD (2000) Slit inhibition of retinal axon growth and its role in retinal axon pathfinding and innervation patterns in the diencephalon. *J Neurosci* 20:4983-4991.
- Rothberg JM, Hartley DA, Walther Z, Artavanis-Tsakonas S (1988) *slit*: an EGF-homologous locus of *D. melanogaster* involved in the development of the embryonic central nervous system. *Cell* 55:1047-1059.
- Rothberg JM, Jacobs JR, Goodman CS, Artavanis-Tsakonas S (1990) *slit*: an extracellular protein necessary for development of midline glia and commissural axon pathways contains both EGF and LRR domains. *Genes Dev* 4:2169-2187.
- Sadler TW (1978) Distribution of surface coat material on fusing neural folds of mouse embryos during neurulation. *Anat Rec* 191:345-349.
- Sah VP, Attardi LD, Mulligan GJ, Williams BO, Bronson RT, Jacks T (1995) A subset of p53-deficient embryos exhibit exencephaly. *Nat Genet* 10:175-180.
- Sasai Y, Lu B, Piccolo S, De Robertis EM (1996) Endoderm induction by the organizer-secreted factors chordin and noggin in *Xenopus* animal caps. *Embo J* 15:4547-4555.
- Sasai Y, Lu B, Steinbeisser H, Geissert D, Gont LK, De Robertis EM (1994) *Xenopus* chordin: a novel dorsalizing factor activated by organizer-specific homeobox genes. *Cell* 79:779-790.

- Sausedo RA, Smith JL, Schoenwolf GC (1997) Role of nonrandomly oriented cell division in shaping and bending of the neural plate. *J Comp Neurol* 381:473-488.
- Scheiffele P (2003) Cell-cell signalling during synapse formation in the CNS. *Annu Rev Neurosci* 26:485-508.
- Schoenwolf GC, Smith JL (2000) Mechanisms of neurulation. *Methods Mol Biol* 136:125-134.
- Serafini T, Colamarino SA, Leonardo ED, Wang H, Beddington R, Skarnes WC, Tessier-Lavigne M (1996) Netrin-1 is required for commissural axon guidance in the developing vertebrate nervous system. *Cell* 87:1001-1014.
- Shimogori T, Banuchi V, Ng HY, Strauss JB, Grove EA (2004) Embryonic signalling centers expressing BMP, WNT and FGF proteins interact to pattern the cerebral cortex. *Development* 131:5639-5647.
- Shum AS, Copp AJ (1996) Regional differences in morphogenesis of the neuroepithelium suggest multiple mechanisms of spinal neurulation in the mouse. *Anat Embryol (Berl)* 194:65-73.
- Smith JL, Schoenwolf GC (1987) Cell cycle and neuroepithelial cell shape during bending of the chick neural plate. *Anat Rec* 218:196-206.
- Smith JL, Schoenwolf GC (1988) Role of cell-cycle in regulating neuroepithelial cell shape during bending of the chick neural plate. *Cell Tissue Res* 252:491-500.
- Smith JL, Schoenwolf GC (1989) Notochordal induction of cell wedging in the chick neural plate and its role in neural tube formation. *J Exp Zool* 250:49-62.
- Smith WC, Harland RM (1992) Expression cloning of noggin, a new dorsalizing factor localized to the Spemann organizer in *Xenopus* embryos. *Cell* 70:829-840.
- Song H, Poo M (2001) The cell biology of neuronal navigation. *Nat Cell Biol* 3:E81-88.
- Song HJ, Ming GL, Poo MM (1997) cAMP-induced switching in turning direction of nerve growth cones. *Nature* 388:275-279.
- Spemann HaM, H. (1924) Über Induktion von Embryonalanlagen durch Implantation artfremder Organisatoren. *Roux's Arch EntwMech Org*:599-638.
- Sperry RW (1963) Chemoaffinity in the Orderly Growth of Nerve Fiber Patterns and Connections. *Proc Natl Acad Sci U S A* 50:703-710.
- Srinivasan K, Strickland P, Valdes A, Shin GC, Hinck L (2003) Netrin-1/neogenin interaction stabilizes multipotent progenitor cap cells during mammary gland morphogenesis. *Dev Cell* 4:371-382.

- Stahl B, Muller B, von Boxberg Y, Cox EC, Bonhoeffer F (1990) Biochemical characterization of a putative axonal guidance molecule of the chick visual system. *Neuron* 5:735-743.
- Stein E, Tessier-Lavigne M (2001) Hierarchical organization of guidance receptors: silencing of netrin attraction by slit through a Robo/DCC receptor complex. *Science* 291:1928-1938.
- Stern CD (2005) Neural induction: old problem, new findings, yet more questions. *Development* 132:2007-2021.
- Stern CD (2004) Neural Induction. In: *Gastrulation: From Cells to Embryo* (Stern CD, ed), pp 419-432. New York: Cold Spring Harbor Press.
- Steup A, Ninnemann O, Savaskan NE, Nitsch R, Puschel AW, Skutella T (1999) Semaphorin D acts as a repulsive factor for entorhinal and hippocampal neurons. *Eur J Neurosci* 11:729-734.
- Storey KG, Goriely A, Sargent CM, Brown JM, Burns HD, Abud HM, Heath JK (1998) Early posterior neural tissue is induced by FGF in the chick embryo. *Development* 125:473-484.
- Streit A, Berliner AJ, Papanayotou C, Sirulnik A, Stern CD (2000) Initiation of neural induction by FGF signalling before gastrulation. *Nature* 406:74-78.
- Streit A, Lee KJ, Woo I, Roberts C, Jessell TM, Stern CD (1998) Chordin regulates primitive streak development and the stability of induced neural cells, but is not sufficient for neural induction in the chick embryo. *Development* 125:507-519.
- Strong CF, Barnett MW, Hartman D, Jones EA, Stott D (2000) Xbra3 induces mesoderm and neural tissue in *Xenopus laevis*. *Dev Biol* 222:405-419.
- Suzuki A, Ueno N, Hemmati-Brivanlou A (1997a) *Xenopus* msx1 mediates epidermal induction and neural inhibition by BMP4. *Development* 124:3037-3044.
- Suzuki A, Chang C, Yingling JM, Wang XF, Hemmati-Brivanlou A (1997b) Smad5 induces ventral fates in *Xenopus* embryo. *Dev Biol* 184:402-405.
- Tamagnone L, Artigiani S, Chen H, He Z, Ming GI, Song H, Chedotal A, Winberg ML, Goodman CS, Poo M, Tessier-Lavigne M, Comoglio PM (1999) Plexins are a large family of receptors for transmembrane, secreted, and GPI-anchored semaphorins in vertebrates. *Cell* 99:71-80.
- Tanaka E, Sabry J (1995) Making the connection: cytoskeletal rearrangements during growth cone guidance. *Cell* 83:171-176.
- Taniguchi M, Yuasa S, Fujisawa H, Naruse I, Saga S, Mishina M, Yagi T (1997) Disruption of semaphorin III/D gene causes severe abnormality in peripheral nerve projection. *Neuron* 19:519-530.

- Tessier-Lavigne M, Goodman CS (1996) The molecular biology of axon guidance. *Science* 274:1123-1133.
- Umemori H, Linhoff MW, Ornitz DM, Sanes JR (2004) FGF22 and its close relatives are presynaptic organizing molecules in the mammalian brain. *Cell* 118:257-270.
- Vielmetter J, Kayyem JF, Roman JM, Dreyer WJ (1994) Neogenin, an avian cell surface protein expressed during terminal neuronal differentiation, is closely related to the human tumor suppressor molecule deleted in colorectal cancer. *J Cell Biol* 127:2009-2020.
- Walter J, Muller B, Bonhoeffer F (1990) Axonal guidance by an avoidance mechanism. *J Physiol (Paris)* 84:104-110.
- Wang H, Copeland NG, Gilbert DJ, Jenkins NA, Tessier-Lavigne M (1999) Netrin-3, a mouse homolog of human NTN2L, is highly expressed in sensory ganglia and shows differential binding to netrin receptors. *J Neurosci* 19:4938-4947.
- Williams ME, Strickland P, Watanabe K, Hinck L (2003a) UNC5H1 induces apoptosis via its juxtamembrane region through an interaction with NRAGE. *J Biol Chem* 278:17483-17490.
- Williams SE, Mann F, Erskine L, Sakurai T, Wei S, Rossi DJ, Gale NW, Holt CE, Mason CA, Henkemeyer M (2003b) Ephrin-B2 and EphB1 mediate retinal axon divergence at the optic chiasm. *Neuron* 39:919-935.
- Wilson PA, Hemmati-Brivanlou A (1995) Induction of epidermis and inhibition of neural fate by Bmp-4. *Nature* 376:331-333.
- Wilson SI, Graziano E, Harland R, Jessell TM, Edlund T (2000) An early requirement for FGF signalling in the acquisition of neural cell fate in the chick embryo. *Curr Biol* 10:421-429.
- Wilson SI, Rydstrom A, Trimborn T, Willert K, Nusse R, Jessell TM, Edlund T (2001) The status of Wnt signalling regulates neural and epidermal fates in the chick embryo. *Nature* 411:325-330.
- Winberg ML, Noordermeer JN, Tamagnone L, Comoglio PM, Spriggs MK, Tessier-Lavigne M, Goodman CS (1998) Plexin A is a neuronal semaphorin receptor that controls axon guidance. *Cell* 95:903-916.
- Wright TJ, Ladher R, McWhirter J, Murre C, Schoenwolf GC, Mansour SL (2004) Mouse FGF15 is the ortholog of human and chick FGF19, but is not uniquely required for otic induction. *Dev Biol* 269:264-275.
- Ybot-Gonzalez P, Cogram P, Gerrelli D, Copp AJ (2002) Sonic hedgehog and the molecular regulation of mouse neural tube closure. *Development* 129:2507-2517.



Yoshikawa S, McKinnon RD, Kokel M, Thomas JB (2003) Wnt-mediated axon guidance via the Drosophila Derailed receptor. *Nature* 422:583-588.

Yu TW, Bargmann CI (2001) Dynamic regulation of axon guidance. *Nat Neurosci* 4 Suppl:1169-1176.

Zimmerman LB, De Jesus-Escobar JM, Harland RM (1996) The Spemann organizer signal noggin binds and inactivates bone morphogenetic protein 4. *Cell* 86:599-606.



## **Chapter 2:**

# ***RGM* Gene Function Is Required for Neural Tube Closure but not Retinal Topography in the Mouse Visual System**

## **Chapter 2: RGM Gene Function Is Required for Neural Tube Closure but not Retinal Topography in the Mouse Visual System**

Vera Niederkofler\*, Rishard Salie\*, Markus Sigrist & Silvia Arber *J. Neurosci.* **24**, 808-18.(2004).

\* indicates equal contribution

### **2.1 Abstract**

The establishment of topographic projections in the developing visual system depends on spatially and temporally controlled expression of axon guidance molecules. In the developing chick tectum, the graded expression of Repulsive Guidance Molecule (*RGM*) has been proposed to be involved in controlling topography of retinal ganglion cell (RGC) axon termination zones along the anterior-posterior axis of the tectum. We now show that there are three mouse proteins homologous to chick *RGM* displaying similar proteolytic processing but exhibiting differential cell surface targeting by GPI anchor addition. Two members of this gene family (*mRGMa* and *mRGMb*) are expressed in complementary patterns in the nervous system, and *mRGMa* is expressed prominently in the superior colliculus at the time of anterior-posterior targeting of RGC axons. The third member of the family (*mRGMc*) is expressed almost exclusively in skeletal muscles. Functional studies in the mouse reveal a role for *mRGMa* in controlling cephalic neural tube closure thus defining an unexpected role for *mRGMa* in early embryonic development. In contrast, *mRGMa* mutant mice do not exhibit defects in anterior-posterior targeting of RGC axons to their stereotypic termination zones in the superior colliculus.

## 2.2 Introduction

The precise temporal and spatial interplay of different extracellular proteins is essential for the establishment of correct morphology and patterning of the nervous system at early developmental stages as well as for the assembly of neuronal circuits later in development. Many extracellular proteins have been studied for their role in controlling axon outgrowth to target regions in an attempt to address the question of how axonal projections of different neuronal populations achieve precise targeting to the region they innervate in the mature nervous system. These studies have led to the concept that extracellular guidance molecules can act in both attractive and repulsive manners (Tessier-Lavigne and Goodman, 1996) and much is known about the mechanisms by which these molecules direct axons towards their targets (Yu and Bargmann, 2001; Dickson, 2002).

One system where the underlying molecular mechanisms controlling the development of precise axonal projections have been studied extensively is the projection of retinal ganglion cells (RGCs) to either the chick tectum or the rodent superior colliculus (Sperry, 1963; McLaughlin et al., 2003a). The anatomical arrangement of retinocollicular projections during rodent development and in the mature system has been well-defined (Simon and O'Leary, 1992). In the mature retinocollicular system there is a precise topography of projections from the retina to the superior colliculus: Temporal RGC axons consistently terminate in the anterior superior colliculus whereas nasal RGC axons project to the posterior superior colliculus (Sperry, 1963; McLaughlin et al., 2003a). This observation has led to the proposal that RGC axons terminating in the anterior superior colliculus may be

repelled by molecular cues found at a higher concentration in the posterior relative to the anterior superior colliculus (Sperry, 1963). Consistent with this model, temporal RGCs are repelled by membranes isolated from the posterior chick tectum and grow preferentially on anterior tectal membranes (Walter et al., 1987). The isolation of molecules expressed in a low anterior to high posterior gradient in the chick tectum led to the discovery that members of the Ephrin family (in particular Ephrin-A2 and Ephrin-A5) possess such a repulsive activity (Drescher et al., 1995; Nakamoto et al., 1996; Monschau et al., 1997). Both *Ephrin-A2* and *Ephrin-A5* are expressed in a gradient in the chick tectum and the mouse superior colliculus (Drescher et al., 1995; Cheng et al., 1995; Feldheim et al., 2000). Functional evidence supports the idea that Ephrin-A2 and Ephrin-A5 act as repulsive guidance cues confining the termination zones of temporal RGCs to more anterior positions (Nakamoto et al., 1996; Feldheim et al., 2000; McLaughlin et al., 2003a).

Chick RGM (cRGM) has been reported to possess an *in vitro* activity similar to the Ephrins, causing growth cone collapse and preferential guidance of temporal RGC axons (Monnier et al., 2002). In contrast to Ephrins however, the *in vivo* role of RGM remains unclear. To determine whether *RGM* does indeed play a role in the establishment of retinocollicular projections *in vivo* we decided to isolate the corresponding mouse gene and examine the neural phenotype of mice lacking *RGM* gene function.

We discovered three genes with homology to *cRGM* within the mouse genome. All three murine members of this protein family – mRGMa, mRGMb and mRGMc – show a carboxy terminal GPI-anchor consensus sequence, but the

efficiency of cell surface transport of the different family members is highly variable. The expression of *mRGMa* and *mRGMb* is largely confined to the nervous system where they are expressed in complementary patterns. In contrast, the most prominent expression of *mRGMc* is found in skeletal muscles. Analysis of *mRGMa* mutant mice demonstrates that the development of RGC projections from the retina to the colliculus and topographic mapping of these projections to defined anterior-posterior positions within the superior colliculus is normal. In contrast, ~ 50% of *mRGMa* mutant mice show defects in cephalic neural tube closure. Together, these findings identify a novel family of extracellular GPI anchored proteins in the mouse with homology to cRGM and reveal an unexpected role for *mRGMa* in the process of neural tube closure.

## 2.3 Results

### 2.3.1 Isolation of Three Genes in the Mouse Genome Homologous to *cRGM*

To isolate genes homologous to *cRGM* (Monnier et al., 2002) in the mouse genome, we searched the database for mouse expressed sequence tags (ESTs) and genomic sequences with a high degree of identity to *cRGM*. We found that the mouse genome contains three genes with homology to *cRGM* (in this paper now referred to as *cRGMa*). Mouse RGMa (*mRGMa*) is most closely related to *cRGMa* and shows an identity of 80% to *cRGMa* at the amino acid level (Figure 6A). The two more distantly related members of the RGM family of proteins, which we called *mRGMb* and *mRGMc*, show identities to *cRGMa* of 50% and 42%, respectively (Figure 6A). Additional evidence that *mRGMb* may be more closely related to *mRGMa* than *mRGMc* comes from an analysis of the organization of the respective genomic loci. The positions of intron-exon junctions as well as the sizes of introns are highly conserved between *mRGMa* (chromosome 7) and *mRGMb* (chromosome 17; data not shown). In addition, two homologous genes – chromodomain helicase DNA binding protein 1 (*CHD1*) and chromodomain helicase DNA binding protein 2 (*CHD2*) – are located in close proximity to *mRGMb* (*mRGMb/CHD1*) and *mRGMa* (*mRGMa/CHD2*) respectively, suggesting that *mRGMa* and *mRGMb* may have evolved by gene duplication. In contrast, the genomic organization of *mRGMc* is highly divergent to *mRGMa* or *mRGMb* (data not shown).

We found that like *cRGMa*, all three members of the mouse family of RGM proteins contain an amino terminal consensus signal peptide for targeting to the endoplasmic reticulum (Figure 6A, grey box) and a carboxy terminal GPI anchor



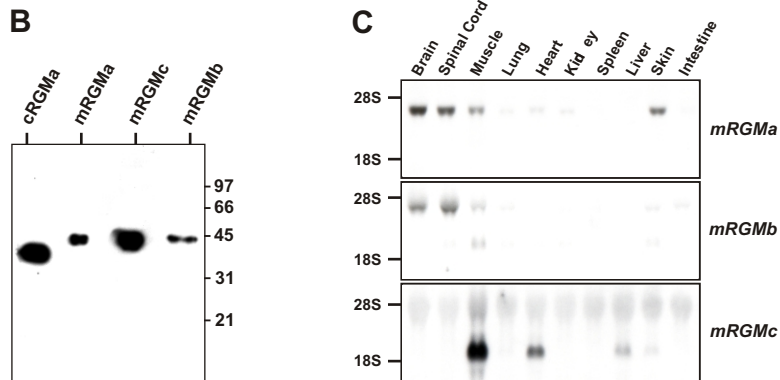


**Figure 6. Characterization of the murine RGM protein family.**

(A) Protein sequence alignment of cRGMa, mRGMa, mRGMb and mRGMc. Stars indicate identical amino acids, pink lines: intron-exon junctions, the grey box: predicted signal peptides, the blue box: potential integrin binding sites (RGD), green boxes: predicted N-glycosylation sites, the yellow box: mature carboxy terminal RGM fragments after full proteolytic cleavage and carboxy terminal GPI anchor addition (proteolytic cleavage sites indicated by arrowheads).

(B) Western blot analysis of supernatant collected from COS-7 cells transfected with carboxy terminally truncated Histidine-Myc labelled cRGMa, mRGMa, mRGMc and mRGMb detected with an anti-Myc antibody. MW standards are indicated to the right.

(C) Northern blot analysis on total RNA from a variety of postnatal day 3 (P3) mouse tissues as indicated, using *mRGMa*, *mRGMb* and *mRGMc* as probes.

consensus sequence (Figure 6A). However, the quality and score of the best site predicted for the addition of a GPI anchor varied significantly amongst the three mouse homologues of RGM and cRGMa (cRGMa: 7.93; mRGMa: 1.14; mRGMb: 2.72; mRGMc: 6.63), raising the possibility that not all members of the RGM family are processed by the addition of a carboxy terminal GPI anchor with the same efficiency. Since differential processing could affect the efficiency of protein targeting to the plasma membrane where GPI anchored proteins are usually localized to lipid rafts (Sharom and Lehto, 2002), we assessed the subcellular localization of cRGMa, mRGMa, mRGMb and mRGMc by transfecting full-length RGMs and a cDNA encoding nuclear  $\beta$ -galactosidase from a bicistronic mRNA into COS-7 cells. To label cell surface accumulated proteins, we incubated live transfected cells with primary antibodies specific to individual RGM family members before fixation and permeabilization of cells. For the identification of transfected cells we stained them with an antibody to  $\beta$ -galactosidase after fixation and permeabilization. While strong cell surface labeling was detected on cells transfected with cRGMa and mRGMc, mRGMa expressing cells were labeled less intensely, and very low if any staining was detected on the plasma membrane of cells transfected with mRGMb (Figure 7A-D). When transfected cells were fixed and permeabilized before incubation with the primary antibody, all four RGMs displayed strong labeling (Figure 7E-H). However, mRGMb protein was highly concentrated in the perinuclear endoplasmic reticulum/Golgi compartment, consistent with the observation that mRGMb protein is not efficiently targeted to the cell surface (Figure 7G). To determine whether this differential subcellular distribution was also found in neurons *in vivo* we electroporated embryonic day 3 (E3) chick spinal cords with vectors expressing mRGMa, mRGMb or mRGMc. Whereas mRGMa and mRGMc proteins were

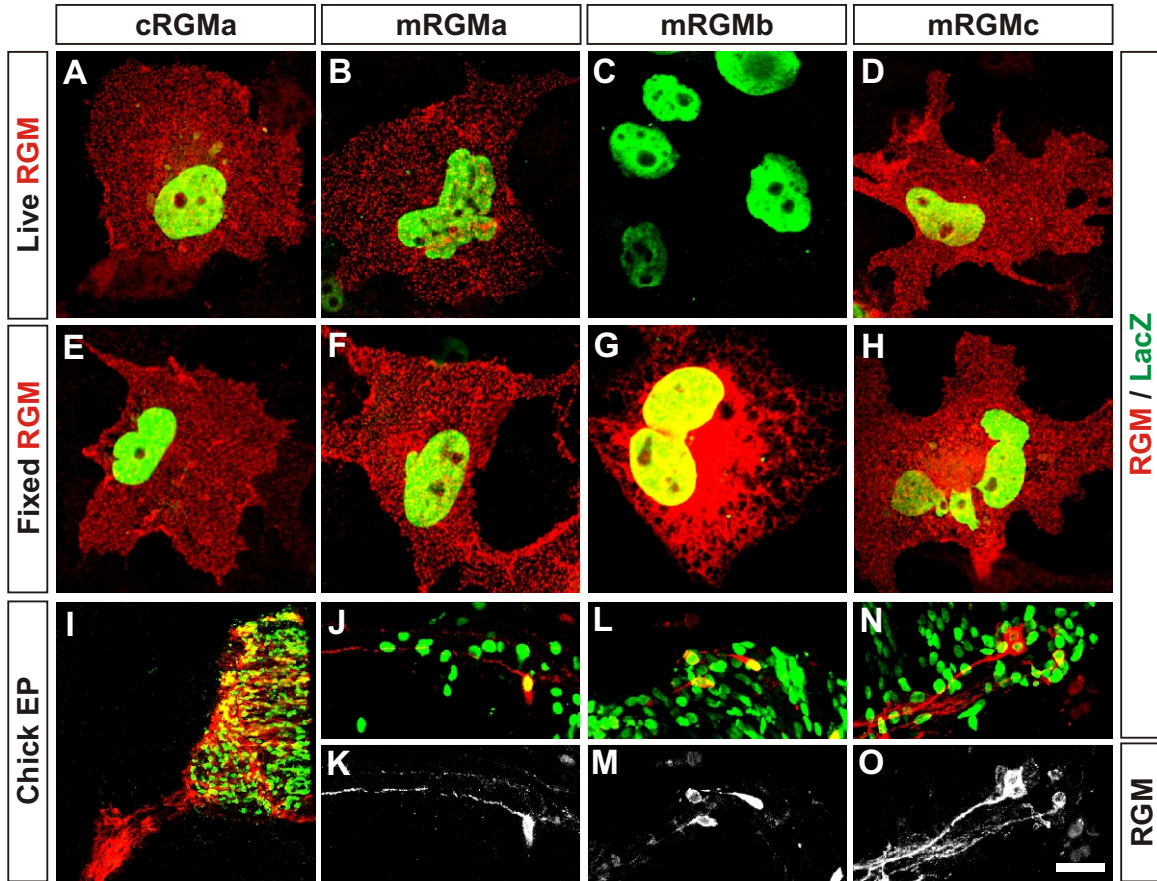


### Figure 7. Differential Cell Surface Targeting of mRGMs.

(A-H) Expression of full length cDNAs coding for *cRGMa* (A, E), *mRGMa* (B, F), *mRGMb* (C, G) and *mRGMc* (D, H) and  $\beta$ -galactosidase on the same plasmid using an IRES in COS-7 cells. Transfected COS-7 cells are identified by staining for  $\beta$ -galactosidase after fixation and permeabilization of cells (green). RGMs (red) are detected either before fixation and permeabilization of cells (A-D) to detect cell surface accumulated RGM or after fixation and permeabilization of cells (E-H) to detect all RGM in transfected cells.

(I-O) Chick spinal cords electroporated with cDNAs coding for *cRGMa* (I), *mRGMa* (J, K), *mRGMb* (L, M) and *mRGMc* (N, O) and  $\beta$ -galactosidase on the same plasmid using an IRES. Sections were stained for either RGM (red) and  $\beta$ -galactosidase (green; I, J, L, N) or RGM (white; K, M, O). Note extensive labeling of axonal processes in (I, J, K, N, O) and predominant cell body and proximal axonal labeling in (L, M).

Scale bar: (A-H)=15mm, (I)= 150mm, (J-O)=60mm.

expressed and efficiently transported into neuronal processes by embryonic day 5 (E5), mRGMb appeared to be concentrated predominantly in neuronal cell bodies and proximal axonal processes, consistent with our findings in transfected COS-7 cells (Figure 7I-O).

It has been shown previously that in addition to the proteolytic processing of the amino terminal signal peptide, cRGMa is cleaved once more to yield two proteolytic fragments – an amino terminal fragment containing an integrin binding RGD motif and a carboxy terminal GPI anchored fragment (Monnier et al., 2002). To determine whether this is also the case for mRGM proteins, we expressed mRGMa, mRGMb and mRGMc in COS-7 cells replacing the GPI anchor consensus sequence by a Myc labeled hexahistidine tag. The molecular weights of these mRGM proteins collected from COS-7 cell supernatants were ~42kD whereas the molecular weight of cRGMa expressed using the same strategy was ~35kD (Figure 6B). Nevertheless, amino terminal end sequencing using Edman degradation showed identical cleavage sites within cRGMa, mRGMa, mRGMb and mRGMc (Figure 6A). The difference in the detected molecular weight is most likely due to glycosylation (Figure 6A, green boxes) or other posttranslational modifications. In summary, the three murine members of the RGM family are proteolytically processed in a manner analogous to cRGMa, but whereas mRGMa and mRGMc are transported to the plasma membrane, mRGMb appears to be predominantly accumulated in intracellular compartments.

### 2.3.2 Differential Expression of *mRGM* Family Members During Development

Using a Northern blot analysis we found that the most abundant expression of *mRGMa* and *mRGMb* was detected in the nervous system whereas *mRGMc* was expressed predominantly in striated muscle tissues, with the highest level of expression detected in skeletal muscles (Figure 6C). To determine the specific sites of expression of *mRGMa* and *mRGMb* during embryonic development, we performed *in situ* hybridization experiments. Both *mRGMa* and *mRGMb* are expressed specifically at the tips of the neural folds of mouse embryos from E8 to E9, coincident with the expression of *mEphrinA5* (Figure 8A-C; Holmberg et al., 2000). Later, both *mRGMa* and *mRGMb* are expressed at discrete sites in the developing CNS, but in non-overlapping and highly complementary patterns. *mRGMa* expression in the brain is found surrounding the ventricles, whereas *mRGMb* expression is often found laterally apposed to *mRGMa* in early postmitotic neurons (e.g. E12.5 spinal cord, Figure 8E-G; E14.5 thalamus, Figure 8H-K). In addition, a high level of *mRGMb* expression was also detected in developing dorsal root ganglia (DRG; Figure 8F, G) and at later developmental stages, *mRGMa* and *mRGMb* are also expressed in distinct nuclei of the brain (E17.5; data not shown). Consistent with the data from our Northern blot analysis, expression of *mRGMc* is confined to striated muscles where it is found in both the muscles of the extremities, (Figure 8L-O) and of the face (Figure 8J, K). No expression of *mRGMc* was detected in embryonic brain or spinal cord (Figure 8J, data not shown).

In summary, the most striking feature revealed by this *in situ* hybridization analysis was an essentially complete lack of overlap and a strong complementarity in the expression of *mRGMa* and *mRGMb* in the developing nervous system. Whereas

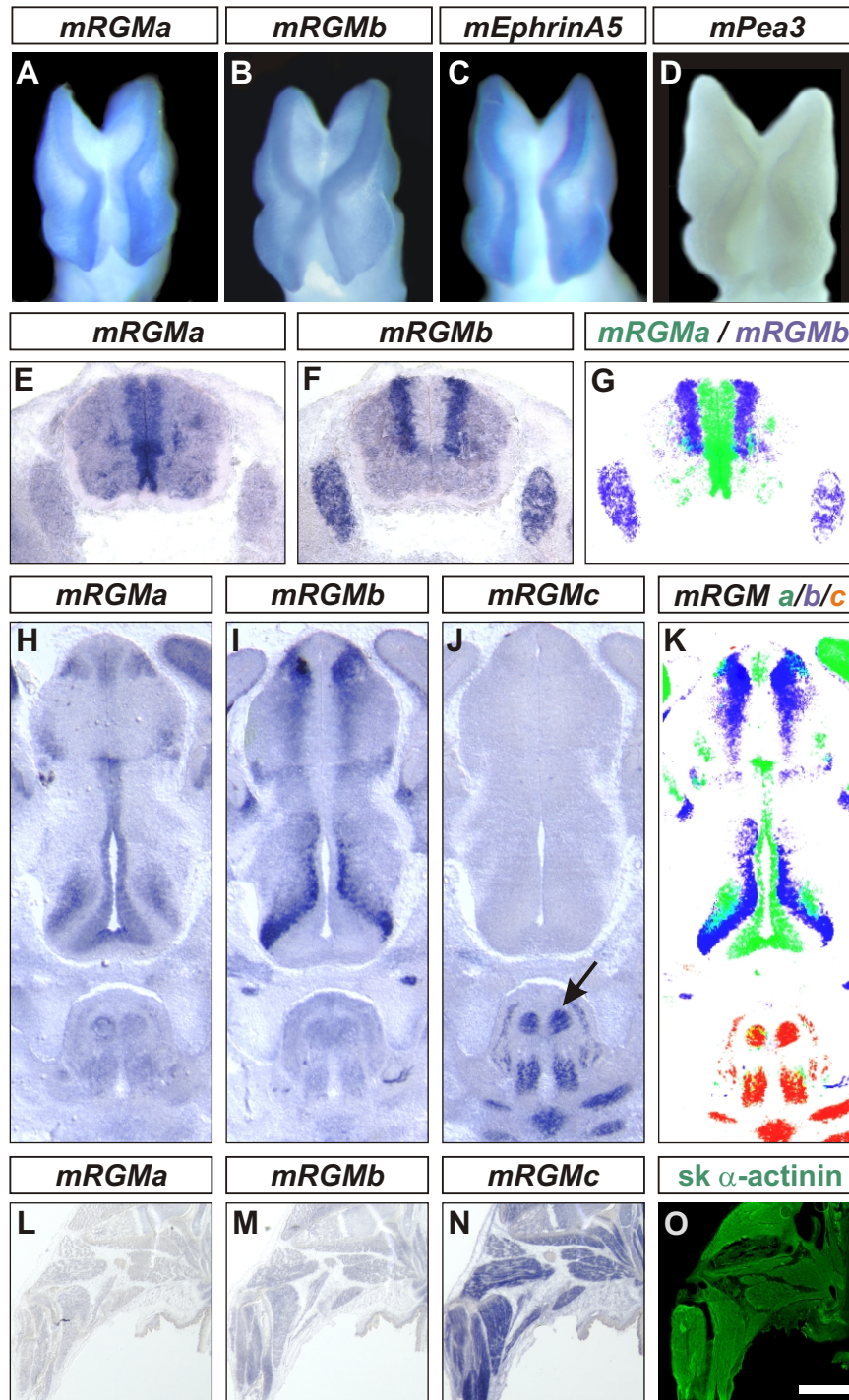


**Figure 8. Embryonic Expression of *mRGMs* in Complementary Patterns.**

(A-D) Whole-mount *in situ* hybridization of E8.5 mouse embryos using *mRGMa* (A), *mRGMb* (B), *mEphrinA5* (C) and *mPea3* (D) as probes. Note absence of *mPea3* expression from the tips of neural folds.

(E-G) Expression of *mRGMa* (E) and *mRGMb* (F) in E12.5 mouse spinal cord and dorsal root ganglia detected by *in situ* hybridization on transverse sections. (G) shows an artificial overlay (*mRGMa* in green, *mRGMb* in blue) to demonstrate complementarity of expression patterns.

(H-K) Expression of *mRGMa* (H), *mRGMb* (I) and *mRGMc* (J) in E14.5 mouse thalamus by *in situ* hybridization on coronal brain sections. Arrow in (J) points to signal of *mRGMc* in skeletal muscles. (K) shows an artificial overlay (*mRGMa* in green, *mRGMb* in blue and *mRGMc* in red) to demonstrate complementarity of expression patterns.

(L-O) Expression of *mRGMa* (L), *mRGMb* (M) and *mRGMc* (N) by *in situ* hybridization and skeletal  $\alpha$ -actinin (O) by immunocytochemistry on E17.5 mouse hindlimbs.

Scale bar: (A-D)=0.15mm, (E-G)=0.35mm, (H-K)=0.32mm, (L-O)=1.8mm.

*mRGMa* expression is consistently found in subventricular zones surrounding the ventricles, *mRGMb* expression is often found laterally apposed to *mRGMa* and *mRGMc* is expressed predominantly in skeletal muscles.

### 2.3.3 Expression Analysis of Mouse *RGMs* in the Visual System

To address which of the mouse *RGM* family members might play a dominant role in the development of the retinocollicular system, we performed *in situ* hybridization experiments in the mouse superior colliculus at P0, a stage just before targeting of RGC axons to defined anterior-posterior positions occurs (Simon and O'Leary, 1992). We found that *mRGMa*, the closest homologue of *cRGMa*, was prominently expressed in the superior colliculus at this stage (Figure 9A, D). However, in contrast to chick (Monnier et al., 2002; Figure 9F), we failed to detect a gradient in the level of *mRGMa* expression along the anterior-posterior axis of the superior colliculus (Figure 9A, D). In addition, and as described previously, *mEphrinA5* was expressed in a clear anterior-posterior gradient in the mouse superior colliculus (Figure 9B, E; Frisen et al., 1998; Feldheim et al., 2000). At earlier developmental stages (E15.5), *mRGMa* is also expressed prominently in the superior colliculus, whereas only faint expression of *mRGMb* was detected (Figure 9G-I). In the retina, *mRGMb* but not *mRGMa* or *mRGMc* is expressed in RGCs (Figure 9J-L). Thus the *mRGM* family member expressed most prominently in the superior colliculus, at a time just before targeting of RGC axons to defined anterior-posterior positions occurs, is *mRGMa*.

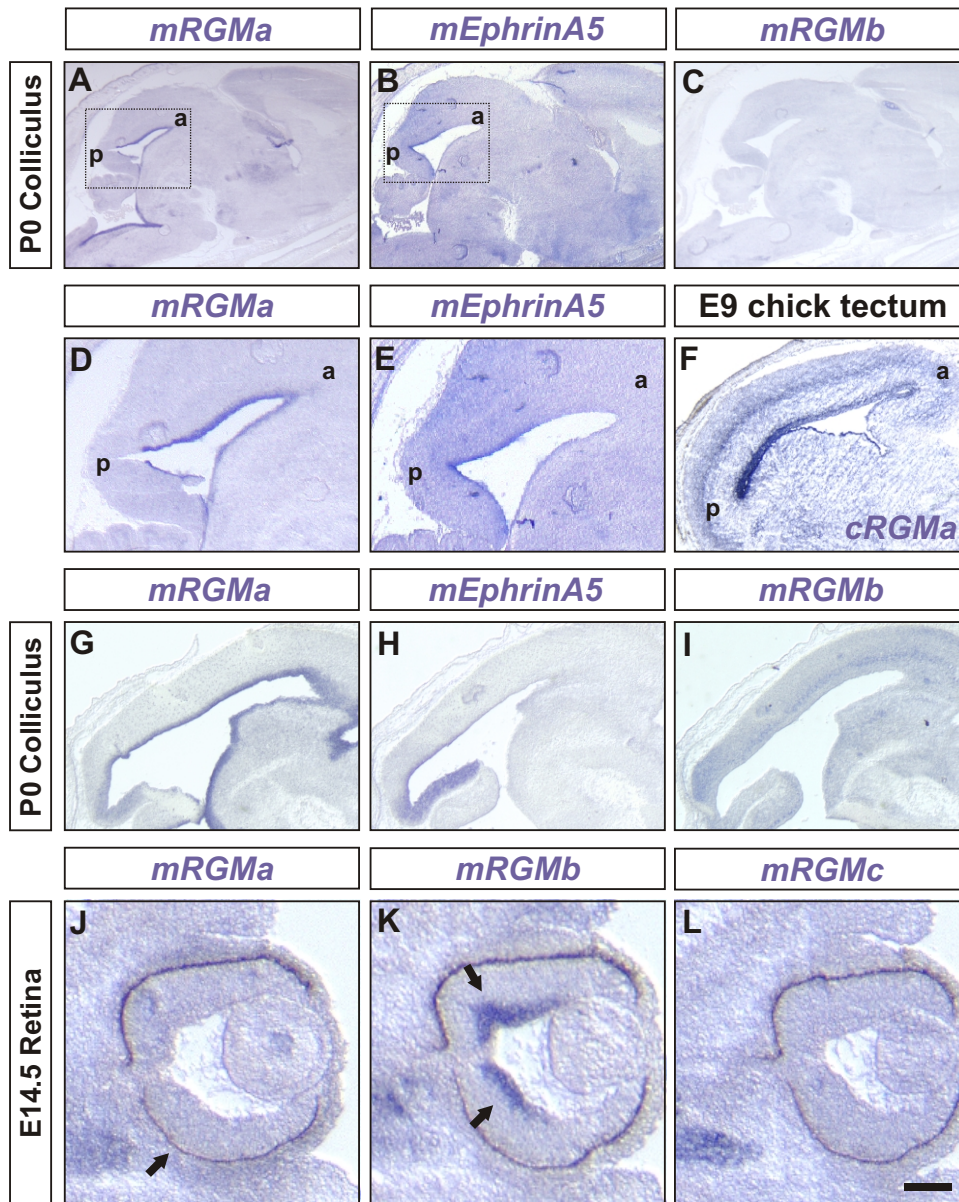


**Figure 9. Expression of *mRGMs* in the developing retinocollicular system.**

(A–E) Expression of *mRGMa* (A, D), *mEphrinA5* (B, E), and *mRGMb* (C) in the superior colliculus of P0 sagittal brain sections detected by *in situ* hybridization. Boxes in (A) and (B) indicate regions shown in higher magnification in (D) and (E). a, anterior; p, posterior.

(F) Expression of *cRGMa* in E9 chick tectum detected by *in situ* hybridization.

(G–I) Expression of *mRGMa* (G), *mEphrinA5* (H), and *mRGMb* (long exposure to detect faint expression; I) in the superior colliculus of E15.5 sagittal brain sections detected by *in situ* hybridization.

(J–L) Expression of *mRGMa* (J), *mRGMb* (K), and *mRGMc* (L) in E14.5 retina detected by *in situ* hybridization. Note the expression of *mRGMb* in RGCs (K, arrows). Pigment epithelium is marked by an arrow in (J).

Scale bar: (in L) (A–C)=1mm; (D, E)= 0.4 mm; (F)= 0.85 mm; (G–I)= 0.25 mm; ( J–L)= 0.13 mm.



#### 2.3.4 Generation of *mRGMa* Mutant Mice

To investigate the function of *mRGMa* in retinocollicular topographic mapping, we performed homologous recombination in embryonic stem cells to eliminate *mRGMa* gene function. We replaced the exon encoding the amino terminal signal peptide responsible for targeting mRGMa protein to the endoplasmic reticulum with a TK-Neomycin cassette (Figure 10A). The transfection of a cDNA construct coding for the remaining carboxy terminal exons of mRGMa into COS-7 cells showed that none of the transfected (eGFP<sup>+</sup>) COS-7 cells expressed the carboxy terminal fragment of mRGMa, thus demonstrating that all cell-surface targeted mRGMa protein is eliminated with this targeting strategy (Figure 10E-H).

Successful homologous recombination in embryonic stem cells using this targeting construct was detected at a very low frequency (~1:2000). Heterozygous *mRGMa*<sup>+/-</sup> mice were phenotypically normal and interbreeding resulted in the generation of homozygous viable *mRGMa*<sup>-/-</sup> mice (Figure 10I; data not shown). Both PCR from genomic DNA as well as RT-PCR from total RNA of homozygous *mRGMa*<sup>-/-</sup> mice showed successful elimination of the exon encoding the signal peptide of mRGMa (Figure 10D). While *mRGMa*<sup>-/-</sup> mice were detected at postnatal stages, the frequency of recovered viable mutants was non-Mendelian (Figure 10I).

#### 2.3.5 Mutation in *mRGMa* Results in an Exencephalic Phenotype *in Utero*

To assess whether a fraction of *mRGMa*<sup>-/-</sup> embryos die *in utero*, we examined the frequency and appearance of *mRGMa*<sup>-/-</sup> embryos at various prenatal stages. At E16.5, we recovered two phenotypically different types of *mRGMa*<sup>-/-</sup> embryos: ~ 50% of *mRGMa*<sup>-/-</sup> embryos had an appearance indistinguishable from wild type embryos

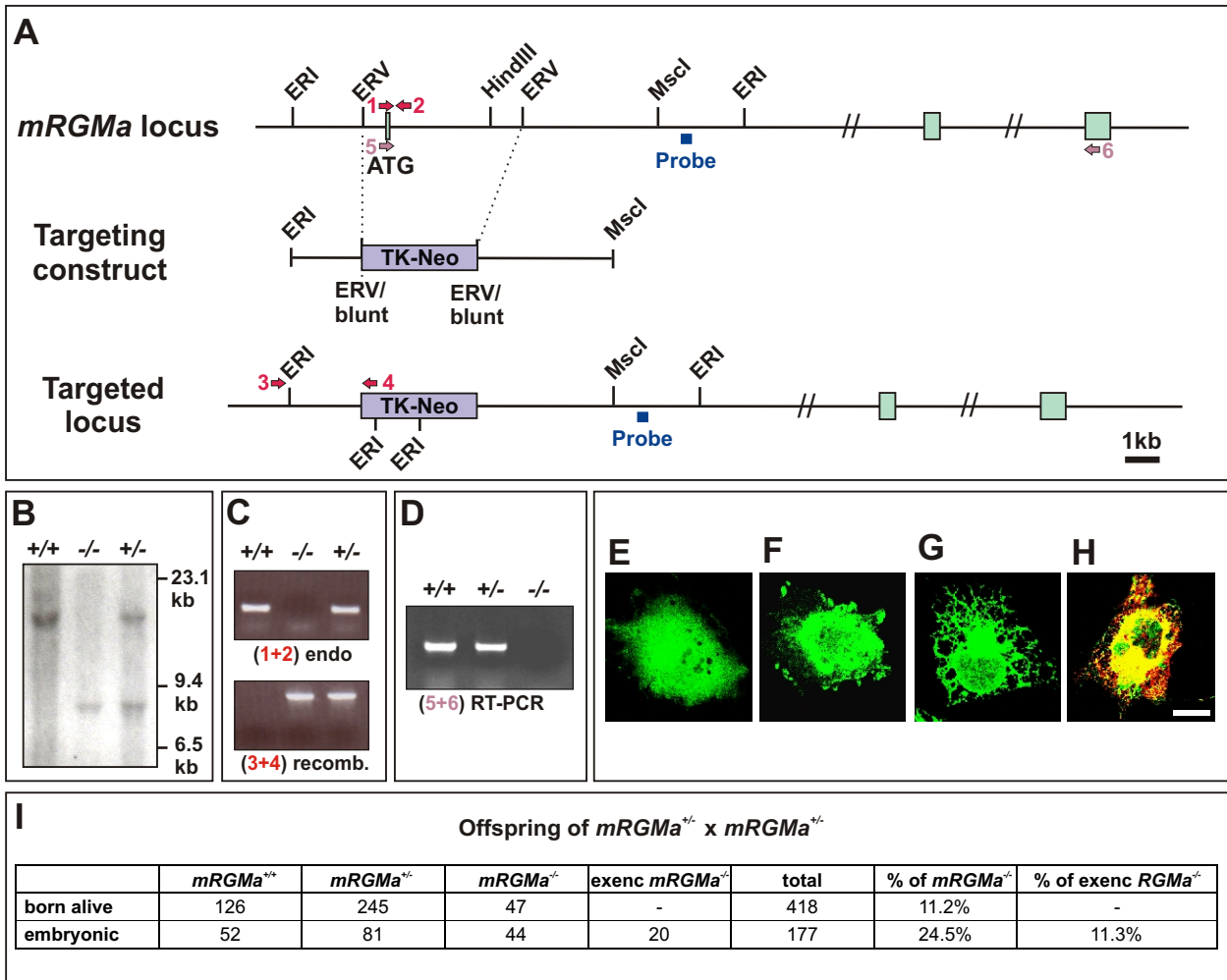


### Figure 10. Generation of $mRGMa$ Mutant Mice.

(A-C) Targeting strategy for homologous recombination in ES cells to eliminate  $mRGMa$  gene function. An EcoRV fragment including the exon containing the methionine of the signal peptide for targeting of  $mRGMa$  to the endoplasmic reticulum was replaced by a TK-Neomycin resistant cassette (purple). Coding exons for  $mRGMa$  are indicated in green, the probe used for genomic Southern analysis (B) in blue, oligonucleotides to determine absence of methionine containing exon in red (arrows 1 and 2; C), oligonucleotides to verify 5' homologous recombination in red (arrows 3 and 4; C) and oligonucleotides used for RT-PCR in pink (arrows 5 and 6; D).

(D) RT-PCR analysis to verify absence of exon containing signal peptide on  $mRGMa$  mRNA in  $mRGMa$  mutant mice (arrows 5 and 6 in A).

(E-H) Immunocytochemistry of COS-7 cells transfected with a cDNA construct containing  $mRGMa$  exons 3' of the targeted exon and eGFP on a bicistronic plasmid (E, F) or a cDNA construct containing an additional artificial in-frame amino terminal methionine and an eGFP containing a signal peptide for targeting to the endoplasmic reticulum (G, H). Cells were stained for eGFP (green) and  $mRGMa$  (red). In (E, G), incubation of cells with antibody to  $mRGMa$  was performed before fixation and permeabilization of cells to label cell-surface associated  $mRGMa$ . In (F, H), fixation and permeabilization of cells was performed before incubation with antibodies. Note that even the addition of an artificial amino terminal methionine in frame with the carboxy terminal  $mRGMa$  exons did not result in cell-surface exposed  $mRGMa$  after transfection (G, H). Scale bar = 15mm.

(I) Statistical analysis of the offspring recovered from matings of  $mRGMa^{+/-}$  breeder pairs. Exencephalic  $mRGMa^{-/-}$  embryos are indicated as exenc in the table.

(Figure 10I; data not shown) whereas in the remaining ~ 50% of *mRGMa*<sup>-/-</sup> embryos, the brain was exposed to the exterior environment and cranial skull tissue was absent (Figure 11D). Dissection of the brains from these affected *mRGMa*<sup>-/-</sup> embryos revealed that the ventral side of the brains as well as the brainstem and spinal cord were anatomically normal when compared to wild type brains and spinal cords (Figure 11E, F). In contrast, dorsal and lateral views of the brain from affected *mRGMa*<sup>-/-</sup> embryos revealed major defects in the morphogenesis of dorsal brain structures (Figure 11B, E; data not shown).

In order to define the nature of the observed defects more precisely, we performed a time course analysis at different embryonic stages. At E8, all *mRGMa*<sup>-/-</sup> embryos were indistinguishable from wild type embryos (data not shown). By E8.5 to E9, when the closure of neural folds in wild type embryos has been initiated at both cephalic and spinal cord levels (Theiler, 1989), ~ 50% of *mRGMa*<sup>-/-</sup> embryos did not show signs of efficient cephalic closure leading to a lack of closure at the cephalic level by E10.5 (Figure 11G-J; data not shown). In contrast, the closure of the neural folds at the level of the spinal cord was never affected in *mRGMa*<sup>-/-</sup> embryos (Figure 11I, J; data not shown). This defect has previously been described as exencephaly (Harris and Juriloff, 1997). Exencephaly is caused by a failure of the cephalic neural folds to fuse, resulting in an exvagination of the developing cephalic tissue at later developmental stages when many neurons are born and brain size increases (Harris and Juriloff, 1997). By E14.5, exencephalic *mRGMa*<sup>-/-</sup> embryos show a pronounced exposure of the developing brain structures and third ventricle to the external environment, as well as a lack of development of cranial skull tissue (Figure 11K-N). In addition, the exencephalic tissue of *mRGMa*<sup>-/-</sup> embryos was highly vascularized

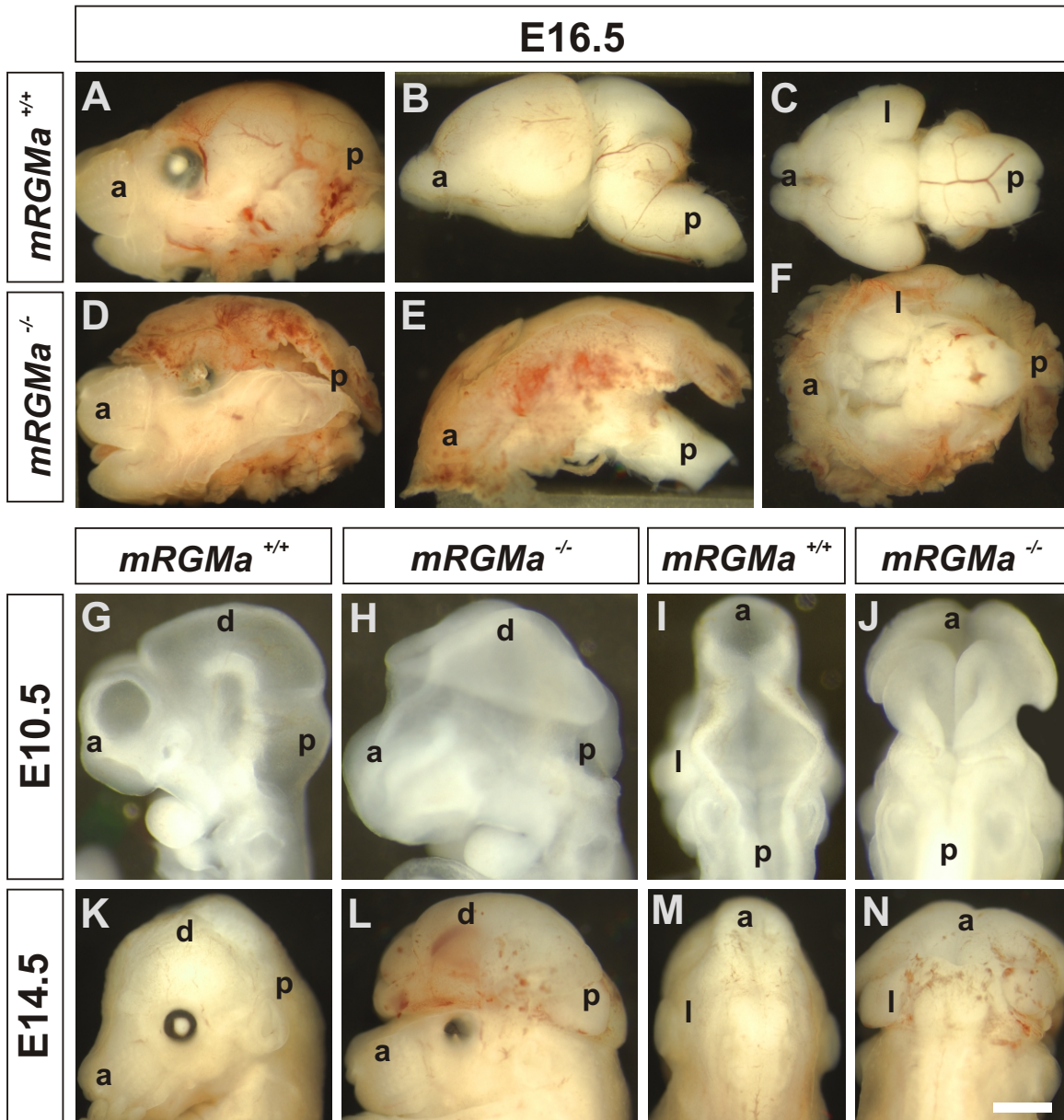


**Figure 11. *mRGMa* Mutant Mice Show an Exencephalic Phenotype.**

(A-F) Lateral (A, B, D, E) or ventral (C, F) view of E16.5 heads (A, D) or dissected brains (B, C, E, F) from *mRGMa*<sup>+/+</sup> (A-C) and exencephalic *mRGMa*<sup>-/-</sup> (D-F) embryos.

(G-J) Lateral (G, H) or dorsal (I, J) head view of E10.5 *mRGMa*<sup>+/+</sup> (G, I) and *mRGMa*<sup>-/-</sup> (H, J) embryos.

(K-N) Lateral (K, L) or dorsal (M, N) head view of E14.5 *mRGMa*<sup>+/+</sup> (K, M) and *mRGMa*<sup>-/-</sup> (L, N) embryos

a, anterior; p, posterior; d, dorsal; l, lateral.

Scale bar: (A, D)=1.5mm, (B, E)=1mm, (C, F)=1.1mm, (G-J)=0.6mm, (K-N)=1.2mm

(Figure 11E, L), another feature frequently observed in exencephalic brains (Harris and Juriloff, 1997). Exencephalic *mRGMa*<sup>-/-</sup> embryos removed surgically immediately prior to birth (E19) displayed reflexive motion and breathing behaviour but died shortly thereafter (data not shown). In contrast, exencephalic *mRGMa*<sup>-/-</sup> embryos delivered by natural birth were stillborn and anencephalic (lacking brain tissue entirely), presumably due to a lack of protection of the brain by the overlying skull during the process of birth (data not shown). These findings suggest that an early function of mRGMA at the site of neural tube closure where both *mRGMa* and *mRGMb* are expressed at this time may be responsible for the exencephalic phenotype observed in ~ 50% of *mRGMa*<sup>-/-</sup> embryos.

### **2.3.6 Exencephalic *mRGMa* Mutants Show no Defects in Early Brain Patterning**

Does the absence of *mRGMa* lead to defects in neuronal patterning, cell proliferation or apoptosis? We first performed BrdU pulse labeling experiments to assess proliferation and neuronal differentiation in *mRGMa*<sup>-/-</sup> embryos. We found that the amount of cellular proliferation was not obviously changed in either exencephalic or anatomically normal *mRGMa*<sup>-/-</sup> embryos when compared to wild type brains or spinal cords (Figure 12A-H; data not shown). However, due to the lack of brain closure in exencephalic *mRGMa*<sup>-/-</sup> embryos proliferating cells in dorsal brain structures now appeared on the outside of the brain whereas GAP43<sup>+</sup> differentiating neurons were facing the lumen (Figure 12B, D, F, H). BrdU<sup>+</sup> and GAP43<sup>+</sup> cells were not intermingled in exencephalic *mRGMa*<sup>-/-</sup> embryos, indicating that *mRGMa* is not required for initial segregation of proliferating cells and differentiating neurons in the brain. We also did not find defects in cellular proliferation and pan-neuronal differentiation in spinal cords of *mRGMa*<sup>-/-</sup> embryos (data not shown). Similarly, many

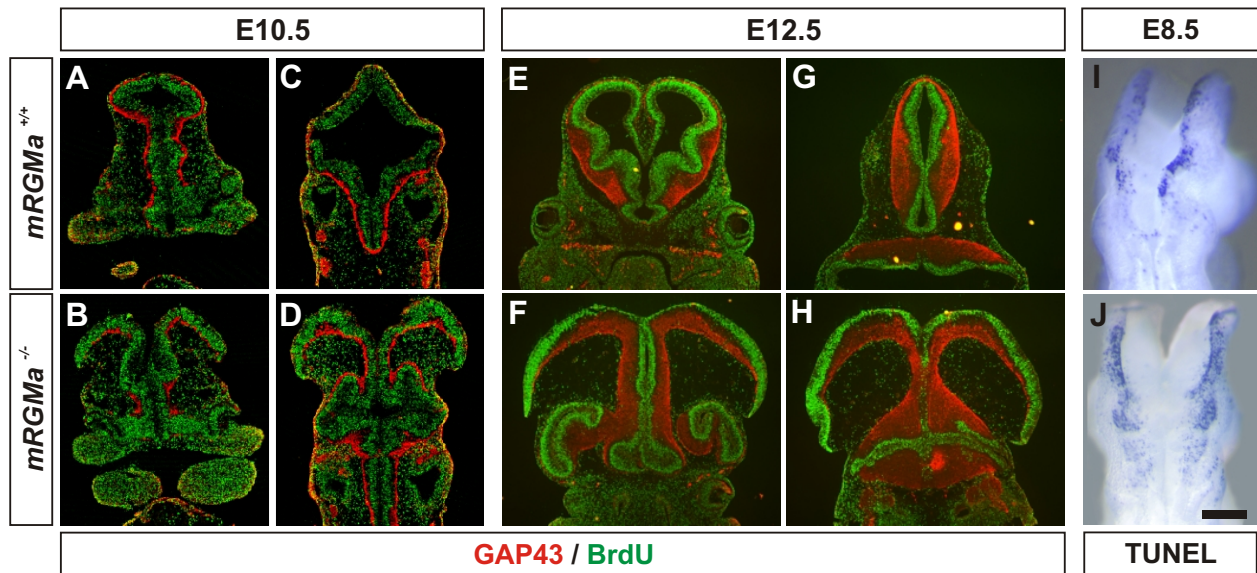


**Figure 12. Exencephalic *mRGMa* Mutant Embryos Do Not Show Defects in Proliferation in the Brain.**

(A-H) Immunocytochemical analysis (GAP-43: red; BrdU: green) of coronal brain sections from E10.5 (A-D) and E12.5 (E-H) BrdU pulse labelled *mRGMa*<sup>+/+</sup> (A, C, E, G) and exencephalic *mRGMa*<sup>-/-</sup> (B, D, F, H) embryos.

(I, J) Whole-mount TUNEL labeling of E8.5 *mRGMa*<sup>+/+</sup> (I) and exencephalic *mRGMa*<sup>-/-</sup> (J) embryos in dorsal view.

genes expressed in defined cell types of the brain and spinal cord were expressed normally in *mRGMa*<sup>-/-</sup> embryos (data not shown). In addition, no aberrant increase or decrease in apoptotic cell death could be observed in cephalic neural folds of exencephalic *mRGMa*<sup>-/-</sup> embryos at E8.5 (Figure 12I, J). Together these findings suggest that the exencephalic phenotype observed in a subpopulation of *mRGMa*<sup>-/-</sup> embryos is most likely not caused by defects in neuronal patterning or cell proliferation, nor does the exencephalic phenotype caused by absence of *mRGMa* lead to such defects.

### **2.3.7 Viable *mRGMa* Mutants Show no Defects in Retinocollicular Projections**

To determine whether the surviving *mRGMa*<sup>-/-</sup> mice show defects in the anterior-posterior mapping of retinocollicular projections as suggested from *in vitro* studies in the developing chick embryo (Monnier et al., 2002), we first injected the lipophilic tracer Dil into the eyes of postnatal day 0 (P0) mice, attempting to label many RGC axons projecting from the retina to the brain. In viable *mRGMa*<sup>-/-</sup> as in wild type mice, the entire superior colliculus was filled with axons and, as expected at this developmental stage (Simon and O'Leary, 1992), a significant number of axons also projected into the inferior colliculus (n=5; Figure 13A, B).

By postnatal day 8 (P8) RGC axons within the superior colliculus have segregated into defined anterior-posterior positions, reaching topographic positions found in the mature superior colliculus (Simon and O'Leary, 1992; Frisen et al., 1998). To determine whether in viable *mRGMa*<sup>-/-</sup> mice, retinocollicular axonal projections terminate in the appropriate anterior-posterior position within the superior colliculus we focally injected Dil into specific regions of the retina of postnatal day 9

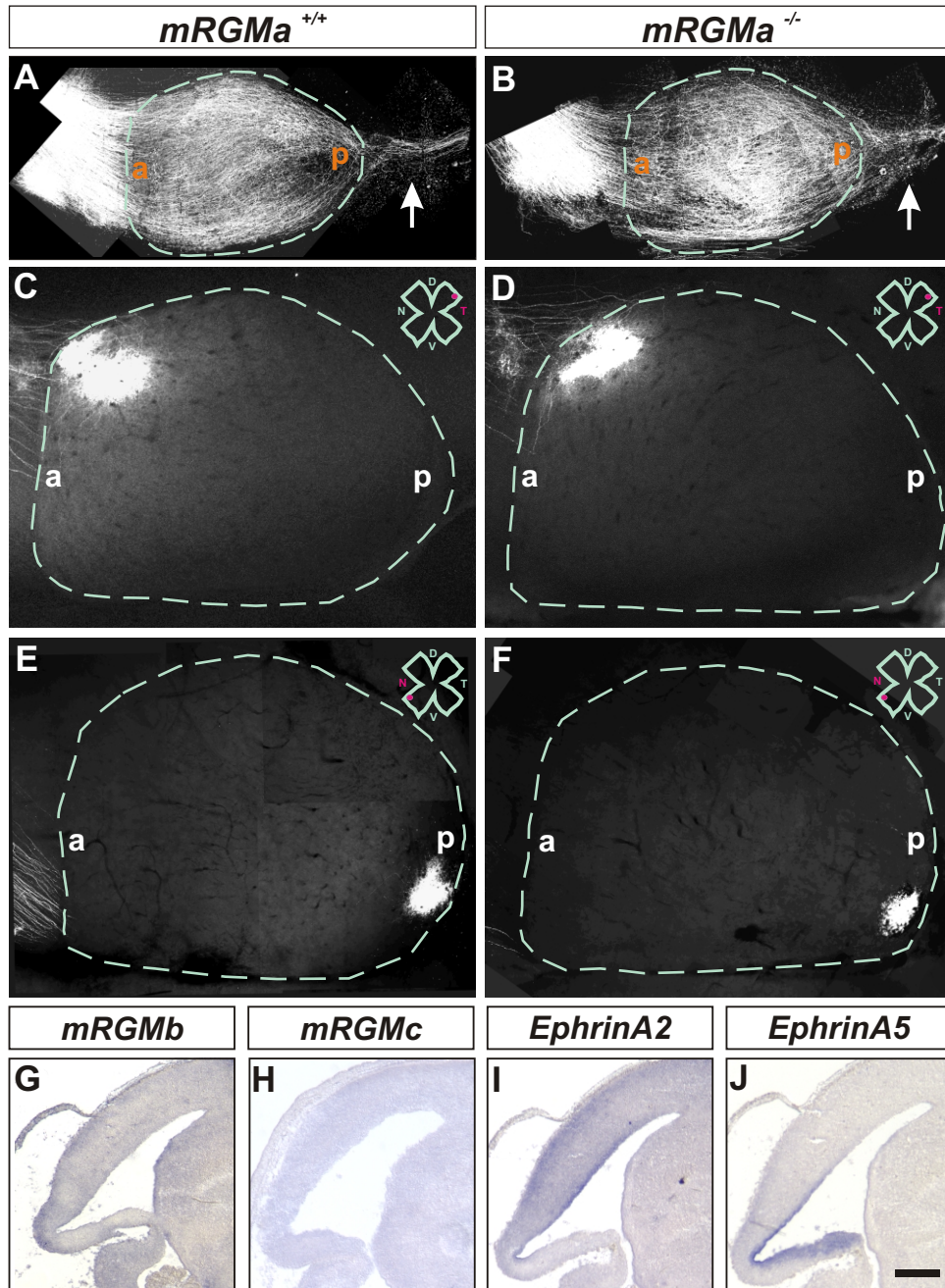


**Figure 13. Lack of Retino-Collicular Projection Phenotype in *mRGMa* Mutant Mice.**

(A, B) Dorsal views of superior and inferior colliculi from *mRGMa*<sup>+/+</sup> (A) and *mRGMa*<sup>-/-</sup> (B) mice after anterograde Dil labeling from the retina at P0 to label many RGC axons. Green dashed line outlines the superior colliculus (a=anterior, p=posterior), arrows point to RGC axons projecting to the inferior colliculus.

(C-F) Anterograde Dil labeling from the temporal (C, D) or nasal (E, F) retina to the superior colliculus (outlined by green dashed lines) after focal Dil injection into the retina of *mRGMa*<sup>+/+</sup> (C, E) and *mRGMa*<sup>-/-</sup> (D, F) mice at P10 (injection point in the retina indicated by red dot in the top right corner. (T=temporal, N=nasal, D=dorsal, V=ventral).

(G-J) Expression of *mRGMb* (G), *mRGMc* (H), *EphrinA2* (I) and *EphrinA5* (J) in superior colliculi of E16.5 sagittal brain sections from *mRGMa*<sup>-/-</sup> mice detected by *in situ* hybridization.



to 12 (P9-P12) animals. In this analysis we first focused our attention on injections into the temporal RGC population known to normally project to the anterior and to be repelled by the posterior superior colliculus (Walter et al., 1987; Godement and Bonhoeffer, 1989; Roskies and O'Leary, 1994). Analysis of the projections of these Dil<sup>+</sup> temporal RGC axons showed a single focal termination zone, in the predicted anterior posterior position of both wild type and viable *mRGMa*<sup>-/-</sup> mice (n≥15, Figure 13C, D). In addition, focal injections of Dil into the nasal retina of both wild type and viable *mRGMa*<sup>-/-</sup> mice revealed that these axons also project and terminate normally in the posterior superior colliculus (n=10, Figure 13E, F). To assess whether the lack of phenotype observed in retinocollicular projections of viable *mRGMa*<sup>-/-</sup> mice could be due to compensatory upregulation of either other *mRGM* family members, or members of the *Ephrin* family of genes, we performed *in situ* hybridization experiments. We found that expression of *mRGMb*, *mRGMc*, *Ephrin-A2*, *Ephrin-A5* in the superior colliculus of *mRGMa*<sup>-/-</sup> mice was not altered when compared to wild-type littermates (Figure 13G-J). Taken together these findings suggest that the lack of *mRGMa* gene function does not seem to impair anterior-posterior mapping of RGC axons to the superior colliculus.

## 2.4 Discussion

In this study we found that *cRGMa* is a member of a novel family of GPI-anchored proteins of which we identified and characterized three murine members: *mRGMa*, *mRGMb* and *mRGMc*. Two members of this gene family are expressed predominantly in the developing nervous system in non-overlapping and distinct expression patterns (*mRGMa* and *mRGMb*) whereas the third member is expressed most abundantly in skeletal muscles (*mRGMc*). Previous *in vitro* studies in the chick have suggested that *cRGMa* may play a role in the establishment of appropriate anterior-posterior RGC termination zones within the tectum. Our functional studies in the mouse now show that *mRGMa* mutant mice do not exhibit defects in the development of topographically appropriate projections in the anterior-posterior dimension of the superior colliculus. Instead, a significant proportion of *mRGMa* mutant mice show an exencephalic defect due to failure of the cephalic neural tube to close during development. We will discuss these findings in the context of (1) the distinct sites of expression and subcellular localization of different RGM family members and (2) the *in vivo* function of *mRGMa* in the developing mouse nervous system.

### 2.4.1 Identification of a Novel Family of GPI-Anchored Proteins Homologous to *cRGMa*

The identification of three genes homologous to *cRGMa* in the mouse genome has allowed us to study the precise developmental time course of expression, subcellular targeting and proteolytic processing of these proteins. Two members of

this gene family – *mRGMa* and *mRGMb* – show abundant expression in the developing mouse nervous system. It is interesting to note that the two genes expressed in the nervous system appear to have evolutionarily arisen by gene duplication. Preliminary evidence suggests that there is a homologue of *mRGMb* in the chick genome with an expression pattern confined to the nervous system (R. Salie, V. Niederkofler, and S. Arber, unpublished observations), indicating that this gene duplication must have occurred evolutionarily earlier than in the chick. A striking feature we observed in the expression of *mRGMa* and *mRGMb* within the nervous system is that their sites of expression are highly distinct and non-overlapping. While *mRGMa* is consistently expressed in ventricular zones where proliferating cells are found, the expression of *mRGMb* is almost exclusive to domains where early postmitotic neurons are found and not in ventricular zones. In addition to these sites of expression, distinct groups of postmitotic neurons also express *mRGMa* or *mRGMb* in non-overlapping patterns. In contrast, the third member of the family (*mRGMc*) is expressed in skeletal muscles and is evolutionarily more distantly related to *mRGMa* and *mRGMb*. Given the function of *mRGMa* in controlling the process of alignment of dorsal neural folds ultimately leading to neural tube closure, it is tempting to speculate that *mRGMc* might be involved in the process of myogenesis where mononucleated myoblasts fuse to form multinucleated myotubes. Consistent with this idea, *mRGMc* expression is upregulated during the process of myogenic differentiation *in vitro* (V. Niederkofler, R. Salie, and S. Arber, unpublished observations).

All three mouse homologues of *cRGMa* have predicted GPI anchor consensus sequences and undergo proteolytic cleavage at several sites within the protein

raising the question of the subcellular localization of the mature mRGM proteins. Our analysis revealed that there is an internal cleavage site within all three mRGM proteins that is highly conserved in sequence between the three mRGM members and cRGMa. This internal protein cleavage produces two fragments, one amino-terminal fragment containing an integrin-binding RGD site and a carboxy terminal fragment with a GPI anchor consensus site. To our knowledge, the sequence of this cleavage site has not been previously described in other proteins and it will be interesting to determine which protease(s) recognize(s) this cleavage site and whether similar proteolytic cleavage sites are present in other proteins. In addition, such a protease may be expressed differentially in different cell types leading to variable efficiencies in proteolytic processing depending on the amount and activity of protease present in a given cell type.

In contrast to the proteolytic cleavage reactions in the amino-terminal region detected in all mRGM proteins, subcellular targeting of different mRGM members to the cell surface does not occur with equal efficiency for all RGM family members. While mRGMc is as efficiently targeted to the cell surface as cRGMa, less mRGMa and almost no mRGMb appears to reach the cell surface. This differential subcellular localization of the RGM family of proteins could be due to differential efficiency in the addition of GPI anchors and may have important implications for the function of individual RGM family members in the extracellular space. Differential subcellular targeting has recently been suggested as a mechanism by which several proteins with proposed extracellular functions regulate their activities. For example, only small amounts of NogoA protein reach the cell surface of oligodendrocytes and the most prominent localization of NogoA is found in the endoplasmic reticulum (Chen et al.,

2000; GrandPre et al., 2000). It has been suggested that NogoA protein may only be released from oligodendrocytes after lesion of the nervous system, thus preventing NogoA from acting under normal circumstances (Brittis and Flanagan, 2001). Moreover, Comm in *Drosophila* has recently been described to sort Robo, the receptor for the repulsive guidance molecule Slit, to the endosomal compartment in order to prevent commissural neurons from responding to Slit before midline crossing (Keleman et al., 2002). Similarly, differential *in vivo* processing and subcellular localization of different members of the RGM family of proteins could regulate the degree of activity in a particular cell.

#### **2.4.2 *In Vivo* Function of *mRGMA* in the Developing Nervous System**

Two major candidate protein families have been implicated in anterior-posterior topographic mapping in the retinocollicular system (McLaughlin et al., 2003a). Ephrins and cRGMA have both been shown to exhibit comparable *in vitro* activities guiding RGC axons (Drescher et al., 1995; Cheng et al., 1995; Monschau et al., 1997). However, whereas genetic evidence supports a role for *Ephrins* in anterior-posterior topographic mapping in the superior colliculus (Feldheim et al., 2000; McLaughlin et al., 2003a), our data on *mRGMA*<sup>-/-</sup> mice suggest that *mRGMA* is not essential for this process. Our findings reveal however, that while there does not appear to be a similarity in the phenotype of *EphrinA5*<sup>-/-</sup> and *mRGMA*<sup>-/-</sup> mice in the retinocollicular system, both *mRGMA* and *EphrinA5* are involved in the process of cephalic neural tube closure albeit at a different level of genetic penetrance (Holmberg et al., 2000). Consistent with this phenotype, both *EphrinA5* (Holmberg et al., 2000) and *mRGMA* are expressed in the dorsal edges of the cranial neural folds.

Why do *mRGMa*<sup>-/-</sup> mice not show a defect in the establishment of anterior-posterior retinocollicular topographic mapping? It is unlikely that a compensatory upregulation of gene expression of other *mRGM* or *Ephrin* family member(s) can account for the lack of phenotype in retinocollicular mapping of *mRGMa*<sup>-/-</sup> mice since the expression of both *mRGMb* and *mRGMc* as well as *EphrinA2* and *EphrinA5* is unchanged in *mRGMa*<sup>-/-</sup> mice. Moreover, *mRGMa* appears to be the member of the *mRGM* gene family expressed at the highest level in the mouse superior colliculus at the time RGC axons segregate into their final anterior-posterior position within the target region suggesting that *mRGMa* should play the dominant role amongst *mRGM* family members in controlling RGC targeting. In contrast, developing RGCs express high levels of *mRGMb* and no or only low levels of *mRGMa*. Since previous evidence suggests that the expression of Ephrins does not only contribute to the development of retinocollicular projections through expression in the target region itself but also through expression in RGCs (Hornberger et al., 1999), it will be interesting to determine in future experiments how *mRGMb* gene function contributes to the development of retinocollicular projections. Another possible explanation for a lack of phenotype in *mRGMa*<sup>-/-</sup> mice could come from the observation that while the expression of *EphrinA2* and *EphrinA5* in the mouse superior colliculus is graded (Feldheim et al., 2000), *mRGMa* exhibits no such anterior-posterior gradient. Thus the function of *mRGMa* may have changed during evolution, maybe because the chick tectum is significantly bigger than the mouse superior colliculus (McLaughlin et al., 2003a) potentially requiring additional cues to acquire precision in the development of projections from the retina to the tectum. Alternatively, *mRGMa* may only function in combination with *EphrinA2* and *EphrinA5* present in the superior colliculus of the mouse and to reveal a retinocollicular phenotype may require the

generation of *mRGMa*<sup>-/-</sup>/*EphrinA2*<sup>-/-</sup>/*EphrinA5*<sup>-/-</sup> mice. It has indeed been suggested that in addition to *EphrinA2* and *EphrinA5* other guidance cues ought to be present in the mouse to explain the anterior-posterior topographic mapping in the superior colliculus since disruption of both *EphrinA2* and *EphrinA5* does not lead to a complete loss in anterior-posterior retinocollicular topography (Feldheim et al., 2000). Future work will determine whether *mRGMa* does indeed act as a cofactor in combination with other guidance molecules to restrict RGC axons to their correct anterior-posterior position in the superior colliculus.

## 2.5 Methods

### 2.5.1 Characterization of *mRGM* Gene Family and Histology

The three members of the *mRGM* gene family were isolated by database searches (Accession numbers: *mRGMa*: AI118914; *mRGMb*: BG519283; *mRGMc*: AA656608). Signal peptide and GPI anchor cleavage sites were determined using the following programs (<http://www.cbs.dtu.dk/services/SignalP-2.0/#submission>; Nielsen et al., 1999 and [http://mendel.imp.univie.ac.at/gpi/gpi\\_server.html](http://mendel.imp.univie.ac.at/gpi/gpi_server.html); Eisenhaber et al., 1999). Percentages of identities of *mRGM* family members to *cRGMa* were determined using NCBI BlastP version 2.2.6. To determine amino-terminal proteolytic cleavage sites, *cRGMa* (Monnier et al., 2002) and *mRGMs* were cloned into pSecTag2A (Invitrogen, San Diego, CA) in frame with the His-tag (*cRGMa*: bp 93-1217; *mRGMa*: bp 91-1232; *mRGMb*: bp 144-1243; *mRGMc*: bp 94-1178). COS-7 cell conditioned medium was collected 2-5 days after transfection and proteins were purified over a Ni-NTA-column (Qiagen, Basel, Switzerland). Amino-

terminal sequencing was performed by Edman degradation (ARS, University of Bern, Switzerland).

For *in situ* hybridization analysis, sections were hybridized with digoxigenin-labelled probes (Schaeren-Wiemers et al., 1993) directed against mouse *mRGMa*, *mRGMb*, *mRGMc*, *cRGMa* (Monnier et al., 2002), *mEphrinA5* (BG921710), *mEphrinA2* (AA170896) and *mPea3* (Livet et al., 2002). Antibodies used in this study were: rabbit anti-GAP-43 (Arber et al., 1999), rabbit anti-*mRGMa* (peptide antibody to aa 316 to 331), rabbit anti-*mRGMb* (peptide antibody to aa 256 to 270), rabbit anti-*mRGMc* (peptide antibody to aa 314 to 328), rabbit anti-*cRGMa* (peptide antibody to aa 319 to 332), mouse anti-BrdU (Beckton Dickinson, San Jose, CA), mouse anti-Myc (9E10; ATTC), mouse anti-skeletal  $\alpha$ -actinin (Sigma, Buchs, Switzerland), goat anti- $\beta$ -Galactosidase (Arnel, New York, NY) and sheep anti-eGFP (Biogenesis, Kingston, NH). Chick electroporations were performed as previously described (Briscoe et al., 2000). Cryostat sections were processed for immunohistochemistry as previously described (Arber et al., 1999) using fluorophore-conjugated secondary antibodies (Molecular Probes, Eugene, OR) (1:1000).

### **2.5.2 Generation and Analysis of *mRGMa* Mutant Mice**

A mouse genomic library was screened using a *mRGMa* specific probe (Incyte Genomics, Palo Alto, CA). An EcoRV genomic fragment containing the exon coding for the amino-terminal methionine and signal peptide was replaced by a TK-Neomycin cassette using homologous recombination in ES cells (targeting frequency ~1:2000). ES cell recombinants were screened by genomic Southern blot (EcoRI digest; 3' probe (~ 200bp): oligonucleotides (A) 5'TTGACCTGCCGCTGAGCACA 3'



and (B) 5'CTGGGCACTGAGTGGTAAGG 3') and verified by PCR (see Figure 10 for position of oligonucleotides: [3]: 5'CATCCAACAAG GCTCCACTGGAAGG 3', [4]: 5'TGCGAAGTGGACCTGGGACCGCG 3'). The identification of *mRGMa*<sup>-/-</sup> mice was performed by genomic Southern blot and PCR (see Figure 10 for position of oligonucleotides: [1]: 5'CAGGTAGGCACAACCTCCTTGGTGG 3' and [2]: 5'TTAGCACGTCTGAGCCTGTGTCCG 3'). RT-PCR was performed following the instructions of the manufacturer (Promega, Madison, WI) using P0 mouse brain total RNA and the following oligonucleotides: [5]: 5'CTTCCTTCTCTGCAGCTTCCCCGC 3' and [6]: 5'CTGGCGCGCCAGCTTGGTAGACTTTCTGGTCC 3'. Lack of antibodies recognizing endogenous mRGMa prohibited us from confirming the absence of mRGMa protein in *mRGMa*<sup>-/-</sup> mice.

BrdU experiments were performed by intraperitoneal injection of BrdU (Sigma, Buchs, Switzerland; 50µg/g body weight) 2 hr before sacrifice and detection of BrdU was performed as previously described (Arber et al., 1999). TUNEL labeling to detect apoptotic cells in whole-mount embryos was performed as described by the manufacturer (Roche, Rotkreuz, Switzerland). Anterograde labeling of retinocollicular projections was done essentially as described (Simon and O'Leary, 1992). Briefly, 5% Dil (Molecular Probes, Eugene, OR) in dimethyl formamide solution was injected into the retina at P0 or the nasal or temporal extreme of the retina at P9-P12 with a fine glass micropipette using a Picospritzer III (Parker, Fairfield, NJ). One day later for fills at P0 or two days later for focal injections, colliculi were analyzed blind to genotype with confocal microscopy (Olympus, Hamburg, Germany). Retinas were examined to verify a single injection point for focal injections.

## 2.6 References

- Arber S, Han B, Mendelsohn M, Smith M, Jessell TM, Sockanathan S (1999) Requirement for the homeobox gene Hb9 in the consolidation of motor neuron identity. *Neuron* 23:659-674.
- Babitt JL, Zhang Y, Samad TA, Xia Y, Tang J, Campagna JA, Schneyer AL, Woolf CJ, Lin HY (2005) Repulsive guidance molecule (RGMa), a DRAGON homologue, is a bone morphogenetic protein co-receptor. *J Biol Chem*.
- Bredesen DE, Mehlen P, Rabizadeh S (2004) Apoptosis and dependence receptors: a molecular basis for cellular addiction. *Physiol Rev* 84:411-430.
- Brinks H, Conrad S, Vogt J, Oldekamp J, Sierra A, Deitinghoff L, Bechmann I, Alvarez-Bolado G, Heimrich B, Monnier PP, Mueller BK, Skutella T (2004) The repulsive guidance molecule RGMa is involved in the formation of afferent connections in the dentate gyrus. *J Neurosci* 24:3862-3869.
- Briscoe J, Pierani A, Jessell TM, Ericson J (2000) A homeodomain protein code specifies progenitor cell identity and neuronal fate in the ventral neural tube. *Cell* 101:435-445.
- Brittis PA, Flanagan JG (2001) Nogo domains and a Nogo receptor: implications for axon regeneration. *Neuron* 30:11-14.
- Chen MS, Huber AB, van der Haar ME, Frank M, Schnell L, Spillmann AA, Christ F, Schwab ME (2000) Nogo-A is a myelin-associated neurite outgrowth inhibitor and an antigen for monoclonal antibody IN-1. *Nature* 403:434-439.
- Cheng HJ, Nakamoto M, Bergemann AD, Flanagan JG (1995) Complementary gradients in expression and binding of ELF-1 and Mek4 in development of the topographic retinotectal projection map. *Cell* 82:371-381.
- Dickson BJ (2002) Molecular mechanisms of axon guidance. *Science* 298:1959-1964.
- Drescher U, Kremoser C, Handwerker C, Loschinger J, Noda M, Bonhoeffer F (1995) In vitro guidance of retinal ganglion cell axons by RAGS, a 25 kDa tectal protein related to ligands for Eph receptor tyrosine kinases. *Cell* 82:359-370.
- Eisenhaber B, Bork P, Eisenhaber F (1999) Prediction of potential GPI-modification sites in proprotein sequences. *J Mol Biol* 292:741-758.
- Feldheim DA, Kim YI, Bergemann AD, Frisen J, Barbacid M, Flanagan JG (2000) Genetic analysis of ephrin-A2 and ephrin-A5 shows their requirement in multiple aspects of retinocollicular mapping. *Neuron* 25:563-574.
- Frisen J, Yates PA, McLaughlin T, Friedman GC, O'Leary DD, Barbacid M (1998)

- Ephrin-A5 (AL-1/RAGS) is essential for proper retinal axon guidance and topographic mapping in the mammalian visual system. *Neuron* 20:235-243.
- Godement P, Bonhoeffer F (1989) Cross-species recognition of tectal cues by retinal fibers in vitro. *Development* 106:313-320.
- GrandPre T, Nakamura F, Vartanian T, Strittmatter SM (2000) Identification of the Nogo inhibitor of axon regeneration as a Reticulon protein. *Nature* 403:439-444.
- Harris MJ, Juriloff DM (1997) Genetic landmarks for defects in mouse neural tube closure. *Teratology* 56:177-187.
- Holmberg J, Clarke DL, Frisen J (2000) Regulation of repulsion versus adhesion by different splice forms of an Eph receptor. *Nature* 408:203-206.
- Hornberger MR, Dutting D, Ciossek T, Yamada T, Handwerker C, Lang S, Weth F, Huf J, Wessel R, Logan C, Tanaka H, Drescher U (1999) Modulation of EphA function by coexpressed ephrinA ligands on retinal ganglion cell axons. *Neuron* 22: 731-742.
- Keleman K, Rajagopalan S, Cleppien D, Teis D, Paiha K, Huber LA, Technau GM, Dickson BJ (2002) Comm sorts robo to control axon guidance at the *Drosophila* midline. *Cell* 110:415-427.
- Livet J, Sigrist M, Stroebel S, De Paola V, Price SR, Henderson CE, Jessell TM, Arber S (2002) ETS gene Pea3 controls the central position and terminal arborization of specific motor neuron pools. *Neuron* 35:877-892.
- Matsunaga E, Tauszig-Delamasure S, Monnier PP, Mueller BK, Strittmatter SM, Mehlen P, Chedotal A (2004) RGM and its receptor neogenin regulate neuronal survival. *Nat Cell Biol* 6:749-755.
- McLaughlin T, Hindges R, O'Leary DD (2003) Regulation of axial patterning of the retina and its topographic mapping in the brain. *Curr Opin Neurobiol* 13:57-69.
- Monnier PP, Sierra A, Macchi P, Deitinghoff L, Andersen JS, Mann M, Flad M, Hornberger MR, Stahl B, Bonhoeffer F, Mueller BK (2002) RGM is a repulsive guidance molecule for retinal axons. *Nature* 419:392-395.
- Monschau B, Kremoser C, Ohta K, Tanaka H, Kaneko T, Yamada T, Handwerker C, Hornberger MR, Loschinger J, Pasquale EB, Siever DA, Verderame MF, Muller BK, Bonhoeffer F, Drescher U (1997) Shared and distinct functions of RAGS and ELF-1 in guiding retinal axons. *Embo J* 16:1258-1267.
- Nakamoto M, Cheng HJ, Friedman GC, McLaughlin T, Hansen MJ, Yoon CH, O'Leary DD, Flanagan JG (1996) Topographically specific effects of ELF-1 on retinal axon guidance in vitro and retinal axon mapping in vivo. *Cell* 86:755-766.

- Nielsen H, Brunak S, von Heijne G (1999) Machine learning approaches for the prediction of signal peptides and other protein sorting signals. *Protein Eng* 12:3-9.
- Roskies AL, O'Leary DD (1994) Control of topographic retinal axon branching by inhibitory membrane-bound molecules. *Science* 265:799-803.
- Schaeren-Wiemers N, Gerfin-Moser A (1993) A single protocol to detect transcripts of various types and expression levels in neural tissue and cultured cells: in situ hybridization using digoxigenin-labelled cRNA probes. *Histochemistry* 100:431-440.
- Sharom FJ, Lehto MT (2002) Glycosylphosphatidylinositol-anchored proteins: structure, function, and cleavage by phosphatidylinositol-specific phospholipase C. *Biochem Cell Biol* 80:535-549.
- Simon DK, O'Leary DD (1992) Development of topographic order in the mammalian retinocollicular projection. *J Neurosci* 12:1212-1232.
- Sperry R (1963) Chemoaffinity in the orderly growth of nerve fiber patterns and connections. *Proc Natl Acad Sci USA* 50:703-710.
- Tessier-Lavigne M, Goodman CS (1996) The molecular biology of axon guidance. *Science* 274:1123-1133.
- Theiler K (1989) *The house mouse: Atlas of embryonic development*. New York: Springer-Verlag.
- Walter J, Henke-Fahle S, Bonhoeffer F (1987) Avoidance of posterior tectal membranes by temporal retinal axons. *Development* 101:909-913.
- Yu TW, Bargmann CI (2001) Dynamic regulation of axon guidance. *Nat Neurosci* 4 Suppl:1169-1176.



## **Chapter 3:**

### **mRGMb is Essential for Survival Until Adulthood, but its Function Remains Unknown**

## **Chapter 3: mRGMb is Essential for Survival Until Adulthood, but its Function Remains Unknown**

### **Chapter 3.1: A Potential Role for *mRGMb* in Axon Guidance and Establishment of Cutaneous Afferent Projections**

#### **3.1.1 Introduction**

*mRGMb*, the second member of the mouse RGM family known to be expressed in the developing CNS (Niederkofler et al., 2004), was also discovered in an independent screen searching for genes regulated by the paired homeodomain transcription factor DRG11 (Samad et al., 2004), previously shown to play a role in the development of nociceptive sensory circuits (Chen et al., 2001). There is high level of conservation of *mRGMb* expression between zebrafish (Samad et al., 2004), chick (R. Salie and V. Niederkofler, unpublished results), and mouse (Niederkofler et al., 2004), however, at present its function remains to be discovered. *In vitro* neuronal adhesion assays suggest an adhesive role for mRGMb in development (Samad et al., 2004) however, these results contradict data from COS cell transfections and chick electroporation experiments performed in our own lab which indicate a very low level of mRGMb found at the cell surface (Chapter 2, Niederkofler et al., 2004).

While both *mRGMa* and *mRGMb* are expressed in the developing visual system their expression patterns are markedly different (Figure 9). *mRGMb* is strongly expressed in the RGC layer of the retina throughout the stages of axonal initiation and elongation (Niederkofler et al., 2004). *mRGMb* is expressed in the

superior colliculus, but at much lower level than *mRGMa* and in different layers of the colliculus (Niederkofler et al., 2004). This expression pattern, in addition to the fact that disruption of *mRGMa* does not disturb retinocollicular mapping raises the question: Does *mRGMb* contribute to the development of the topographic visual map?

## 3.2 Results and Discussion

### 3.2.1 *mRGMb* Mutant Mice Do Not Exhibit Defects in Retinocollicular Topography

In order to investigate the *in vivo* function of *mRGMb* in retinocollicular mapping, we performed homologous recombination in embryonic stem cells to eliminate *mRGMb* gene function. We disrupted the second coding exon with a eGFP-IRES-NLS-LacZ-pA-TK-neomycin cassette (Figure 14A). Successful homologous recombination in embryonic stem cells using this targeting construct was confirmed by Southern blot (Figure 14B). Heterozygous *mRGMb*<sup>+/-</sup> mice were phenotypically normal and interbreeding resulted in the generation of homozygous *mRGMb*<sup>-/-</sup> offspring in a Mendelian frequency. Northern blots of total brain extracts from neonatal mice (P0) homozygous for the disrupted *mRGMb* allele showed a complete absence of *mRGMb* mRNA providing evidence for a complete null mutation (Figure 14C).

Topographic projections of RGCs along the anterior-posterior axis were analyzed by focal Dil injections into the temporal and nasal extreme of the retina of postnatal day 9 to 12 (P9-P12) animals. Temporal RGCs project stereotypically to the



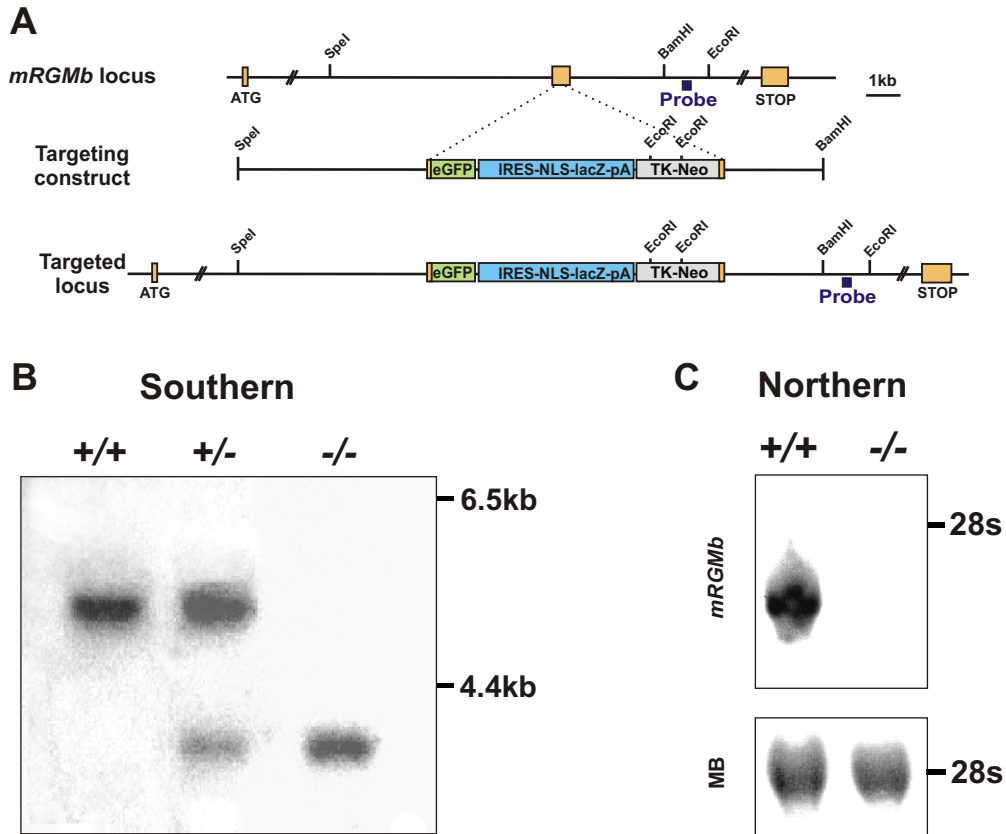


**Figure 14. Generation of *mRGMb* Mutant Mice.**

(A, B) Targeting strategy for homologous recombination in ES cells to eliminate *mRGMb* gene function. The second coding exon was disrupted with an eGFP-IRES-NLS-lacZ-pA-TK-Neo cassette. Exons are indicated in yellow. Probe used for genomic Southern analysis (B) is depicted in dark blue.

(C) Northern blot analysis demonstrates the absence of *mRGMb* mRNA in *mRGMb* mutant animals. Methylene Blue (MB) staining served as a loading control.

anterior part of the superior colliculus, while nasal RGC axons project to the posterior. Focal termination zones were detected in the predicted location in the superior colliculus in both *wild-type* and *mRGMb* mutant mice (Figure 15) (temporal:  $n \geq 3$ ; nasal:  $n \geq 6$ ). No shift in location or ectopic termination zones could be detected.

While *mRGMb* mutant mice lack defects in topographic mapping of the RGC projections to the superior colliculus along the anterior-posterior axis, the absence of retinocollicular anomalies in both *mRGMa* and *mRGMb* mutant mice might be due to functional redundancy between these two molecules. The analysis of *mRGMa/mRGMb* double mutants will elucidate this issue. It is also possible that *mRGMa* and *mRGMb* mutants only reveal their function in combination with *Ephrin-A2/Ephrin-A5* disruption. An alternative possibility is that any retinocollicular guidance function of *mRGMa* and *mRGMb* has been superseded during evolution. The chick optic tectum is approximately four times bigger than the mouse superior colliculus, and thus may require additional guidance cues for proper precise mapping. It will be interesting to observe larger mammals defective in *mRGMa* to determine if there is a requirement for *mRGMa* function in their retinotopic mapping. It would also be of interest to study smaller avians to see if RGMs in these species still retain guidance potential when the size of the optic tectum is reduced.

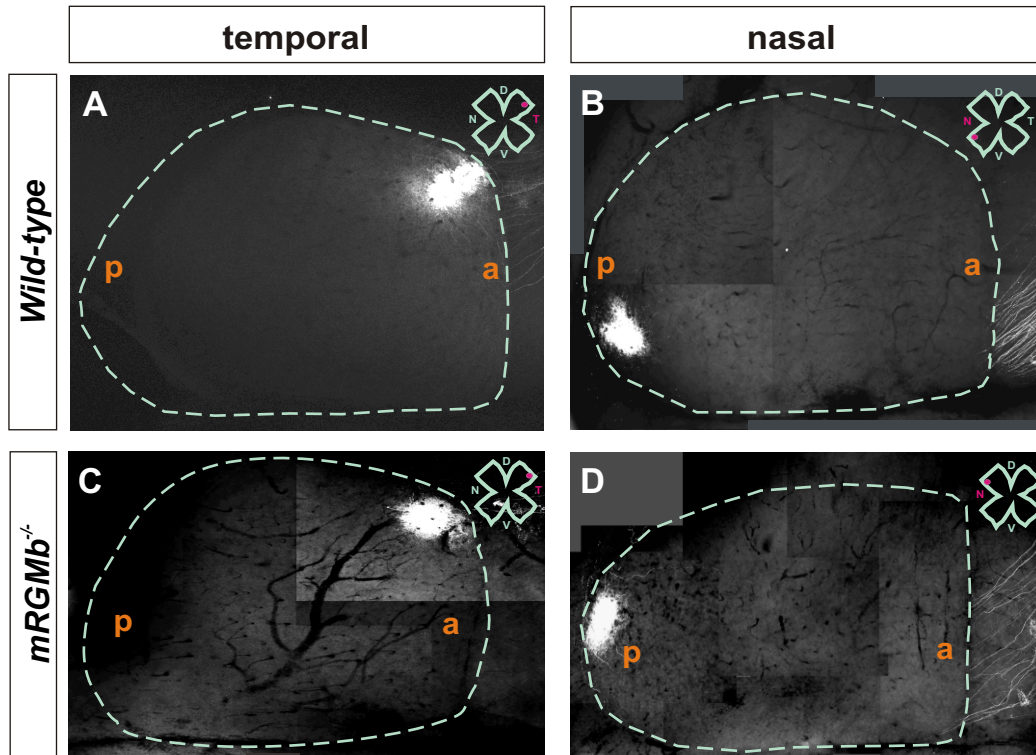


**Figure 15. Lack of Retinocollicular Projection Defects in *mRGMb* Mutant Mice.**

(A-D) Dorsal view of anterograde Dil tracing from temporal (A, C) or nasal (B, D) RGCs to the superior colliculus (outlined by green dashed lines) after focal Dil injection into the retina of *wild-type* (A, B) or *mRGMb*<sup>-/-</sup> (C, D) mice at P10 (injection points indicated by pink dot in top right corner). (T=temporal, N=nasal, D=dorsal, V=ventral, a=anterior, p=posterior)

### **3.3 *mRGMb* Mutant Mice Do Not Exhibit Defects in Establishment of Cutaneous Afferent Projections**

#### **3.3.1 Introduction**

Sensory neurons, which reside within dorsal root ganglia (DRG), transmit information about sensations such as temperature, pain, touch and body position. Diverse neuronal cell types mediate this sensory input and are associated with stereotypic development of specifically localized terminations of the projections within the spinal cord. Proprioceptive sensory neurons, which detect body position project to the ventral spinal cord, while cutaneous sensory neurons, delivering information from the skin terminate in superficial laminae I and II of the dorsal horn. It is believed that the specificity of these projections is controlled, in part, by differential expression of transcription factors in the sensory neurons and their corresponding targets. In the chick, the ETS transcription factor *Er81* has been shown to be expressed specifically in proprioceptive afferents and in subpopulations of the motor neurons to which they connect (Lin et al., 1998). The same principle holds true for the paired homeodomain transcription factor *DRG11*, which is expressed in cutaneous afferents and the dorsal horn of the spinal cord (Chen et al., 2001).

Recently, a genetic screen for the promoter regions of genes regulated by *DRG11* identified *mRGMb/DRAGON* as transcriptionally regulated by *DRG11* (Samad et al., 2004). The same study also shows that *mRGMb* is coexpressed with *DRG11* in the embryonic DRG and spinal cord, that its expression is reduced in *DRG11* null mutants and that *mRGMb* can interact homophilically in an adhesive manner. Interestingly, both *mRGMb* and *DRG11* mutant mice die of unknown

causes within the first postnatal month. Due to the proposed role of DRG11 as a regulator of *mRGMb*, and the similarity of *mRGMb* and *DRG11* expression in the DRGs and developing spinal cord, we hypothesised that *mRGMb* might be the downstream target of DRG11 responsible for spinal cord defects seen in the *DRG11* mutant animals.

### **3.4 Results and Discussion**

To address the functional implications of *mRGMb* regulation by DRG11, we assessed *mRGMb* mutant mice for defects observed in the *DRG11* mutant animals. Mouse embryos deficient in *DRG11* display abnormalities in the spatio-temporal patterning of cutaneous sensory afferent projections into the dorsal horn, as well as dorsal horn morphogenesis (Chen et al., 2001).

#### **3.4.1 Projection Pattern of Primary Sensory Afferents in the Dorsal Horn**

To determine if there is any gross central projection defect in *mRGMb* mutant mice we immunostained spinal cords of embryonic day 15.5 (E15.5) animals, three days after the initial ingrowth of sensory fibers into the grey matter, for parvalbumin, which marks proprioceptive afferents (Ernfors et al., 1994), and TrkA, which labels cutaneous afferents (Mu et al., 1993) (Figure 16C, D; data not shown). We could not detect an obvious sensory projection defect in *mRGMb* mutant mice compared to *wild-type* littermates, for either proprioceptive or cutaneous afferents. In contrast,

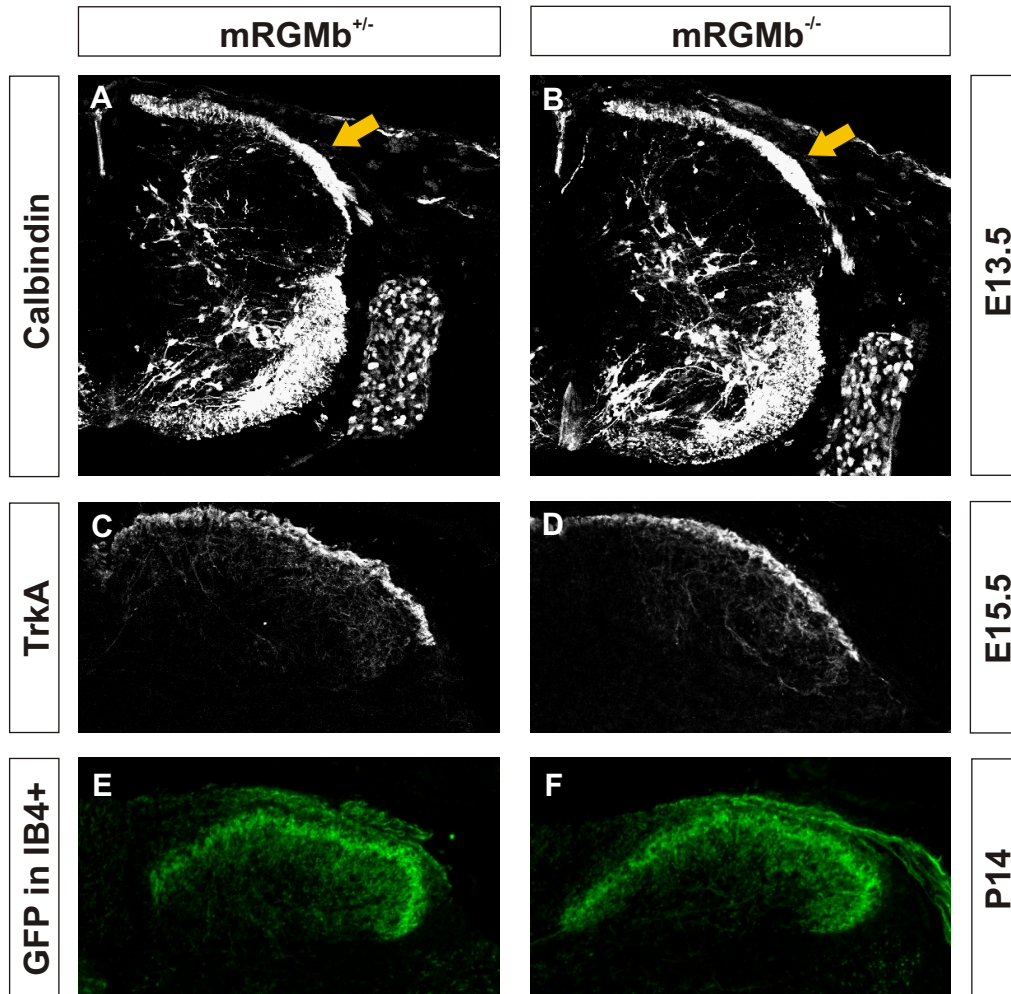


**Figure 16. *mRGMB* Mutant Mice Do Not Exhibit a Defect in Central Cutaneous Afferent Projections.**

(A-D) Spinal cords of *mRGMB*<sup>+/-</sup> (A, C) and *mRGMB*<sup>-/-</sup> (B, D) embryos were immunostained with Calbindin-28K (A, B) or TrkA (C, D). Arrows in (A, B) indicate Calbindin positive cutaneous afferents.

(E, F) GFP driven by the *Thy1* promoter labels specifically IB4 positive cutaneous afferents.

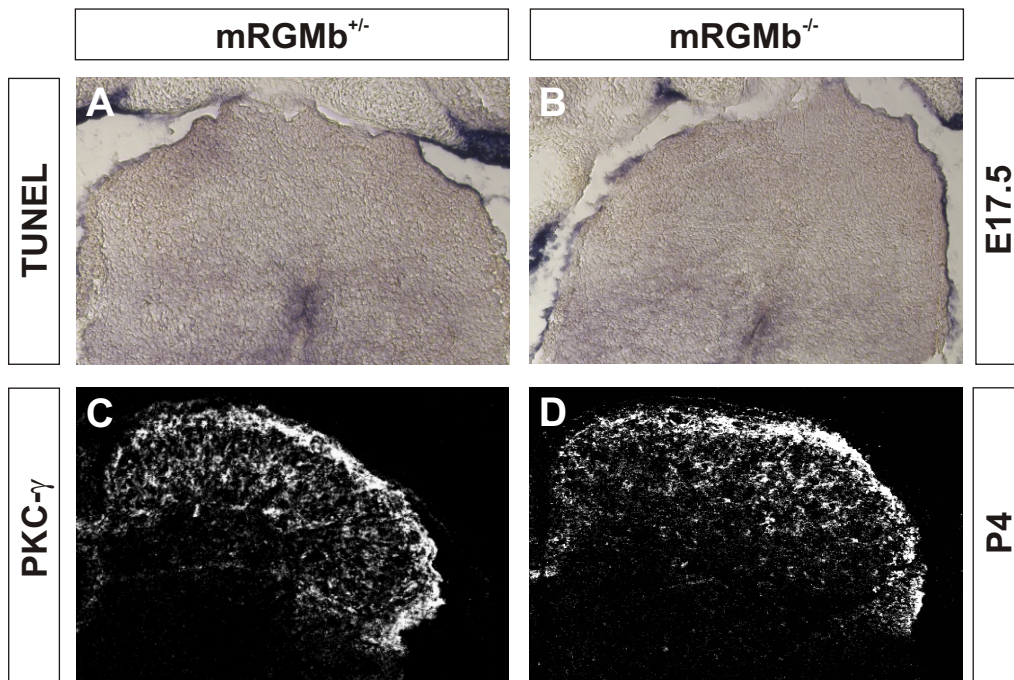


**Figure 17. Apoptosis and PKC- $\gamma$  Are Not Affected in *mRGMb* Mutant Mice.**

(A, B) TUNEL labeling does not reveal increased apoptosis in *mRGMb*<sup>-/-</sup> (B) compared to *mRGMb*<sup>+/-</sup> (A) embryos.

(C, D) PKC- $\gamma$  positive neurons are unchanged in *mRGMb*<sup>-/-</sup> (D) compared to *mRGMb*<sup>+/-</sup> (C) animals.

*DRG11* mutant animals exhibit a delayed ingrowth of TrkA positive afferent fibers into the gray matter relative to *wild-type*. In addition, these fibers are also biased toward the medial region and depleted from the lateral region in *DRG11* mutant animals.

To assess more subtle potential projection defects, we examined subsets of cutaneous afferents. We analyzed nonpeptidergic nociceptive fibers (IB4+), known to project specifically to lamina III in the dorsal horn (Molliver et al., 1995), by utilizing a transgenic mouse line expressing *eGFP* under the control of the *Thy1* promoter selectively in this sensory afferent subpopulation (Caroni, 1997; M. Sigrist and S. Arber, unpublished observation). The projection pattern was indistinguishable in both *mRGMb* mutant and *wild-type* mice. (Figure 16E, F). In contrast, *DRG11* mutant embryos have reduced nonpeptidergic nociceptive fibers with incorrectly localized terminations within the grey matter.

We also stained for Calbindin, which marks another subset of cutaneous afferents. These projections start to invade the dorsal horn at E12.5-E13.5 in *wild-type* embryos. In *DRG11<sup>-/-</sup>* embryos no Calbindin positive fibers are detected in the dorsal horn of at E13.5 (Chen et al., 2001). This defect in *DRG11* mutant animals appears to be a transient delay, since later in development the majority of Calbindin positive fibers project into the dorsal horn, although with slightly disturbed pattern. In contrast, no delay in invasion was observed in Calbindin positive cutaneous projections in *mRGMb* mutant mice when compared to *wild-type* littermates (Figure 16A, B).



### 3.4.2 Dorsal Horn Morphogenesis

*DRG11* mutant embryos exhibit increased cell death in the dorsal horn at E17.5, which results in an altered dorsal horn morphology (Chen et al., 2001). We performed TUNEL labelling at E17.5 to determine if there were changes in cell death within the dorsal horn. *mRGMB* mutant embryos did not show an increase in apoptotic cells as compared to their *wild-type* littermates (Figure 17A, B). In addition, *DRG11* mutant mice lack the protein kinase C- $\gamma$  (PKC- $\gamma$ ) expression which normally first appears in the dorsal horn at P2 (Chen et al., 2001). We observed PKC- $\gamma$  expression using immunostaining on P4 *mRGMB* mutant spinal cord. No decrease in PKC- $\gamma$  positive neurons was detectable in the dorsal horn of early postnatal *mRGMB* mutant mice (Figure 17C, D).

Together, our preliminary data do not provide any evidence for a function of *mRGMB* in the establishment of cutaneous afferent projections. Interestingly, although *mRGMB* is co-expressed with *DRG11* in embryonic DRG and spinal cord, *mRGMB* is expressed earlier than *DRG11* in the neural tube. In addition to a different temporal expression, the spatial expression of *DRG11* and *mRGMB* is also different. As well as being expressed in the developing DRG and spinal cord, *mRGMB* is also expressed in the brain and developing retina (Niederkofler et al., 2004). This suggests that also other regulatory elements play a role in controlling *mRGMB* expression. Furthermore, *DRG11* likely regulates multiple genes which might mediate its effect on neuronal differentiation instead of *mRGMB*. Backcrosses into the outbred CD-1 genetic background extended the life span of *DRG11* mutant animals significantly (Chen et al., 2001). These mice, when tested for behavioural defects, revealed a reduced sensitivity to nociceptive and mechanical stimuli. It would be

interesting to determine if a comparable change in genetic background would extend the life of *mRGMB* mutant mice, and whether they would exhibit similar behavioural defects to the *DRG11* mutant mice.

### 3.5 Material and Methods

#### 3.5.1 Generation of *mRGMb* Mutant Mice

A mouse genomic library was screened using a *mRGMb* specific probe (Incyte Genomics, Palo Alto, CA). The second coding exon of *mRGMb* was disrupted by inserting a cassette containing an *eGFP* in frame with the endogenous ATG, followed by an *IRES-NLS-LacZ-pA* and a thymidine kinase (TK)-neomycin cassette using homologous recombination in embryonic stem (ES) cells (targeting frequency, ~ 1:50)(Figure 14). ES cell recombinants were screened by genomic Southern blot (EcoRI digest; 3' probe (~ 250bp): oligonucleotides (A) 5' cca tgc tgc tca gcc ctg c-3' and (B) 5' ctt aga acg tgt ttt gta agg 3'). The identification of *mRGMb* mutant mice was performed by genomic Southern blotting and PCR ([1] 5'-gtt cct agg gag aat agc gtc tcc-3'; [2] 5'-aca ggc acg ttc gtc act tga acc-3')(Figure 14). Northern blot analysis of *mRGMb*<sup>-/-</sup> animals confirmed the absence of *mRGMb* mRNA using a *mRGMb* specific probe (BG519283) (Figure 14).

#### 3.5.2 Analysis of Retinocollicular Projections

Anterograde labeling of retinocollicular projections was done as described (Simon and O'Leary, 1992). Briefly, 5% Dil (Molecular Probes, Eugene, OR) in dimethyl formamide solution was injected into the retina at P0 or the nasal or temporal extreme of the retina at P9-P12 with a fine glass micropipette using a Picospritzer III (Parker, Fairfield, NJ). One day later for fills at P0 or two days later for focal injections, colliculi were analyzed blind to genotype with confocal microscopy (Olympus, Hamburg, Germany). Retinas were examined to verify a single injection point for focal injections.

### **3.5.3 Histology**

Antibodies used in this study were: rabbit anti-parvalbumin (Swant), rabbit anti-TrkA (Upstate), rabbit anti-PKC- $\gamma$  (C19) (Santa Cruz), rabbit anti-Calbindin D-28k (Swant), sheep anti-GFP (Biogenesis). Cryostat sections were processed for immunohistochemistry as previously described (Arber et al., 1999) using fluorophore-conjugated secondary antibodies (Molecular Probes, Eugene, OR) (1:1000). TUNEL labelling to detect apoptotic cells was performed as described by the manufacturer (Roche, Rotkreuz, Switzerland)

### 3.6 References

- Arber S, Ladle DR, Lin JH, Frank E, Jessell TM (2000) ETS gene Er81 controls the formation of functional connections between group Ia sensory afferents and motor neurons. *Cell* 101:485-498.
- Chen ZF, Rebelo S, White F, Malmberg AB, Baba H, Lima D, Woolf CJ, Basbaum AI, Anderson DJ (2001) The paired homeodomain protein DRG11 is required for the projection of cutaneous sensory afferent fibers to the dorsal spinal cord. *Neuron* 31:59-73.
- Ernfors P, Lee KF, Kucera J, Jaenisch R (1994) Lack of neurotrophin-3 leads to deficiencies in the peripheral nervous system and loss of limb proprioceptive afferents. *Cell* 77:503-512.
- Lin JH, Saito T, Anderson DJ, Lance-Jones C, Jessell TM, Arber S (1998) Functionally related motor neuron pool and muscle sensory afferent subtypes defined by coordinate ETS gene expression. *Cell* 95:393-407.
- Molliver DC, Radeke MJ, Feinstein SC, Snider WD (1995) Presence or absence of TrkA protein distinguishes subsets of small sensory neurons with unique cytochemical characteristics and dorsal horn projections. *J Comp Neurol* 361:404-416.
- Mu X, Silos-Santiago I, Carroll SL, Snider WD (1993) Neurotrophin receptor genes are expressed in distinct patterns in developing dorsal root ganglia. *J Neurosci* 13:4029-4041.
- Niederkofler V, Salie R, Sigrist M, Arber S (2004) Repulsive guidance molecule (RGM) gene function is required for neural tube closure but not retinal topography in the mouse visual system. *J Neurosci* 24:808-818.
- Samad TA, Srinivasan A, Karchewski LA, Jeong SJ, Campagna JA, Ji RR, Fabrizio DA, Zhang Y, Lin HY, Bell E, Woolf CJ (2004) DRAGON: a member of the repulsive guidance molecule-related family of neuronal- and muscle-expressed membrane proteins is regulated by DRG11 and has neuronal adhesive properties. *J Neurosci* 24:2027-2036.
- Samad TA, Rebbapragada A, Bell E, Zhang Y, Sidis Y, Jeong SJ, Campagna JA, Perusini S, Fabrizio DA, Schneyer AL, Lin HY, Brivanlou AH, Attisano L, Woolf CJ (2005) DRAGON: a bone morphogenetic protein co-receptor. *J Biol Chem*.
- Xia Y, Sidis Y, Mukherjee A, Samad TA, Brenner G, Woolf CJ, Lin HY, Schneyer A (2005) Localization and Action of Dragon (Repulsive Guidance Molecule b), a Novel Bone Morphogenetic Protein Coreceptor, throughout the Reproductive Axis. *Endocrinology* 146:3614-3621.



## **Chapter 4:**

### **mRGMc Plays a Role in Iron Metabolism**

## **Chapter 4: mRGMc Plays a Role in Iron Metabolism**

### **4.1 Iron Homeostasis**

#### **4.1.1 The Role of Iron in the Body**

Iron is an essential element incorporated into a variety of proteins in nearly all organisms (Aisen et al., 2001). In mammals, the majority of body iron is utilized for hemoglobin synthesis, but is also necessary for production of myoglobin, cytochromes and various other proteins required in cellular metabolism. Lack of iron leads to anemia, a reduced number of erythrocytes measured by decreased hemoglobin content of the blood. Iron has the capacity to accept and donate single electrons, interconverting between its ferric ( $\text{Fe}^{3+}$ ) and ferrous ( $\text{Fe}^{2+}$ ) forms. While the redox properties of iron make it an indispensable component of some proteins, the same properties also make iron dangerous to cells unless tightly regulated. Ferrous iron ( $\text{Fe}^{2+}$ ) reacts with hydrogen peroxide or lipid peroxides, common cellular constituents, to produce free radicals. These free radicals are highly reactive species that damage lipid membranes, proteins, and nucleic acids. Because either too much or too little iron is hazardous to the organism, iron uptake, storage and export must be tightly regulated. Any disturbance in iron metabolism can lead to hematological, metabolic and neurodegenerative disorders, which are potentially lethal (Andrews, 2000b; Hentze et al., 2004).

The human body contains a total of ~3,000 mg to 4,000 mg iron, the majority of which is incorporated into the oxygen binding hemoglobin of red blood cells (Ponka, 1997; Andrews, 1999) (Figure 18). While the human body requires 20 mg of iron every day to maintain erythropoiesis, only 1-2 mg of iron is absorbed per day. In addition, the body loses 1-2 mg of iron per day to natural tissue loss such as desquamation (loss of dead skin), menstruation, or loss of dead enterocytes into the



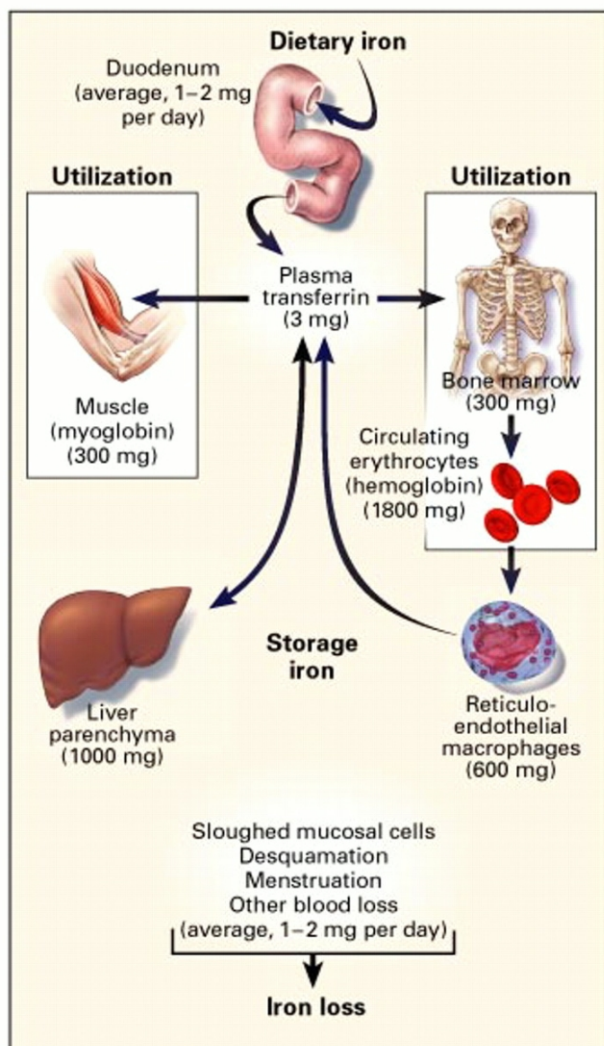


**Figure 18. Distribution of Iron in Adults.**

In the balanced state, 1 to 2 mg of iron enters and leaves the body each day. Dietary iron is absorbed by duodenal enterocytes. It circulates in plasma bound to transferrin. Most of the iron in the body is incorporated into hemoglobin in erythroid precursors and mature red cells. Approximately 10 to 15 percent is present in muscle fibers (in myoglobin) and other tissues (in enzymes and cytochromes). Iron is stored in parenchymal cells of the liver and reticuloendothelial macrophages. These macrophages provide most of the usable iron by degrading hemoglobin in senescent erythrocytes and reloading ferric iron onto transferrin for delivery to cells. (From Andrews, 1999)

digestive tract (Figure 18). How does the body acquire the iron it needs to maintain red blood cell production? Recycling of iron from hemoglobin of senescent erythrocytes allows for erythropoiesis with minimal iron absorption. Excess body iron is stored in hepatocytes and reticuloendothelial macrophages, from where it can be mobilized in response to acute need. As the body cannot actively excrete iron, the body iron levels must be tightly regulated at the point of absorption, across the mature enterocytes of the duodenum (Figure 18).

#### 4.1.2 Regulation of Iron Absorption

Iron must pass from the gut lumen through both apical and basolateral membranes of the duodenal enterocyte to reach the plasma (Andrews, 2000b; Chorney et al., 2003) (Figure 19). The acidic nature of the digestive lumen contents and the brush-border reductase, DcytB (a cytochrome b) allow reduction of insoluble ferric iron to its ferrous form.  $\text{Fe}^{2+}$  is transported into the enterocyte by the divalent-metal transporter DMT1, where it is either stored in association with the protein ferritin or transferred across the basolateral membrane by ferroportin (FPN1), an iron exporter. Upon leaving the enterocyte,  $\text{Fe}^{2+}$  is oxidized to  $\text{Fe}^{3+}$  by hephaestin, a basolateral ferroxidase where it is bound by transferrin (Tf), a plasma protein with a high affinity for iron at physiological pH, and transported across the vascular endothelium into the blood. The iron-transferrin complex (Fe-Tf) is bound by the ubiquitously expressed transferrin receptor 1 (TfR), and the entire Fe-Tf-TfR complex is endocytosed. Proton pumps acidify the internalized endosome reducing the affinity of transferrin for iron. Iron is released from transferrin, reduced to  $\text{Fe}^{2+}$  at which point it exits the endosome via DMT1 into the cytoplasm. Tf and TfR return to the cell surface, where they dissociate and transferrin is returned to the circulating pool where it may participate in further rounds of iron delivery. If not immediately

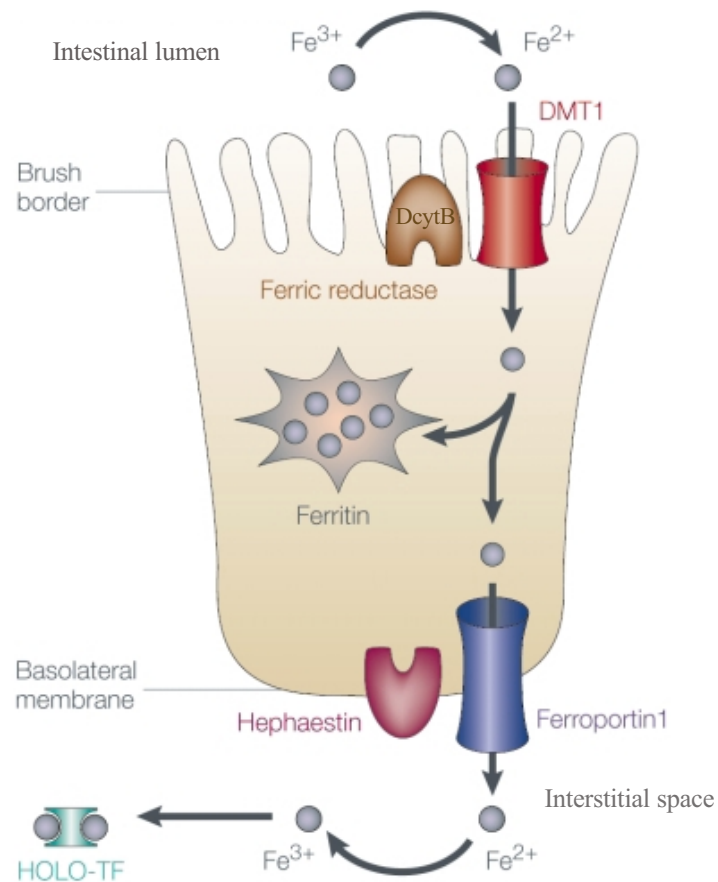


**Figure 19. Cellular Iron Transport.**

Duodenal enterocytes absorb iron from the diet. Non-heme iron is reduced by a ferric reductase (DcytB) in the brush border and is transported into the cell through the transmembrane iron transporter DMT1 (for divalent metal transporter 1). Some iron is stored within the cell in ferritin; the remainder must pass through the basolateral membrane to reach the plasma. An iron exporter, ferroportin, carries out basolateral iron transfer in cooperation with hephaestin, a ferroxidase. Absorbed iron is loaded onto transferrin (TF) to give holotransferrin (HOLO-TF) and transported across the vascular endothelium into the blood. (From Andrews, 2000b )

incorporated into protein, iron may also be sequestered by ferritin until it is needed (Figure 19).

#### **4.1.3 IREs and IRPs: Translational Regulators of Iron Metabolism Proteins**

In order to keep strict control of body iron levels it is also necessary to regulate the proteins involved in iron uptake, storage and export. Iron regulatory proteins (IRP1 and IRP2) are cytoplasmic polypeptides that modify translation of several proteins involved in iron metabolism by binding to iron responsive elements (IREs), conserved mRNA stem loop structures (Thomson et al., 1999; Cairo and Pietrangelo, 2000; Aisen et al., 2001, Eisenstein, 2003 #422; Pantopoulos, 2004). IREs are located within the 5' or the 3' untranslated regions of mRNAs coding for multiple proteins involved in iron homeostasis. mRNA of ferritin heavy and light chains, transferrin receptor-1 (TfR), ferroportin (FPN1) and the divalent metal transporter-1 (DMT-1) all contain IREs (McKie et al., 2000; Gunshin et al., 2001; Frazer et al., 2003). Affinity of IRPs for their IREs is regulated by the availability of iron within the organism. When intracellular iron levels are elevated, binding affinity of IRPs to the IREs is low. In contrast, reduced cellular iron availability activates binding activity of IRPs, thus stabilizing mRNAs which bear their IREs within the 3' untranslated region, such as TfR and DMT1. This serves to increase the amount of iron brought into the cell. Proteins with IREs within the 5' untranslated region, such as ferritin or ferroportin, are translationally blocked by IRP binding thus reducing iron efflux from the cell.

#### **4.1.4 Iron Homeostasis: Regulation in Response to Multiple Factors**

Several mechanisms regulate intestinal iron uptake. First, iron uptake can be modulated at the enterocyte by the amount of recently consumed iron in the diet, a

mechanism referred to as the “mucosal block” (Stewart et al., 1950; O'Neil-Cutting and Crosby, 1987; Frazer et al., 2003). After the consumption of a high amount of iron, absorptive enterocytes transiently block any further uptake. This block seems to be caused by a rapid decrease of the divalent-metal transporter DMT1 and the brush-border reductase DcytB at both the transcriptional and translational levels, likely mediated by IRP-IRE interactions, decreasing iron absorption at the apical membrane (Frazer et al., 2003). The mucosal block may even occur in the presence of systemic iron deficiency (Stewart et al., 1950). Intestinal iron absorption is also regulated in response to the amount of iron present in the body – the “stores regulator” (Finch, 1994; Gavin et al., 1994). When the amount of iron in the body stores decreases, iron absorption increases maintaining homeostatic levels. Iron absorption also changes in response to the requirements for erythropoiesis (Finch, 1994; Andrews, 1999). During periods of increased erythropoiesis, i.e. after severe blood loss, iron absorption from the diet increases in addition to iron released from hepatic and reticuloendothelial stores into the circulating iron pool. Iron regulation by proinflammatory cytokines is responsible for the withdrawal of iron to create a hostile environment to invading pathogens (Andrews, 1999; Hentze et al., 2004). Duodenal iron absorption is decreased and iron from senescent erythrocytes is withheld from recirculation into the transferrin pool by tissue macrophages. This generates a hypoferremic environment depriving pathogens of iron essential for their survival (Luft, 2004).

#### **4.1.5 Hepcidin, the Iron Regulatory Hormone**

How is the iron status of the body conveyed to the various responding cells that respond to it? Hepcidin, a small peptide hormone secreted predominantly by the liver, is the key regulator in iron absorption in response to dietary iron, iron stores,

anemia/hypoxia and inflammation (Andrews, 1999, 2004; Hentze et al., 2004). Heparin was first identified as a 20-25 amino acid antimicrobial peptide in urine (Park et al., 2001) and plasma (Krause et al., 2000). Heparin was first linked to iron metabolism when mRNA for mouse *Hamp*, the gene encoding heparin, was found to be increased in livers of mice fed a high iron diet (Pigeon et al., 2001). Additional evidence from transgenic mouse models indicates that heparin is the predominant negative regulator of iron absorption (Nicolas et al., 2001; Nicolas et al., 2002b). *Hamp* mutant mice show a progressive iron deposition in the liver and other organs (Nicolas et al., 2001). In contrast, mice overexpressing heparin under the control of a liver-specific promoter were born with lethal iron deficiency anemia (Nicolas et al., 2002b). In addition to responding to the iron levels of the body, heparin also responds to the hypoxia and the inflammatory stimuli. Animals subjected to hypoxia or hemolytic anemia showed a decrease in hepatic *Hamp* mRNA compared to controls (Nicolas et al., 2002a). *Hamp* mRNA levels are increased in mice injected with the inflammatory agents bacterial lipopolysaccharide (LPS) or turpentine (Pigeon et al., 2001; Nicolas et al., 2002a) as well as in fish infected with pathogenic bacteria (Shike et al., 2002). In addition, heparin is increased, in humans, during transfusion-induced iron overload, infections, and inflammatory states (Nemeth et al., 2003). Confirmation of the essential role of heparin in human iron metabolism came from a study of juvenile hereditary hemochromatosis, a severe iron overload disease whose affected members were found to be homozygous for mutations in *Hamp*. (Roetto et al., 2003).

By what mechanism does heparin function? In the last two years, several research groups have observed an inverse relationship between heparin and ferroportin mRNA and protein levels (Frazer et al., 2002; Yang et al., 2002; Mok et al., 2004; Yeh et al., 2004). This proposed interaction was recently confirmed by

Nemeth et al. who showed in cell culture experiments, that hepcidin binds to ferroportin on the cell surface, and induces its internalization and degradation (Nemeth et al., 2004c). Removal of ferroportin from the cell surface reduces release of iron into the plasma by enterocytes and macrophages. Since hepcidin expression is increased by a high level of serum iron, its production reduces ferroportin, in turn decreasing the amount of serum iron. As the iron level falls, hepcidin expression is reduced, allowing for the presence of ferroportin on the surface of enterocytes and reticuloendothelial macrophages. The accompaniment of increased *Hamp* mRNA with a decrease of *ferroportin* mRNA (Yeh et al., 2004) in a high iron environment is likely not due to direct interaction, but rather destabilizing effects of IRPs on *ferroportin* mRNA by binding to its 5' IRE.

Future studies will be required to elucidate the molecular circuitry that controls *Hamp* expression in response to iron, inflammation and hypoxia/anemia. One of the major questions that remains unresolved is the nature of the iron sensor. Some component of this sensor is likely to directly bind to iron, while another portion must signal to control the release of hepcidin. While the localization and components of the sensor are presently a mystery, as new molecules involved in iron metabolism are uncovered and more is discovered about the members already known, it is hoped that this question will soon be answered.

#### **4.1.6 Hereditary Hemochromatosis: A Disease of Iron Overload**

While all iron overload disorders are generally described under the blanket term 'hemochromatosis', several specific types have been identified with similar clinical symptoms (Andrews, 2000b). Hereditary hemochromatosis, characterized by a hyperabsorption of iron although the body iron stores are full (Andrews, 2000a;

Beutler et al., 2003; Brissot et al., 2004; Pietrangelo, 2004), has been associated with mutations in several single genes. In an attempt to reduce the serum iron content, iron is sequestered in various tissues, mainly the liver, pancreas, and heart. While these organs can store small excesses of iron safely, massive amounts of iron accumulate over the lifetime of the organism resulting in damage to iron loaded tissues. The most frequent clinical features of this genetic iron overload disease are cirrhosis, cardiomyopathy, diabetes, and hypogonadism. Until recently, therapeutic phlebotomy (deliberate removal of venous blood) to reduce body iron levels was the only treatment for patients suffering from hereditary hemochromatosis (Beutler et al., 2003). Iron chelators, which bind iron and allow it to be excreted in urine and faeces, have only recently been made available as an alternative therapy (Breuer et al., 2001; Boturao-Neto et al., 2002; Tam et al., 2003). The most difficult aspect of clinical treatment of hemochromatosis is appropriate diagnosis. Due to the variety of organs affected, wide variability in symptoms and the gradual progression of damage, hemochromatosis is often misdiagnosed or diagnosed too late, after the organs are irreversibly damaged (Franchini and Veneri, 2005).

Four subclasses of hereditary hemochromatosis have been identified, each caused by disruption of a different gene (Pietrangelo, 2004). The symptoms are similar but vary in their time of onset and severity. Type 1 and type 3 hemochromatosis are caused by mutation of *HFE* or *transferrin receptor 2* respectively, and induce a mild, late onset form of hereditary hemochromatosis. Type 2A and type 2B, also called juvenile hereditary hemochromatosis, are caused by mutation of *Hamp* or human RGMc (also known as *HFE2*) respectively, and result in a severe, early onset form of this disease, which is generally fatal by age 30 if not diagnosed and treated early in life.



Clinical studies, as well as analysis of animals mutant in iron metabolism genes, show all subtypes of hereditary hemochromatosis present with reduced hepcidin levels (Ahmad et al., 2002; Bridle et al., 2003; Papanikolaou et al., 2004; Kawabata et al., 2005; Nemeth et al., 2005), and have lead to the conclusion that hepcidin is the major regulator of iron absorption (Andrews, 2000b; Pietrangelo, 2004). Hyperabsorption of iron is due to failure to upregulate hepcidin in the face of high iron levels. Reduced hepcidin results in continued presence of ferroportin on the cell surface causing persistent iron uptake by enterocytes and release by macrophages although the biological iron levels are already elevated.

#### **4.2 Aim of the Following Study**

Recently, mutation of a gene called *HFE2* on chromosome 1q has been linked by positional cloning to the human disease, type 2B juvenile hereditary hemochromatosis (Papanikolaou et al., 2004). The murine ortholog of human *HFE2* is *mRGMc*, a member of the GPI-anchored RGM protein family (Niederkofler et al., 2004). In the following chapter we show the functional characterization of *mRGMc*. We provide evidence that *mRGMc* mutant mice mimic the iron overload phenotype of human juvenile hereditary hemochromatosis and show a pronounced defect in the upregulation of *Hamp* upon increased iron loading. In contrast, *Hamp* remains inducible in these animals via the inflammatory pathway.

Furthermore, we identify *mRGMc* as the key component in resolution of conflict between dietary iron requirements of the body and hypoferremia induced by inflammation. Upon inflammation, iron levels are reduced to discourage pathogens which are dependent on iron for survival. This is achieved by upregulation of hepcidin, resulting in decreased intestinal iron absorption and increased iron retention in tissue

macrophages, leaving the body in a transient hypoferremic state (Luft, 2004). The body should sense this low iron state and downregulate hepcidin to rectify the hypoferremia, however this is not the case. We believe that the downregulation of *mRGMc* acts as a switch to override the iron-sensing pathway during inflammatory response and provide a possible explanation for how the two conflicting pathways of dietary iron-sensing and inflammation are regulated to prevent conflict at the molecular level.

### 4.3 Hemojuvelin Is Essential For Dietary Iron-Sensing and Its Mutation Leads to Severe Iron Overload

Vera Niederkofler\*, Rishard Salie\* and Silvia Arber. *J. Clin. Invest.* 115(8): 2180-6, (2005)

\* indicates equal contribution

#### 4.3.1 Abstract

Iron homeostasis plays a critical role in many physiological processes, notably synthesis of heme proteins. Dietary iron-sensing and inflammation converge on the control of iron absorption and retention by regulating the expression of hepcidin, a regulator of the iron exporter ferroportin. Human mutations in the GPI-anchored protein Hemojuvelin (HJV/RGMc/HFE2) cause juvenile hemochromatosis, a severe iron overload disease, but it was unclear how HJV intersects with the iron regulatory network. Here we show that within the liver, mouse *Hjv* is selectively expressed by periportal hepatocytes and that *Hjv* mutant mice exhibit iron overload as well as a dramatic decrease in *hepcidin* expression. Our findings define a key role for *Hjv* in dietary iron-sensing and also reveal that cytokine-induced inflammation regulates *hepcidin* expression through an *Hjv*-independent pathway.

### 4.3.2 Introduction

Regulation of iron uptake depends on the ability of an organism to accurately sense systemic iron and adjust its level accordingly. While iron is an essential physiological cofactor for the production of many proteins, most notably heme proteins, excess iron can be harmful to the organism, in part, through the generation of oxygen radicals and is potentially lethal (Hentze et al., 2004). Recent work has established the importance of the peptide hormone hepcidin in iron homeostasis as a negative regulator of iron release into the system by duodenal enterocytes and reticuloendothelial macrophages. Hepcidin binds to the iron exporter ferroportin resulting in its internalization and degradation (Nemeth et al., 2004c). How hepcidin levels are kept in balance through upstream signalling pathways is still under investigation (Nicolas et al., 2002a; Krijt et al., 2004; Lee et al., 2004; Nemeth et al., 2004a).

Multiple pathways are known to regulate expression of *hepcidin* and thus indirectly affect iron uptake and retention (Nicolas et al., 2002a). *Hepcidin* expression is induced by an excess of iron and is downregulated by iron deprivation, consistent with its role as a downstream effector of iron-sensing (Pigeon et al., 2001). In addition, *hepcidin* also responds to acute inflammation with rapid induction of gene expression. Injection of lipopolysaccharide (LPS), a bacterial endotoxin and potent activator of inflammatory response, induces *hepcidin* in mice (Pigeon et al., 2001), an effect believed to be dependent on cytokine production (Lee et al., 2004; Nemeth et al., 2004a). During inflammation induced by pathogenic infection, creation of a hypoferremic environment is thought to be a defense mechanism of the host organism to restrict pathogenic growth, which is partially dependent on physiological iron levels (Luft, 2004). Thus, both dietary iron-sensing and inflammatory pathways

converge on the regulation of the key regulator *hepcidin*, but how these two pathways intersect remains unclear.

An increasing number of genes have been assigned roles in iron homeostasis through their mutational identification in human diseases, some of which cause accumulation of iron and result in disease states of varying severity (Hentze et al., 2004; Pietrangelo, 2004). Human juvenile hemochromatosis is an early onset disorder of iron homeostasis resulting in massive iron overload in various body tissues (Beutler et al., 2003; Brissot et al., 2004; Hentze et al., 2004; Pietrangelo, 2004). Patients suffer from cardiomyopathy, diabetes or cirrhosis attributed to oxidative damage caused by iron loading and often die before 30 years of age. Recently, a mutation causing juvenile hemochromatosis which had been mapped to the human chromosomal position 1q, was identified by positional cloning (Papanikolaou et al., 2004). The corresponding gene was named *HFE2/HJV* and was shown to be a member of a previously identified GPI-anchored gene family named after its founding member RGM (Repulsive Guidance Molecule), the function of which has mainly been studied in the nervous system. The *RGM* gene family is comprised of three members (*RGMa*, *RGMb* and *RGMc*) (Niederkofler et al., 2004). *RGMc* is only different from *HFE2/HJV* in nomenclature (Niederkofler et al., 2004; Papanikolaou et al., 2004), and its mouse homologue will be referred to as *Hjv* in this study. Whereas two mouse homologues of this family, *mRGMa* and *mRGMb*, are mainly expressed in the nervous system, the expression of *Hjv* is enriched in skeletal muscle and liver (Niederkofler et al., 2004; Papanikolaou et al., 2004). Functionally, *RGMa* has been implicated in axon guidance and neural tube closure (Monnier et al., 2002; Niederkofler et al., 2004), whereas the expression of *mRGMb/DRAGON* is

regulated by the transcription factor DRG11 in dorsal root ganglia sensory neurons (Samad et al., 2004). In contrast, no function for *Hjv* had previously been described.

Here we show that *Hjv* is expressed in periportal hepatocytes and disruption of the *Hjv* gene results in severe iron overload. Mice mutant in *Hjv* fail to express *hepcidin* in response to dietary or injected iron, thus providing a molecular explanation for the severe iron accumulation observed in *Hjv* mutant mice. In contrast, these mice retain the ability to upregulate *hepcidin* expression in response to acute inflammation induced either by LPS or its downstream products IL-6 or TNF $\alpha$ . Moreover, we also show that, upon induction of inflammation, *Hjv* expression in wild-type mice is selectively downregulated in the liver, but not in skeletal muscle. Our data, taken together with previous observations (Krijt et al., 2004), suggest that inflammation might induce a temporary elimination of iron-sensing by downregulation of hepatic *Hjv*. In summary, our results imply that *Hjv* plays an essential role in the regulation of *hepcidin* expression which is confined to the iron-sensing pathway.

### **4.3.3 Results**

#### **4.3.3.1 Generation of *Hjv* Mutant Mice and Expression of *Hjv* in Periportal Hepatocytes**

The recent genetic linkage of *HFE2/HJV* to the iron overload disease juvenile hemochromatosis in humans (Papanikolaou et al., 2004) has opened the way to elucidate the function of *Hjv* in iron homeostasis under normal physiological conditions and in disease by use of mouse genetics. We therefore generated *Hjv* mutant mice, coordinately expressing LacZ targeted to the nucleus from the *Hjv* locus (Figure 20A, B). Previous work has shown that the strongest expression of *Hjv* in mice is found in skeletal muscles, but a lower level of expression was also detected

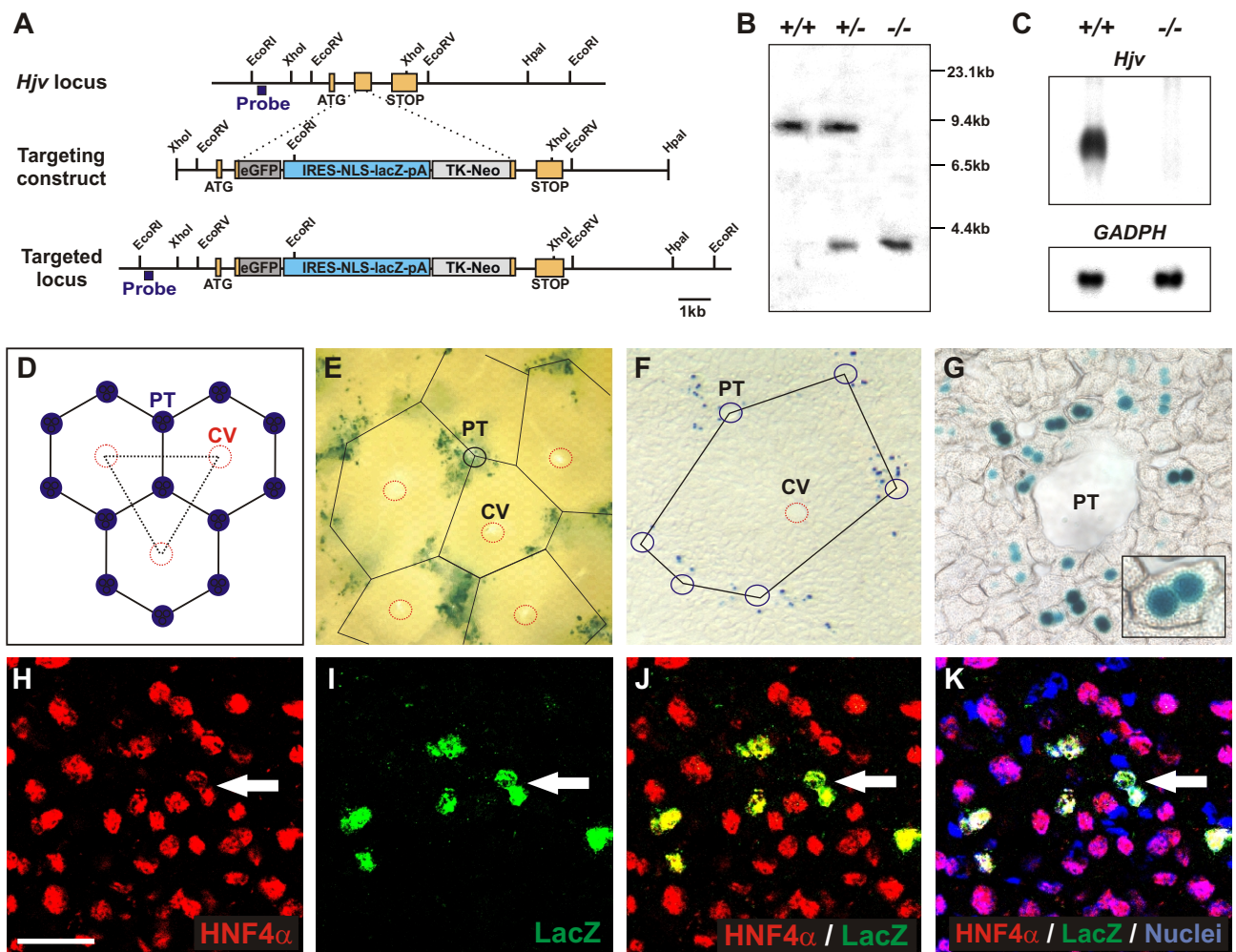


**Figure 20. *Hjv* Expression in Periportal Hepatocytes.**

(A) Targeting strategy used for homologous recombination in ES cells to eliminate *Hjv* gene function. The *Hjv* locus contains three coding exons (yellow; amino-terminal methionine: ATG; carboxy-terminal stop codon: STOP). A targeting construct containing an eGFP (dark grey) followed by an IRES-NLS-LacZ-pA (blue) and TK-Neo (light grey) was integrated in frame into the second coding exon of *Hjv*. The probe used for genomic Southern analysis is indicated in blue. Integrated cassette is not drawn to scale.

(B) Genomic Southern of *Hjv*<sup>+/+</sup>, *Hjv*<sup>+/-</sup> and *Hjv*<sup>-/-</sup> genomic DNA using the probe indicated in (A).

(C) Northern blot analysis of total RNA isolated from P21 hindlimb muscles of *Hjv*<sup>+/+</sup> and *Hjv*<sup>-/-</sup> mice probed for the expression of *Hjv* (top) and *GADPH* (bottom).

(D) Schematic drawing depicting the territories of liver lobules. Portal tracts (PT) are indicated in blue, central veins (CV) are shown in red. Note that solid lines outline the hexagonally shaped hepatic lobule with PTs at the corners.

(E-G) Detection of enzymatic LacZ activity in liver from 3 month old *Hjv*<sup>+/-</sup> mice analyzed on vibratome (E) or cryostat (F, G) sections. Red circles indicate central vein (CV), blue circles indicate portal tract (PT). Inset in (G) depicts high magnification of individual binuclear hepatocyte expressing LacZ.

(H-K) Immunohistochemical detection of HNF4α (H, J, K: red), LacZ (I, J, K: green), and SYTOX green (Nuclei; K: blue) on liver from 3 month old *Hjv*<sup>+/-</sup> mice. Arrow points to binuclear *Hjv* expressing hepatocyte.

Scale bar: (E)=530μm, (F)= 260μm, (G)= 70μm, (inset to G)= 30μm, (H-K)= 40μm.

in the liver (Niederkofler et al., 2004). Mice homozygous for the mutated *Hjv* allele showed a complete absence of *Hjv* mRNA in all tissues analyzed, including skeletal muscles, providing evidence for a complete null mutation (Figure 20C; data not shown).

To determine the exact site of expression of *Hjv* in the liver, we processed vibratome sections of adult liver from *Hjv*<sup>+/-</sup> mice for the presence of LacZ activity (Figure 20E). Interestingly, we found a patterned distribution of *Hjv* expression in the liver whereas skeletal muscles were stained uniformly (Figure 20E; data not shown). To determine the identity of these cells, we analyzed LacZ expression on thin sections and found labeled cells surrounding portal tracts but not central veins (Figure 20F, G). At high magnification, and as described to occur frequently in hepatocytes (Seglen, 1997; Guidotti et al., 2003), LacZ<sup>+</sup> cells often contained two nuclei (Figure 20G). In addition, double labeling immunohistochemistry with an antibody against HNF4 $\alpha$ , a transcription factor expressed in hepatocytes (Parviz et al., 2003), confirmed the hepatocytic identity of these LacZ<sup>+</sup> cells (Figure 20H-K). In contrast, no overlap in the expression of LacZ with several other cell types of the liver was detected, including sinusoidal endothelial cells expressing CD31 (Benten et al., 2005) (data not shown). Together, these findings indicate that *Hjv* expression in the liver is restricted to hepatocytes surrounding the portal tracts.

#### **4.3.3.2 *Hjv* Mutation in Mice Causes Severe Iron Overload**

To assess the consequences of *Hjv* mutation for iron homeostasis in various organs, we used both histological staining procedures as well as quantitative determination of iron content (Figure 21; Figure 22). At 2.5 months of age, a severe increase in iron content was detected in liver (~20 fold; iron accumulation in the parenchymal cells of



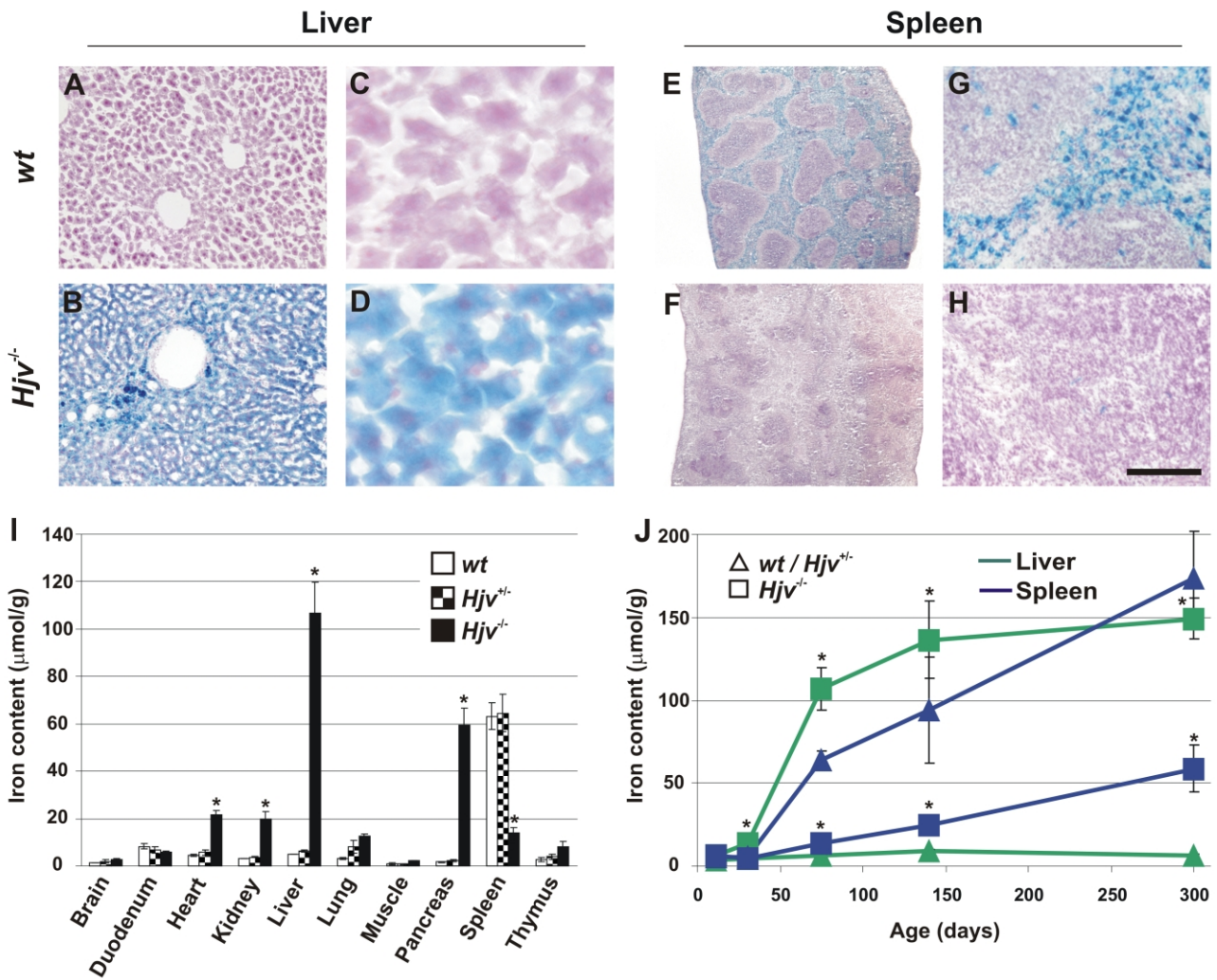


**Figure 21. Iron accumulation in *Hjv* mutant mice.**

(A-H) Histological detection of iron content on cryostat sections of liver (A-D) and spleen (E-H) of *wild-type* (A, C, E, G) and *Hjv*<sup>-/-</sup> (B, D, F, H) mice. Note uniform iron accumulation in the liver of 2.5 month old *Hjv* mutant mice and absence thereof in the red pulp of the spleen.

(I) Quantitative determination of iron content ( $\mu\text{mol/g}$  dry weight) in various organs (brain, duodenum, heart, kidney, liver, lung, skeletal muscle, pancreas, spleen and thymus) of 2.5 month old *wild-type* (white), *Hjv*<sup>+/-</sup> (checkerboard), and *Hjv*<sup>-/-</sup> (black) mice ( $n=5$  for each group). Asterisks indicate significant changes ( $P<0.05$ ) in *Hjv*<sup>-/-</sup> mice as compared to *wild-type* littermates.

(J) Time course (from P12 to P300; indicating days after birth) of iron content ( $\mu\text{mol/g}$  dry weight) determined in *Hjv*<sup>-/-</sup> mice (squares) compared to pooled *wild-type* and *Hjv*<sup>+/-</sup> mice (triangles). Liver (green) and spleen (blue) are depicted in the graph. At least 3 animals per time point and genotype were included in the analysis. Asterisks indicate significant changes ( $P<0.05$ ) in *Hjv*<sup>-/-</sup> mice as compared to pooled *wild-type* and *Hjv*<sup>+/-</sup> littermates.

Scale bar: (A, B)= 270 $\mu\text{m}$ , (C, D)= 45 $\mu\text{m}$ , (E, F)= 1.2mm, (G, H)= 100 $\mu\text{m}$ .

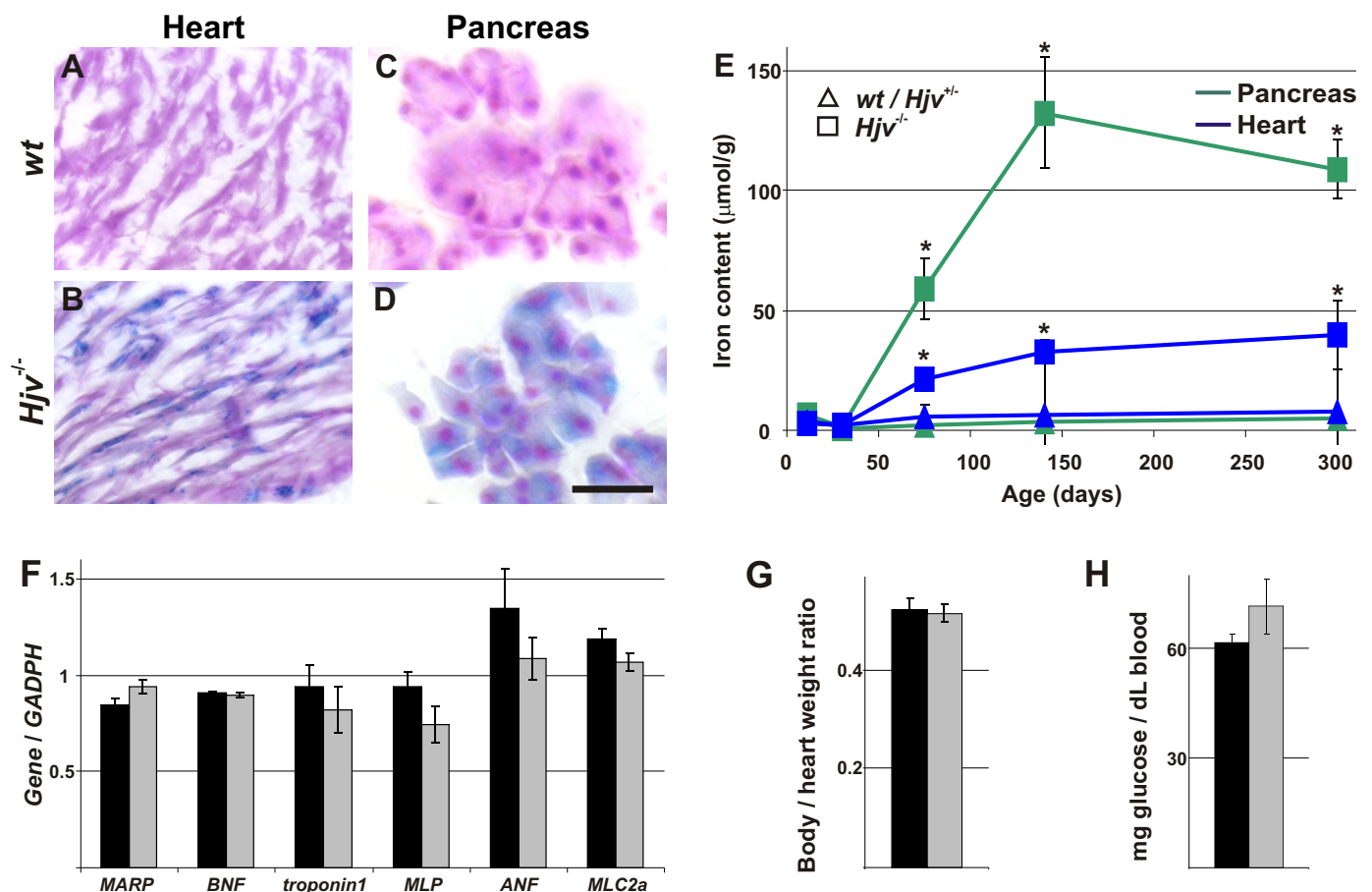


**Figure 22. Iron accumulation, but no indication of cardiomyopathy or diabetes in *Hjv* mutant mice.**

(A-D) Histological detection of iron content on cryostat sections of heart (A, B) and pancreas (C, D) of 2.5 month old *wild-type* (A, C) and *Hjv*<sup>-/-</sup> (B, D) mice.

(E) Time course (from P12 to P300; indicating days after birth) of iron content (μmol/g dry weight) determined in *Hjv*<sup>-/-</sup> mice (squares) compared to pooled *wild-type* and *Hjv*<sup>+/+</sup> mice (triangles). Pancreas (green) and heart (blue) are depicted in the graph. At least 3 animals per time point and genotype were included in the analysis. Asterisks indicate significant changes ( $P < 0.05$ ) in *Hjv*<sup>-/-</sup> mice as compared to pooled *wild-type* and *Hjv*<sup>+/+</sup> littermates.

(F) Quantification of mRNA expression levels as assessed by Northern blot analysis was performed by normalization of each cardiomyopathy related gene to *GADPH* expression probed sequentially on the same blots. Histograms depict *wild-type* mice in black (n=4), *Hjv* mutant mice in grey (n=4). Analyzed animals were 8-10 months old.

(G) Comparison of body weight to heart weight ratio (x100). Histograms depict *wild-type* mice in black (n=4), *Hjv* mutant mice in grey (n=7). Analyzed animals were 8-10 months old.

(H) Comparison of blood glucose (mg glucose/dl blood). Histograms depict *wild-type* mice in black (n=4), *Hjv* mutant mice in grey (n=5). Analyzed animals were 8-10 months old.

Scale bar: (A-D)=70μm, (C, D)=45μm.

the liver), pancreas (~25 fold; iron accumulation in acinar tissue) and heart (~4.5 fold) of *Hjv* mutant mice (Figure 21A-D, I, J; Figure 22). In contrast, we found a reduction in iron accumulation in the spleen (~4.5 fold; Figure 21E-H, I, J), likely due to inability of reticuloendothelial macrophages residing in the red pulp to sequester iron. These findings are consistent with the previously observed distribution of iron content under conditions of hemochromatosis in both human patients and other mouse models of this disease (Zhou et al., 1998; Fleming et al., 2001; Nicolas et al., 2001; Beutler et al., 2003; Pietrangelo, 2004; Kawabata et al., 2005).

A time course to determine the iron content in various tissues at several postnatal developmental stages of *Hjv* mutant mice showed a rapid and permanent increase in iron accumulation, reaching plateau levels by four months of age (Figure 21J; Figure 22E). Importantly, the first signs of hepatic iron overload were already detected by postnatal day 30 (Figure 21J). These findings reveal that mutation of *Hjv* in mice leads to iron accumulation in multiple organs with a time course and tissue distribution comparable to that observed in patients suffering from juvenile hemochromatosis (Pietrangelo, 2004).

In contrast to similarities detected in iron accumulation between human juvenile hemochromatosis patients and *Hjv* mutant mice, we did not observe obvious features of cardiomyopathy in these mice, as assessed by histology, analysis of heart weight and a number of marker genes known to be altered in cardiomyopathy (Figure 22F, G; data not shown). Moreover, *Hjv* mutant mice did not experience an increase in mortality (up to 15 months of age) or show signs of diabetes (Figure 22H; data not shown). While *Hjv* mutant males were sterile, they did not show signs of hypogonadism as assessed by determination of testicular size, a phenotype

frequently observed in human sufferers of juvenile hemochromatosis (Pietrangelo, 2004). Together, these findings suggest that *Hjv* mutant mice show an iron homeostasis phenotype highly similar to human patients but surprisingly, do not develop all of the associated pathological conditions.

#### **4.3.3.3 Lack of *Hepcidin* Expression in *Hjv* Mutant Mice**

We next began to assess the molecular mechanism by which absence of *Hjv* leads to iron accumulation in mice. *Hepcidin* expression is a well-established indicator of iron levels and is upregulated by high body iron (Andrews, 2004). In the liver of wild-type rats, *hepcidin* expression occurs in two waves: an early postnatal (P0-P3) spike which declines rapidly, followed by a second increase during the fourth postnatal week remaining through to adulthood (Courselaud et al., 2002). A very similar time course can be detected in mice in which adult levels of *hepcidin* expression in the liver are reached at P24 (Krijt et al., 2004) (Figure 23A). In contrast to the dynamic expression of *hepcidin*, *Hjv* expression in the liver was already detected at E13.5 and reached a steady level by late embryonic stages (Krijt et al., 2004) (Figure 23A).

We first determined the level of hepatic *hepcidin* expression in adult *Hjv* mutant mice by Northern blot analysis and *in situ* hybridization experiments. We found that *hepcidin* mRNA was virtually undetectable in adult *Hjv* mutant mice when compared to wild-type littermates in which expression was detected broadly throughout the liver ( $\leq 0.3\%$  of wild-type; Figure 23B, D; Figure 24A). Moreover, hepatic *hepcidin* expression in *Hjv* mutant mice was also absent at early postnatal stages when wild-type mice exhibit a naturally occurring spike of *hepcidin* expression (Figure 23B). To determine whether *Hjv* mutant mice exhibit a general block of

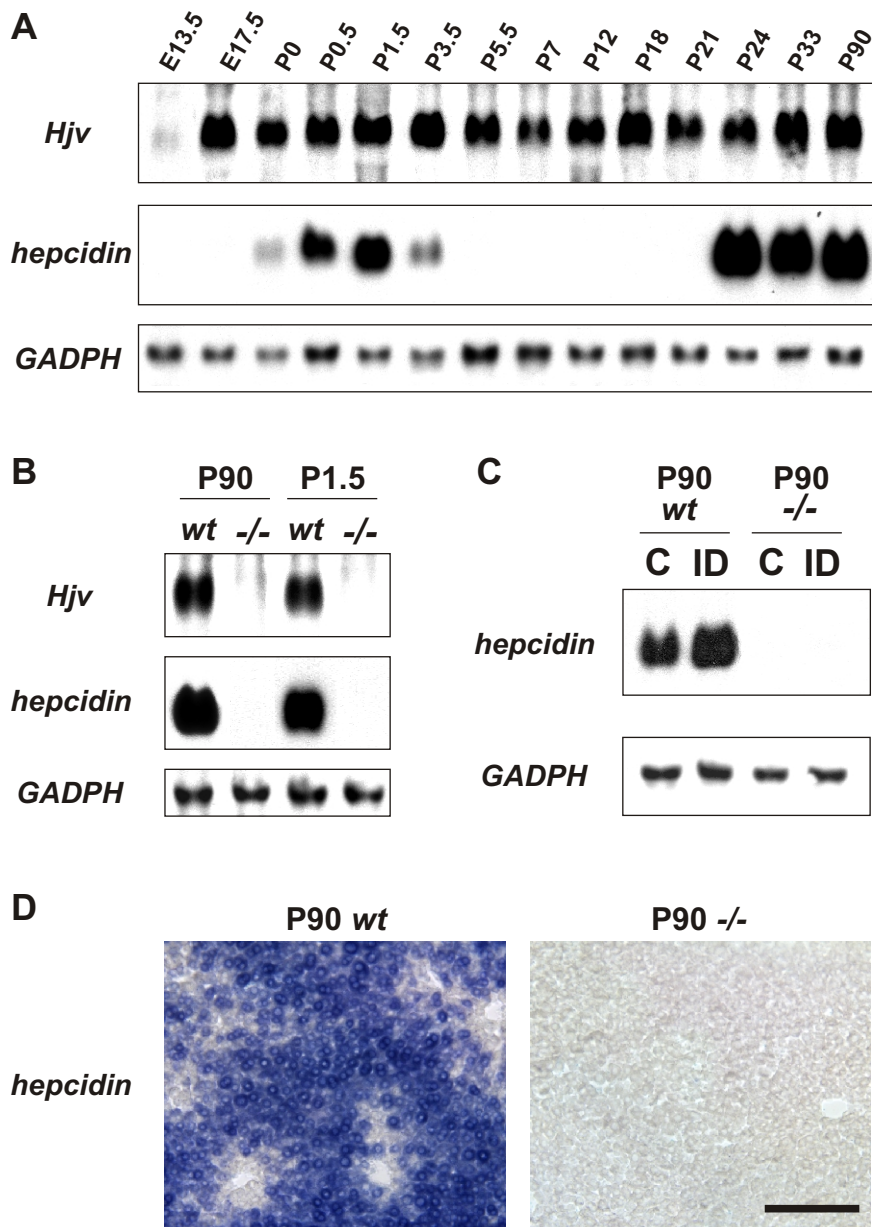


**Figure 23. Lack of *Hepcidin* expression in *Hjv* mutant mice.**

(A) Developmental time course (ages as indicated from E13.5 to P90) of *Hjv*, *hepcidin*, *GADPH* expression levels determined by Northern blot analysis on total RNA isolated from liver.

(B) Northern blot analysis of total RNA isolated from adult (P90) or P1.5 liver of *wild-type* and *Hjv*<sup>-/-</sup> mice probed for the expression of *Hjv*, *hepcidin* and *GADPH*.

(C) Northern blot analysis of total RNA isolated from adult (P90) liver of *wild-type* and *Hjv*<sup>-/-</sup> mice sacrificed seven days after sham injection (C) or injection with iron-dextran (ID) and probed for the expression of *hepcidin* and *GADPH*.

(D) *In situ* hybridization on cryostat sections of liver isolated from adult (P90) *wild-type* and *Hjv*<sup>-/-</sup> mice probed for the expression of *hepcidin*.

Scale bar: (C)= 100 $\mu$ m.

*hepcidin* regulation in response to iron, we assessed whether artificial elevation of iron levels in *Hjv* mutant mice was capable of inducing *hepcidin* expression. We found that subcutaneous injection of iron-dextran (Pigeon et al., 2001) in *Hjv* mutant mice did not increase *hepcidin* expression significantly whereas the same treatment consistently increased *hepcidin* in wild-type mice (Figure 23C).

Together, these findings point to an essential role for *Hjv* in iron-sensing, as an upstream regulator of *hepcidin* expression. Moreover, the massive reduction in *hepcidin* provides a molecular explanation for the continued iron accumulation and lack of effective regulatory mechanisms to decrease iron uptake in *Hjv* mutant mice.

#### **4.3.3.4 Acute Inflammation Can Induce *Hepcidin* Expression in *Hjv* Mutant Mice**

Does the lack of *hepcidin* expression in *Hjv* mutant mice represent an absolute inability to induce hepatic *hepcidin* expression, or is it possible to bypass this deficiency by stimulation of the inflammatory pathway (Pigeon et al., 2001; Nemeth et al., 2004a)? We found that induction of acute inflammation by lipopolysaccharide (LPS) injection led to rapid and robust upregulation of *hepcidin* in *Hjv* mutant mice when compared to levels in sham injected mutant animals (~300 fold; Figure 24A). To determine whether downstream products of LPS were also sufficient to mimic the effect of LPS on *hepcidin* expression in *Hjv* mutant mice, we used injections of either proinflammatory cytokine IL-6 or TNF $\alpha$  (Zetterstrom et al., 1998). We found that either IL-6 or TNF $\alpha$  were sufficient to mimic the effect of LPS, albeit to a lower extent (IL-6 ~130 fold; TNF $\alpha$ ~160 fold; Figure 24A).

We also assessed whether, in *Hjv* mutant mice, inflammation-mediated upregulation of *hepcidin* expression was capable of effectively eliciting appropriate

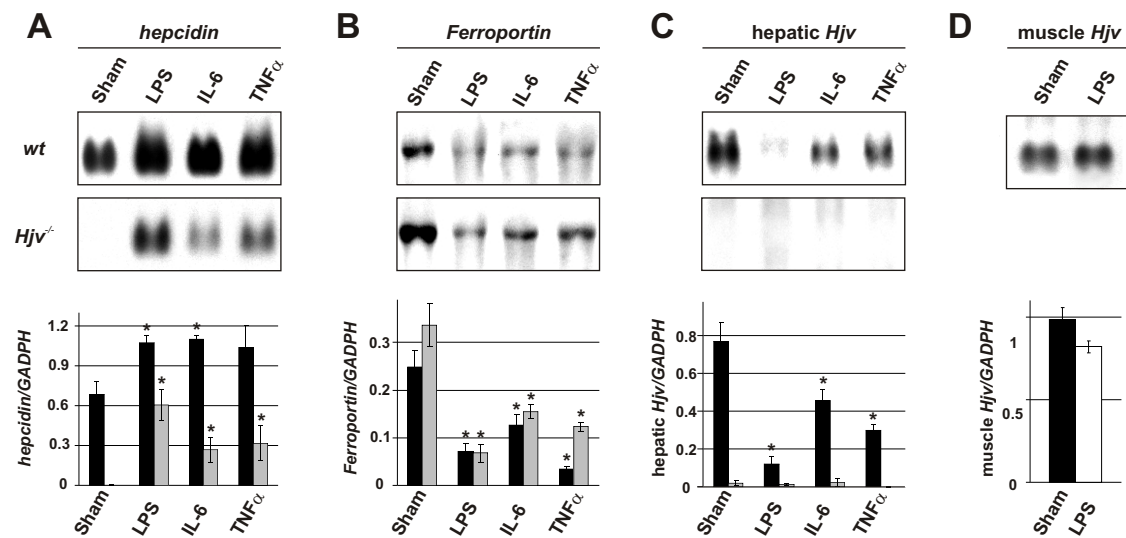


**Figure 24. Selective suppression of *Hjv* during inflammatory response.**

(A-C) Northern blot analysis of *hepcidin* (A), *ferroportin* (B) and *Hjv* (C) expression on total RNA isolated from liver of *wild-type* or *Hjv* mutant mice. Before isolation of total RNA, mice were injected intraperitoneally with PBS (sham), LPS, IL-6, or TNF $\alpha$ . At least three animals per experimental condition were analyzed and one representative example is shown. Quantification of expression levels was performed by normalization of each sample to *GADPH* expression probed sequentially on the same blots (data not shown). Histograms depict *wild-type* mice in black, *Hjv* mutant mice in grey. Asterisks indicate significant changes ( $P < 0.05$ ) in animals treated with LPS, IL-6 or TNF $\alpha$  as compared to sham injected animals of the same genotype.

(D) Northern blot analysis of *Hjv* expression on total RNA isolated from skeletal muscle of *wild-type* mice after sham or LPS injection. Quantification was performed as described in (A-C). Histogram depicts sham injected mice in black, LPS injected mice in white.

downstream responses. The iron exporter ferroportin has been shown to both regulate cellular iron uptake by binding to hepcidin (Nemeth et al., 2004b) and to be transcriptionally downregulated by high hepcidin levels (Yeh et al., 2004). Consistent with the observed lack of *hepcidin* expression, *ferroportin* is highly expressed in untreated or sham-injected *Hjv* mutant mice (Figure 24B; data not shown). In contrast, upon LPS injection (associated with *hepcidin* induction), *ferroportin* mRNA is significantly reduced in *Hjv* mutant mice as well as in wild-type mice (Figure 24B), indicating the presence of intact downstream responses to hepcidin in *Hjv* mutant mice. These findings show that the inflammatory pathway can efficiently bypass a requirement for *Hjv* in the induction of hepatic *hepcidin* expression and assign a role to *Hjv* specifically in the iron-sensing pathway upstream of hepcidin regulation.

#### **4.3.3.5 Inflammation Induces Selective Downregulation of *Hjv* in Liver but not Muscle**

Normal iron balance is subverted during inflammation when hepcidin levels are elevated to create a transient hypoferremic environment inhibitory to pathogenic growth (Luft, 2004). This low serum iron concentration should be perceived as hypoferremia by the dietary iron-sensing pathway and rapidly counteracted; however this is not the case. Interestingly, previous experiments have shown that *Hjv* expression in the liver of wild-type mice is strongly downregulated upon induction of acute inflammation by LPS (Krijt et al., 2004). These findings raise the question of whether the observed effect is selective to the liver and whether other genes involved in iron metabolism (Beutler et al., 2003; Brissot et al., 2004; Hentze et al., 2004; Pietrangelo, 2004) are regulated in a similar manner.



Interestingly, in contrast to the dramatic downregulation of *Hjv* expression observed in the liver of LPS injected animals (Krijt et al., 2004) (Figure 24C), no decrease in the expression of *Hjv* expression in skeletal muscles was detected under these conditions (Figure 24C). Moreover, we also found that the expression levels of several hemochromatosis or iron metabolism related genes, such as *Hfe*, *Tfr2*,  $\beta$ 2-microglobulin or *ceruloplasmin* analyzed in the liver were unchanged following LPS injection (Figure 25). Finally, a decrease in *Hjv* expression in the liver can also be observed in response to IL-6 or TNF $\alpha$  injection (Figure 24D). Together, these findings show that the inflammatory response induces a transcriptional downregulation of *Hjv* specifically in the liver and that such a response is not observed for other genes implicated in iron regulatory pathways.

#### 4.3.4 Discussion

In this study, we provide evidence that *Hjv* expression in the liver is restricted to periportal hepatocytes and that *Hjv* is an essential component of the iron-sensing pathway. Our experiments show that *Hjv* mutant mice exhibit an iron overload phenotype with high similarity to human patients suffering from juvenile hemochromatosis. Despite excessive iron accumulation, *Hjv* mutant mice show a complete lack in *hepcidin* expression providing a molecular explanation for the observed phenotype. Nevertheless, *hepcidin* expression can still be induced in *Hjv* mutant mice by activation of the inflammatory pathway, providing evidence for the selective requirement of *Hjv* in the iron-sensing but not the inflammatory pathway upstream of *hepcidin* regulation. We will discuss our findings with respect to the role of *Hjv* in iron homeostasis and potential mechanisms by which *Hjv* might link iron-sensing and inflammatory pathways in vivo.

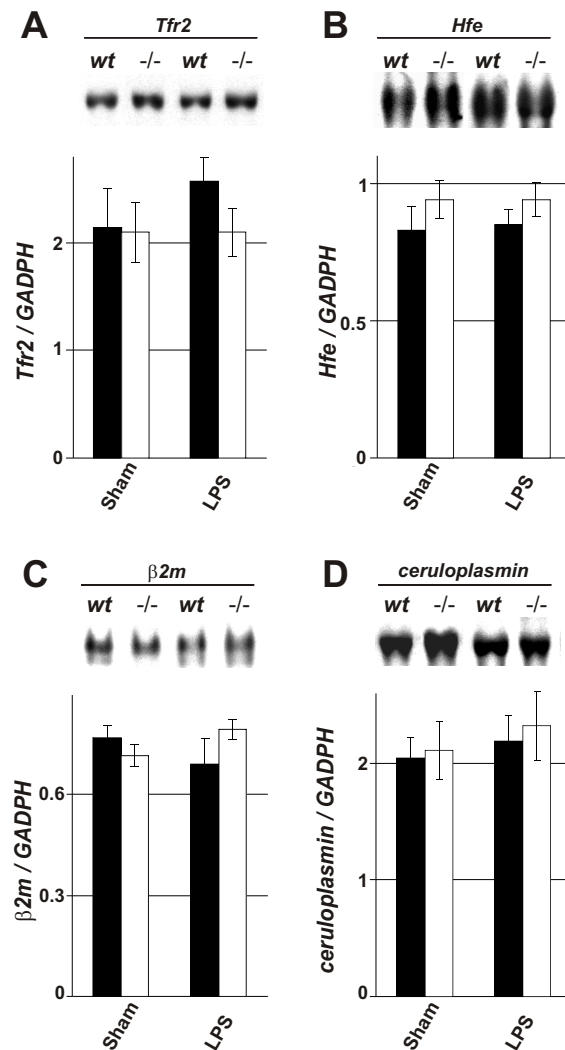


**Figure 25. LPS injection does not influence expression of *Tfr2*, *Hfe*,  $\beta 2$ -microglobulin and *ceruloplasmin*.**

(A-D) Northern blot analysis of *Tfr2*, *Hfe*,  $\beta 2$ -microglobulin, *ceruloplasmin* and *GADPH* expression on total RNA isolated from liver of *wild-type* or *Hfe* mutant mice. 6 hours before isolation of RNA, mice were injected intraperitoneally with PBS (sham) or LPS. At least four animals per experimental condition were analyzed and one representative example is shown. Quantification of expression levels was performed by normalization of each sample to *GADPH* expression probed sequentially on the same blots. Histograms depict *wild-type* mice in black, *Hfe* mutant mice in white

The complex regulatory network underlying systemic regulation of iron homeostasis is tuned to respond to different stimuli by activation of distinct molecular pathways all of which funnel into the regulation of hepatic hepcidin expression (Nicolas et al., 2002a) (Figure 26A, B). In this study, we provide evidence that *Hjv* is essential in the iron-sensing pathway. We found that even experimental elevation of iron levels was not capable of inducing *hepcidin* expression in *Hjv* mutant mice and that these mice were also devoid of the *hepcidin* expression spike normally occurring during the first postnatal week. These findings strongly suggest an essential role for *Hjv* in iron metabolism from birth throughout postnatal life.

In marked contrast to the defects in iron-sensing, induction of *hepcidin* expression upon inflammation is intact in *Hjv* mutant mice. Interestingly, *hepcidin* levels in LPS injected *Hjv* mutant animals do not reach the same level as in wild-type animals. These findings suggest that the total level of *hepcidin* expression observed upon inflammation is additive to the base line level and again argue for the existence of two independent pathways leading to the regulation of *hepcidin* expression. Of these two pathways, only the iron-sensing pathway requires functional *Hjv* (Figure 26).

How do iron-sensing and inflammatory pathways interact and what could be the possible mechanism to prevent interference between the two pathways? Interestingly, previous experiments have shown that hepatic *Hjv* is rapidly downregulated at the transcriptional level upon induction of inflammation by LPS injection in wild-type mice (Krijt et al., 2004). Moreover, we now show that *Hjv* downregulation upon inflammation is selective to the liver but does not occur in skeletal muscle, another prominent site of expression of *Hjv* (Figure 26B). Together

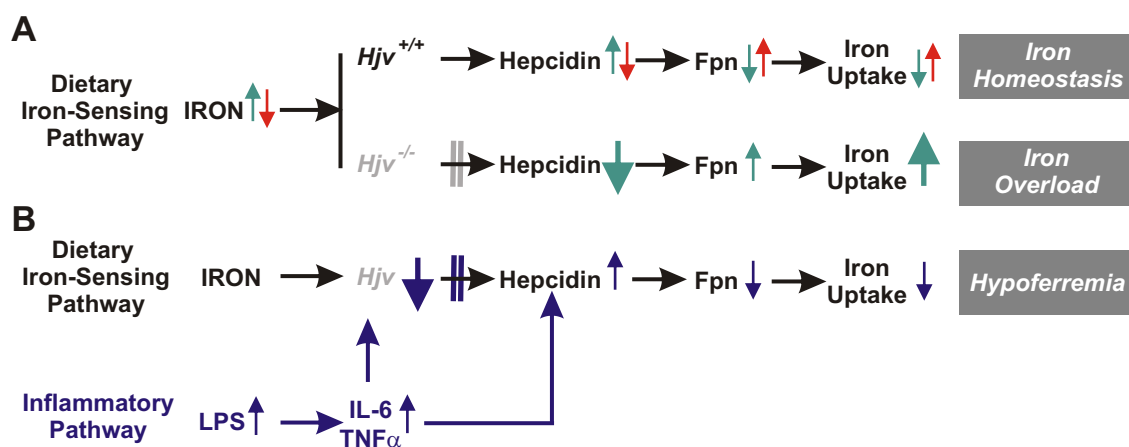


**Figure 26. An essential role for *Hjv* in the iron-sensing pathway.**

(A) Model depicting the dietary iron-sensing pathway in *wild-type* and *Hjv* mutant mice. In *wild-type* mice, green arrows indicate responses in the presence of high iron, red arrows show responses in the presence of low iron. Balanced regulation of this pathway adjusts iron levels to the needs of the healthy organism (follow green or red arrows from left to right). In *Hjv* mutant mice, iron-sensing is defective due to the absence of *Hjv* (indicated by solid vertical double line). Despite high iron, this leads to an essentially complete absence of hepcidin expression, iron overload and hemochromatosis (green arrows in *Hjv* mutant). Abbreviation: Fpn=ferroportin.

(B) Model depicting the impact of acute inflammation on the iron-sensing pathway (blue arrows). Acute phase cytokines IL-6 and TNF $\alpha$  act to coordinately downregulate *Hjv* expression in the liver while simultaneously inducing hepcidin expression. The reduction of *Hjv* results in a blockade of the dietary iron-sensing pathway (indicated by solid vertical double line). This mechanism efficiently suppresses the iron-sensing pathway during inflammatory response resulting in a low iron serum concentration inhibiting pathogenic growth. Abbreviation: Fpn=ferroportin.

with our observations that *Hjv* is not required for *hepcidin* induction during inflammation, these findings provide an intriguing potential mechanistic explanation for how the iron-sensing pathway could be switched off during inflammation, by the rapid and selective extinction of *Hjv* in the liver (Figure 26B). By such a mechanism, interference of individual pathways could be prevented by selective and fast cross-regulatory interactions at the level of transcriptional gene regulation.

This study also provides evidence that the expression of *Hjv* in the liver is restricted to a population of periportal hepatocytes. In contrast, *Hfe*, *Tfr2* and  $\beta$ 2-*microglobulin* have been described to be expressed broadly throughout the liver (Kawabata et al., 2001; Chorney et al., 2003; Zhang et al., 2004). Periportal hepatocytes are located close to the portal veins which deliver blood to the liver from the gut and are thus in a prime position to detect the iron content of blood coming directly from the digestive tract. While we cannot exclude a potential role for *Hjv* in iron-sensing in skeletal muscles with the currently available mouse model, our results nevertheless suggest the possibility that the cellular source assigned to iron-sensing in the liver may be periportal hepatocytes, marked by the expression of *Hjv*. Definitive proof of the importance of hepatic expression of *Hjv* however awaits the generation of either tissue specific *Hjv* mutant mice or attempts to selectively rescue *Hjv* mutant phenotypes by tissue specific expression. Finally, since *hepcidin* expression is not restricted to periportal hepatocytes, this finding excludes a direct molecular link from *Hjv* to the intracellular induction of *hepcidin* expression.

In summary, the findings described in this study reveal a selective role for *Hjv* in one of two pathways both of which converge on the downstream expression of the key regulatory peptide *hepcidin*. Whereas *Hjv* is required for *hepcidin* expression

through the iron-sensing pathway, *Hjv* is dispensable for induction of *hepcidin* through the inflammatory pathway. As such, our findings also provide important insights for future therapeutic strategies to treat diseases affecting iron metabolism.

#### **4.3.5 Methods**

##### **4.3.5.1 Generation, Maintenance and Analysis of *Hjv* Mutant Mice**

A mouse genomic library was screened using an *Hjv*-specific probe. The second coding exon of *Hjv* was disrupted by inserting a cassette containing an *eGFP* in frame with the endogenous ATG, followed by an *IRES-NLS-LacZ-pA* and a thymidine kinase (TK)-neomycin cassette using homologous recombination in embryonic stem (ES) cells (129SvJae1 origin; targeting frequency ~1:100). ES cell recombinants were screened by genomic Southern blot (EcoRI digest; 5' probe (~300bp): oligonucleotides (A) 5'-ctc agt gta tta tgt gta gaa-3' and (B) 5'-aat tcc agg aac gtt ggt ggc-3'; Figure 20A). The identification of *Hjv* mutant mice was performed by genomic Southern blotting (Figure 20B) and PCR ([1] 5'-cca gtg caa gat cct ccg ctg c-3'; [2] 5'-tcc gga tgg tgg tag cgt tgg c-3'). *Hjv* mice were maintained in a 129SvJ genetic background under standard conditions. All experiments were performed using male mice and control littermates were processed in parallel for each experiment.

##### **4.3.5.2 Northern Blot Analysis and Histology**

Northern blot analysis and isolation of total RNA was performed as previously described (Niederkofler et al., 2004), using digoxigenin-labeled probes directed against *Hjv* (Niederkofler et al., 2004), *Hamp* (BC021587), *Tfr2* (BC013654),  $\beta$ 2-microglobulin (BI691504), *Hfe* (AA255260), *ceruloplasmin* (AI225600), *Ferroportin*

(BQ928442) and *GADPH* (gift from P. Matthias, FMI). Expression of *mMLP*, *Marp*, *ANF* (Arber et al., 1997), *BNF* (NM\_008726), *troponin1* (NM\_009406) and *MLC2a* (Gottshall et al., 1997) were assessed by Northern blot analysis on heart total RNA. Signals were quantified using FluoView500 (Olympus) and normalized to the expression level of *GADPH*. Average values were determined from at least three independent experiments for each data point. Cryostat sections (16  $\mu$ m) were processed for immunohistochemistry as described previously (Arber et al., 1999), using fluorophore-conjugated secondary antibodies (1:1000; Molecular Probes). Primary antibodies used in this study were rabbit anti-LacZ (Arber et al., 1999) and goat anti-HNF4 $\alpha$  (Santa Cruz). Nuclei were detected using SYTOX Green (Molecular Probes, Eugene, OR). Vibratome sections (100  $\mu$ m) were cut on a vibratome (Leica). Detection of LacZ enzymatic activity and *in situ* hybridization experiments were performed as previously described (Arber et al., 1999; Niederkofler et al., 2004).

#### **4.3.6.3 Iron Quantification, Blood Glucose Measurement and Statistical Analysis**

Iron was detected on cryostat sections using the Accustain<sup>TM</sup> Iron Stain Kit (Sigma). Non heme-iron in dehydrated tissue was quantified according to a previously described method (Torrance, 1980). Animals were fasted for 6 hours before blood glucose measurement (Glucocard memory 2, Arkray Inc.). For statistical analysis, all *P* values were calculated in Microsoft Excel using a two tailed Student's *t*-test.

#### **4.3.6.4 LPS, Cytokine and Iron Injection**

LPS (1  $\mu$ g/g body weight; serotype O111:B4; Sigma), IL-6 (12.5ng/g body weight; R&D Systems) and TNF- $\alpha$  (12.5ng/g body weight; R&D Systems) were

injected intraperitoneally and organs were isolated for RNA preparation 6 hours after LPS and 4 hours after IL-6 or TNF- $\alpha$  injections (Yeh et al., 2004). Iron-dextran or PBS/dextran/phenol control solution was injected subcutaneously as previously described and animals were analyzed seven days after injection (Pigeon et al., 2001).



#### 4.3.6 References

- Ahmad KA, Ahmann JR, Migas MC, Waheed A, Britton RS, Bacon BR, Sly WS, Fleming RE (2002) Decreased liver hepcidin expression in the Hfe knockout mouse. *Blood Cells Mol Dis* 29:361-366.
- Aisen P, Enns C, Wessling-Resnick M (2001) Chemistry and biology of eukaryotic iron metabolism. *Int J Biochem Cell Biol* 33:940-959.
- Andrews NC (1999) Disorders of iron metabolism. *N Engl J Med* 341:1986-1995.
- Andrews NC (2000a) Inherited iron overload disorders. *Curr Opin Pediatr* 12:596-602.
- Andrews NC (2000b) Iron homeostasis: insights from genetics and animal models. *Nat Rev Genet* 1:208-217.
- Andrews NC (2004) Anemia of inflammation: the cytokine-hepcidin link. *J Clin Invest* 113:1251-1253.
- Arber S, Han B, Mendelsohn M, Smith M, Jessell TM, Sockanathan S (1999) Requirement for the homeobox gene Hb9 in the consolidation of motor neuron identity. *Neuron* 23:659-674.
- Arber S, Hunter JJ, Ross J, Jr., Hongo M, Sansig G, Borg J, Perriard JC, Chien KR, Caroni P (1997) MLP-deficient mice exhibit a disruption of cardiac cytoarchitectural organization, dilated cardiomyopathy, and heart failure. *Cell* 88:393-403.
- Benten D, Follenzi A, Bhargava KK, Kumaran V, Palestro CJ, Gupta S (2005) Hepatic targeting of transplanted liver sinusoidal endothelial cells in intact mice. *Hepatology*.
- Beutler E, Hoffbrand AV, Cook JD (2003) Iron deficiency and overload. *Hematology (Am Soc Hematol Educ Program)*:40-61.
- Boturao-Neto E, Marcopito LF, Zago MA (2002) Urinary iron excretion induced by intravenous infusion of deferoxamine in beta-thalassemia homozygous patients. *Braz J Med Biol Res* 35:1319-1328.
- Breuer W, Ermers MJ, Pootrakul P, Abramov A, Hershko C, Cabantchik ZI (2001) Desferrioxamine-chelatable iron, a component of serum non-transferrin-bound iron, used for assessing chelation therapy. *Blood* 97:792-798.
- Bridle KR, Frazer DM, Wilkins SJ, Dixon JL, Purdie DM, Crawford DH, Subramaniam VN, Powell LW, Anderson GJ, Ramm GA (2003) Disrupted hepcidin regulation

- in HFE-associated haemochromatosis and the liver as a regulator of body iron homoeostasis. *Lancet* 361:669-673.
- Brissot P, Troadec MB, Loreal O (2004) The clinical relevance of new insights in iron transport and metabolism. *Curr Hematol Rep* 3:107-115.
- Cairo G, Pietrangelo A (2000) Iron regulatory proteins in pathobiology. *Biochem J* 352 Pt 2:241-250.
- Chorney MJ, Yoshida Y, Meyer PN, Yoshida M, Gerhard GS (2003) The enigmatic role of the hemochromatosis protein (HFE) in iron absorption. *Trends Mol Med* 9:118-125.
- Courselaud B, Pigeon C, Inoue Y, Inoue J, Gonzalez FJ, Leroyer P, Gilot D, Boudjema K, Guguen-Guillouzo C, Brissot P, Loreal O, Ilyin G (2002) C/EBP $\alpha$  regulates hepatic transcription of hepcidin, an antimicrobial peptide and regulator of iron metabolism. Cross-talk between C/EBP pathway and iron metabolism. *J Biol Chem* 277:41163-41170.
- Finch C (1994) Regulators of iron balance in humans. *Blood* 84:1697-1702.
- Fleming RE, Holden CC, Tomatsu S, Waheed A, Brunt EM, Britton RS, Bacon BR, Roopenian DC, Sly WS (2001) Mouse strain differences determine severity of iron accumulation in Hfe knockout model of hereditary hemochromatosis. *Proc Natl Acad Sci U S A* 98:2707-2711.
- Franchini M, Veneri D (2005) Recent advances in hereditary hemochromatosis. *Ann Hematol* 84:347-352.
- Frazer DM, Wilkins SJ, Becker EM, Vulpe CD, McKie AT, Trinder D, Anderson GJ (2002) Hepcidin expression inversely correlates with the expression of duodenal iron transporters and iron absorption in rats. *Gastroenterology* 123:835-844.
- Frazer DM, Wilkins SJ, Becker EM, Murphy TL, Vulpe CD, McKie AT, Anderson GJ (2003) A rapid decrease in the expression of DMT1 and Dcytb but not Ireg1 or hephaestin explains the mucosal block phenomenon of iron absorption. *Gut* 52:340-346.
- Gavin MW, McCarthy DM, Garry PJ (1994) Evidence that iron stores regulate iron absorption--a setpoint theory. *Am J Clin Nutr* 59:1376-1380.
- Gottshall KR, Hunter JJ, Tanaka N, Dalton N, Becker KD, Ross J, Jr., Chien KR (1997) Ras-dependent pathways induce obstructive hypertrophy in echo-selected transgenic mice. *Proc Natl Acad Sci U S A* 94:4710-4715.
- Guidotti JE, Bregerie O, Robert A, Debey P, Brechot C, Desdouets C (2003) Liver cell polyploidization: a pivotal role for binuclear hepatocytes. *J Biol Chem* 278:19095-19101.

- Gunshin H, Allerson CR, Polycarpou-Schwarz M, Rofts A, Rogers JT, Kishi F, Hentze MW, Rouault TA, Andrews NC, Hediger MA (2001) Iron-dependent regulation of the divalent metal ion transporter. *FEBS Lett* 509:309-316.
- Hentze MW, Muckenthaler MU, Andrews NC (2004) Balancing acts: molecular control of mammalian iron metabolism. *Cell* 117:285-297.
- Kawabata H, Germain RS, Ikezoe T, Tong X, Green EM, Gombart AF, Koeffler HP (2001) Regulation of expression of murine transferrin receptor 2. *Blood* 98:1949-1954.
- Kawabata H, Fleming RE, Gui D, Moon SY, Saitoh T, O'Kelly J, Umehara Y, Wano Y, Said JW, Koeffler HP (2005) Expression of hepcidin is down-regulated in TfR2 mutant mice manifesting a phenotype of hereditary hemochromatosis. *Blood* 105:376-381.
- Krause A, Neitz S, Magert HJ, Schulz A, Forssmann WG, Schulz-Knappe P, Adermann K (2000) LEAP-1, a novel highly disulfide-bonded human peptide, exhibits antimicrobial activity. *FEBS Lett* 480:147-150.
- Krijt J, Vokurka M, Chang KT, Necas E (2004) Expression of Rgmc, the murine ortholog of hemojuvelin gene, is modulated by development and inflammation, but not by iron status or erythropoietin. *Blood* 104:4308-4310.
- Lee P, Peng H, Gelbart T, Beutler E (2004) The IL-6- and lipopolysaccharide-induced transcription of hepcidin in HFE-, transferrin receptor 2-, and beta 2-microglobulin-deficient hepatocytes. *Proc Natl Acad Sci U S A* 101:9263-9265.
- Lin L, Goldberg YP, Ganz T (2005) Competitive regulation of hepcidin mRNA by soluble and cell-associated hemojuvelin. *Blood*. (E-published ahead of print).
- Luft FC (2004) Hepcidin comes to the rescue. *J Mol Med* 82:345-347.
- McKie AT, Marciani P, Rolfs A, Brennan K, Wehr K, Barrow D, Miret S, Bomford A, Peters TJ, Farzaneh F, Hediger MA, Hentze MW, Simpson RJ (2000) A novel duodenal iron-regulated transporter, IREG1, implicated in the basolateral transfer of iron to the circulation. *Mol Cell* 5:299-309.
- Mok H, Jelinek J, Pai S, Cattanach BM, Prchal JT, Youssoufian H, Schumacher A (2004) Disruption of ferroportin 1 regulation causes dynamic alterations in iron homeostasis and erythropoiesis in polycythaemia mice. *Development* 131:1859-1868.
- Monnier PP, Sierra A, Macchi P, Deitinghoff L, Andersen JS, Mann M, Flad M, Hornberger MR, Stahl B, Bonhoeffer F, Mueller BK (2002) RGM is a repulsive guidance molecule for retinal axons. *Nature* 419:392-395.
- Nemeth E, Roetto A, Garozzo G, Ganz T, Camaschella C (2005) Hepcidin is decreased in TFR2 hemochromatosis. *Blood* 105:1803-1806.

- Nemeth E, Valore EV, Territo M, Schiller G, Lichtenstein A, Ganz T (2003) Heparin, a putative mediator of anemia of inflammation, is a type II acute-phase protein. *Blood* 101:2461-2463.
- Nemeth E, Rivera S, Gabayan V, Keller C, Taudorf S, Pedersen BK, Ganz T (2004a) IL-6 mediates hypoferrremia of inflammation by inducing the synthesis of the iron regulatory hormone hepcidin. *J Clin Invest* 113:1271-1276.
- Nemeth E, Tuttle MS, Powelson J, Vaughn MB, Donovan A, Ward DM, Ganz T, Kaplan J (2004b) Heparin regulates cellular iron efflux by binding to ferroportin and inducing its internalization. *Science* 306:2090-2093.
- Nicolas G, Bennoun M, Devaux I, Beaumont C, Grandchamp B, Kahn A, Vaulont S (2001) Lack of hepcidin gene expression and severe tissue iron overload in upstream stimulatory factor 2 (USF2) knockout mice. *Proc Natl Acad Sci U S A* 98:8780-8785.
- Nicolas G, Chauvet C, Viatte L, Danan JL, Bigard X, Devaux I, Beaumont C, Kahn A, Vaulont S (2002a) The gene encoding the iron regulatory peptide hepcidin is regulated by anemia, hypoxia, and inflammation. *J Clin Invest* 110:1037-1044.
- Nicolas G, Bennoun M, Porteu A, Mativet S, Beaumont C, Grandchamp B, Sirtori M, Sawadogo M, Kahn A, Vaulont S (2002b) Severe iron deficiency anemia in transgenic mice expressing liver hepcidin. *Proc Natl Acad Sci U S A* 99:4596-4601.
- Niederkofler V, Salie R, Sigrist M, Arber S (2004) Repulsive guidance molecule (RGM) gene function is required for neural tube closure but not retinal topography in the mouse visual system. *J Neurosci* 24:808-818.
- O'Neil-Cutting MA, Crosby WH (1987) Blocking of iron absorption by a preliminary oral dose of iron. *Arch Intern Med* 147:489-491.
- Pantopoulos K (2004) Iron metabolism and the IRE/IRP regulatory system: an update. *Ann N Y Acad Sci* 1012:1-13.
- Papanikolaou G, Samuels ME, Ludwig EH, MacDonald ML, Franchini PL, Dube MP, Andres L, MacFarlane J, Sakellaropoulos N, Politou M, Nemeth E, Thompson J, Risler JK, Zaborowska C, Babakouf R, Radomski CC, Pape TD, Davidas O, Christakis J, Brissot P, Lockitch G, Ganz T, Hayden MR, Goldberg YP (2004) Mutations in HFE2 cause iron overload in chromosome 1q-linked juvenile hemochromatosis. *Nat Genet* 36:77-82.
- Park CH, Valore EV, Waring AJ, Ganz T (2001) Heparin, a urinary antimicrobial peptide synthesized in the liver. *J Biol Chem* 276:7806-7810.
- Parviz F, Matullo C, Garrison WD, Savatski L, Adamson JW, Ning G, Kaestner KH, Rossi JM, Zaret KS, Duncan SA (2003) Hepatocyte nuclear factor 4alpha controls the development of a hepatic epithelium and liver morphogenesis. *Nat Genet* 34:292-296.

- Pietrangelo A (2004) Hereditary hemochromatosis--a new look at an old disease. *N Engl J Med* 350:2383-2397.
- Pigeon C, Ilyin G, Courselaud B, Leroyer P, Turlin B, Brissot P, Loreal O (2001) A new mouse liver-specific gene, encoding a protein homologous to human antimicrobial peptide hepcidin, is overexpressed during iron overload. *J Biol Chem* 276:7811-7819.
- Ponka P (1997) Tissue-specific regulation of iron metabolism and heme synthesis: distinct control mechanisms in erythroid cells. *Blood* 89:1-25.
- Roetto A, Papanikolaou G, Politou M, Alberti F, Girelli D, Christakis J, Loukopoulos D, Camaschella C (2003) Mutant antimicrobial peptide hepcidin is associated with severe juvenile hemochromatosis. *Nat Genet* 33:21-22.
- Samad TA, Srinivasan A, Karchewski LA, Jeong SJ, Campagna JA, Ji RR, Fabrizio DA, Zhang Y, Lin HY, Bell E, Woolf CJ (2004) DRAGON: a member of the repulsive guidance molecule-related family of neuronal- and muscle-expressed membrane proteins is regulated by DRG11 and has neuronal adhesive properties. *J Neurosci* 24:2027-2036.
- Seglen PO (1997) DNA ploidy and autophagic protein degradation as determinants of hepatocellular growth and survival. *Cell Biol Toxicol* 13:301-315.
- Shike H, Lauth X, Westerman ME, Ostland VE, Carlberg JM, Van Olst JC, Shimizu C, Bulet P, Burns JC (2002) Bass hepcidin is a novel antimicrobial peptide induced by bacterial challenge. *Eur J Biochem* 269:2232-2237.
- Stewart WB, Yuile CL, Claiborne HA, Snowman RT, Whipple GH (1950) Radioiron absorption in anemic dogs; fluctuations in the mucosal block and evidence for a gradient of absorption in the gastrointestinal tract. *J Exp Med* 92:375-382.
- Tam TF, Leung-Toung R, Li W, Wang Y, Karimian K, Spino M (2003) Iron chelator research: past, present, and future. *Curr Med Chem* 10:983-995.
- Thomson AM, Rogers JT, Leedman PJ (1999) Iron-regulatory proteins, iron-responsive elements and ferritin mRNA translation. *Int J Biochem Cell Biol* 31:1139-1152.
- Torrance JD, Bothwell, T.H. (1980) Tissue iron stores. *Methods in Hematology*:90-115.
- Yang F, Liu XB, Quinones M, Melby PC, Ghio A, Haile DJ (2002) Regulation of reticuloendothelial iron transporter MTP1 (Slc11a3) by inflammation. *J Biol Chem* 277:39786-39791.
- Yeh KY, Yeh M, Glass J (2004) Hepcidin regulation of ferroportin 1 expression in the liver and intestine of the rat. *Am J Physiol Gastrointest Liver Physiol* 286:G385-394.

Zetterstrom M, Sundgren-Andersson AK, Ostlund P, Bartfai T (1998) Delineation of the proinflammatory cytokine cascade in fever induction. *Ann N Y Acad Sci* 856:48-52.

Zhang AS, Xiong S, Tsukamoto H, Enns CA (2004) Localization of iron metabolism-related mRNAs in rat liver indicate that HFE is expressed predominantly in hepatocytes. *Blood* 103:1509-1514.

Zhou XY, Tomatsu S, Fleming RE, Parkkila S, Waheed A, Jiang J, Fei Y, Brunt EM, Ruddy DA, Prass CE, Schatzman RC, O'Neill R, Britton RS, Bacon BR, Sly WS (1998) HFE gene knockout produces mouse model of hereditary hemochromatosis. *Proc Natl Acad Sci U S A* 95:2492-2497.



## **Chapter 5:**

### **General Discussion and Perspectives**



## Chapter 5: General Discussion and Perspectives

This section will provide a global discussion concerning how our studies relate to additional findings regarding the RGM family members, as well as addressing some of the numerous open questions that remain unanswered.

### 5.1 Chick RGM

In addition to the proposed activity of cRGM in axon guidance from the chick retina to the optic tectum (Monnier et al., 2002), recent *in ovo* electroporation studies have implicated cRGMa in neuronal survival (Matsunaga et al., 2004). Overexpression of Neogenin, the receptor for cRGM, in the chick optic tectum produced increased levels of apoptotic cell death, while co-expression of cRGM and Neogenin did not. In addition, electroporation of siRNA to knock down endogenous *cRGM* expression in the tectum also caused an increase in apoptosis. Taken together, these results suggest that Neogenin acts as a proapoptotic receptor which acts to mediate cell death in the absence of its ligand, cRGM. Presence of cRGM prevents self activation of Neogenin, preventing triggering of apoptosis. Such activity has been previously described in other receptors such as DCC, the p75<sup>NTR</sup>, as well as Patched (a receptor for Shh) (reviewed in (Bredesen et al., 2004)).

It is interesting to note that, similar to the molecular families that play dual roles both patterning of the CNS, and axon guidance (discussed in Section 1.3), many of the receptors involved in ligand independent apoptosis are also axonal guidance molecules. DCC, Neogenin and Patched are all involved both in axon guidance and cell death (Mehlen and Mazelin, 2003; Porter and Dhakshinamoorthy, 2004; Mehlen and Llambi, 2005). It would be interesting to determine if there is a

relationship between these two developmental processes in the organization of the nervous system.

## 5.2 mRGMA

In addition to the function of *mRGMA* in neural tube closure described in this study, mRGMA has also been described to play a role in formation of afferent connections in the developing dentate gyrus (Brinks et al., 2004). Entorhinal axons, which make connections to the outer molecular layers of the dentate gyrus, are repelled by recombinant mRGMA in the stripe assay and axon outgrowth assays. Additionally, the inner molecular layer of the dentate gyrus, which is free of entorhinal connections, expresses *mRGMA*. Upon incubation of entorhino-hippocampal co-cultures with an antibody that neutralizes mRGMA, entorhinal projections invaded inappropriate areas of the hippocampus. These results suggest that in the developing hippocampus, mRGMA acts as a repellent cue which prevents entorhinal axons from straying from their correct target zone. It would be of interest to determine if *mRGMA* mutant mice have defects in the connections from the entorhinal axons to their appropriate termination zones in the dentate gyrus. This could easily be accomplished by injecting entorhinal cortex of *mRGMA* mutants with an anterograde tracer and performing appropriate histology to see the terminations in the dentate gyrus.

Another potential role recently ascribed to mRGMA is that of a molecule involved in regeneration failure after spinal cord injury. Lack of regeneration in the adult mammalian CNS is attributed to multiple factors, including inhibitory molecules present in CNS myelin, such as Nogo-A and OMgp (reviewed in Ramer et al., 2005). A recent study has shown that mRGMA is upregulated in rats with acute spinal cord

injury (SCI) and maintained in the lesion site into the chronic phase of SCI as the glial scar tissue matures (Schwab et al., 2005). While there is presently no direct evidence, it is possible that mRGMa might contribute to the inability of regenerating axons to cross the lesion site. With this in mind, a function blocking antibody against mRGMa may assist in promotion of regenerative activity in the injured spinal cord.

Until recently Neogenin was the only known binding partner for mRGMa. Recent work has shown that the soluble extracellular domain of mRGMa complexes with BMP type I receptors and binds directly and selectively to BMP-2 and BMP-4 (Babitt et al., 2005). mRGMa enhances BMP signalling *in vitro* via a pathway involving Smad1, 5, and 8 and in addition, upregulates endogenous Inhibitor of Differentiation (Id1) protein, a downstream target of BMP signalling. Furthermore, BMP signalling is present in neurons which express *RGMa in vivo*. Taken together, these data suggest a potential role for *mRGMa* as a BMP co-receptor in the nervous system. While the present known functions for mRGMa are believed to be mediated through its receptor, Neogenin, this finding raises the possibility that mRGMa, like Ephrin-A2 (Holmberg et al., 2005), possesses the capacity to mediate reverse signalling. The mechanism of *mRGMa* function in neural tube closure has yet to be determined, and it would be of interest to determine whether this effect is mediated via Neogenin, or if mRGMa is acting as a BMP co-receptor in this situation. Furthermore, the potential for bi-directional signalling between mRGMa and Neogenin expressing cells during axon guidance or in the control of cell death, adds to the complexity of an already intricate system.

### 5.3 mRGMb

While our preliminary studies of *mRGMb* knockout animals remain inconclusive, mRGMb has also been identified as a BMP co-receptor (Samad et al., 2005). This was concluded from the fact that mRGMb/DRAGON can bind to BMP2 and BMP4, as well as BMP type I and II receptors, enhancing BMP signalling by reducing the threshold of Smad1 activation. A further study has shown that mRGMb is expressed through both the male and female mouse reproductive system and that the protein is present in lipid rafts. It has been proposed that mRGMb plays a role in mammalian reproduction as a modulator of BMP signalling (Xia et al., 2005). This hypothesised role remains to be tested as the disruption of *mRGMb* results in death in the first postnatal month. The production of conditional or inducible *mRGMb* mutant animals might allow for survival of these animals and a more precise assessment of *mRGMb* function in both the nervous and reproductive systems

### 5.4 mRGMc

In addition to our analysis of iron overload in *mRGMc* mutant mice, a recent study has demonstrated that cell-bound hemojuvelin levels positively regulate hepcidin mRNA concentration in a cultured hepatocarcinoma cell line (Lin et al., 2005). In contrast, recombinant soluble hemojuvelin suppressed *Hamp* expression from cultured hepatocytes in a dose dependant manner. From their data, the authors suggest that while GPI-anchored hemojuvelin acts as a ligand (or perhaps even receptor) with unknown binding partner(s) to signal hepcidin, that the soluble form of hemojuvelin acts as a competitive negative regulator of this interaction. By interfering with the interaction of membrane bound hemojuvelin and its binding partner, soluble hemojuvelin can negatively regulate *Hamp* expression. The authors also suggest

that the source of soluble hemojuvelin may not be hepatic in nature, but instead come from the skeletal muscles, which express exceptionally high amounts of *mRGMc*. In agreement with this idea is the log-linear dose dependency curve for the competition (a 100-fold increase in soluble hemojuvelin results in a 50% decrease in hepcidin level), which implies that a massive amount of soluble hemojuvelin would be required to completely block bound hemojuvelin interaction with its binding partner, thus eliminating hepcidin expression. It will be exciting to see whether these ideas are compatible with an *in vivo* system, and how the other iron metabolism molecules fit into this model of *Hamp* regulation. It will also be interesting to determine if, like mRGMa and mRGMb, mRGMc has the ability to act as a co-receptor for BMP signalling. There are presently no known binding partners identified for mRGMc, and it remains to be determined how signalling by proinflammatory cytokines downregulates *mRGMc*, as well as how mRGMc acts to regulate the expression of hepcidin in response to dietary iron. Screening of a hepatic cDNA library with an mRGMc-AP fusion protein may reveal which proteins interact with mRGMc, providing a clearer picture of how it fits into both dietary iron sensing and inflammation mediated hypoferrremia.

## 5.5 References

- Babitt JL, Zhang Y, Samad TA, Xia Y, Tang J, Campagna JA, Schneyer AL, Woolf CJ, Lin HY (2005) Repulsive guidance molecule (RGMa), a DRAGON homologue, is a bone morphogenetic protein co-receptor. *J Biol Chem*.
- Bredesen DE, Mehlen P, Rabizadeh S (2004) Apoptosis and dependence receptors: a molecular basis for cellular addiction. *Physiol Rev* 84:411-430.
- Brinks H, Conrad S, Vogt J, Oldekamp J, Sierra A, Deitinghoff L, Bechmann I, Alvarez-Bolado G, Heimrich B, Monnier PP, Mueller BK, Skutella T (2004) The repulsive guidance molecule RGMa is involved in the formation of afferent connections in the dentate gyrus. *J Neurosci* 24:3862-3869.
- Holmberg J, Armulik A, Senti KA, Edoff K, Spalding K, Momma S, Cassidy R, Flanagan JG, Frisen J (2005) Ephrin-A2 reverse signaling negatively regulates neural progenitor proliferation and neurogenesis. *Genes Dev* 19:462-471.
- Lin L, Goldberg YP, Ganz T (2005) Competitive regulation of hepcidin mRNA by soluble and cell-associated hemojuvelin. *Blood*.
- Matsunaga E, Tauszig-Delamasure S, Monnier PP, Mueller BK, Strittmatter SM, Mehlen P, Chedotal A (2004) RGM and its receptor neogenin regulate neuronal survival. *Nat Cell Biol* 6:749-755.
- Mehlen P, Mazelin L (2003) The dependence receptors DCC and UNC5H as a link between neuronal guidance and survival. *Biol Cell* 95:425-436.
- Mehlen P, Llambi F (2005) Role of netrin-1 and netrin-1 dependence receptors in colorectal cancers. *Br J Cancer* 93:1-6.
- Monnier PP, Sierra A, Macchi P, Deitinghoff L, Andersen JS, Mann M, Flad M, Hornberger MR, Stahl B, Bonhoeffer F, Mueller BK (2002) RGM is a repulsive guidance molecule for retinal axons. *Nature* 419:392-395.
- Porter AG, Dhakshinamoorthy S (2004) Apoptosis initiated by dependence receptors: a new paradigm for cell death? *Bioessays* 26:656-664.
- Ramer LM, Ramer MS, Steeves JD (2005) Setting the stage for functional repair of spinal cord injuries: a cast of thousands. *Spinal Cord* 43:134-161.
- Samad TA, Rebbapragada A, Bell E, Zhang Y, Sidis Y, Jeong SJ, Campagna JA, Perusini S, Fabrizio DA, Schneyer AL, Lin HY, Brivanlou AH, Attisano L, Woolf CJ (2005) DRAGON: a bone morphogenetic protein co-receptor. *J Biol Chem*.
- Schwab JM, Conrad S, Monnier PP, Julien S, Mueller BK, Schluesener HJ (2005) Spinal cord injury-induced lesional expression of the repulsive guidance molecule (RGM). *Eur J Neurosci* 21:1569-1576.

Xia Y, Sidis Y, Mukherjee A, Samad TA, Brenner G, Woolf CJ, Lin HY, Schneyer A (2005) Localization and Action of Dragon (Repulsive Guidance Molecule b), a Novel Bone Morphogenetic Protein Coreceptor, throughout the Reproductive Axis. *Endocrinology* 146:3614-3621.





## **Appendices**

## **Appendix A: Acknowledgments**

I am very grateful to Prof. Dr. Silvia Arber for the opportunity to do my Ph. D. in her laboratory and for her infinite patience. I would especially like to thank her for all the time and effort she put in to make this project a success.

My special thanks to Dr. Vera Niederkofler, I could never have asked for a more intelligent and reliable colleague, or a better friend.

I should also point out my appreciation for the rest of the lab for putting up with my early morning crabbiness, for liberally (and often unknowingly) donating their extra freezer space to Team RGM, and for their general good will throughout my time here.

## Appendix B: Curriculum Vitae

### **RISHARD SALIE**

Gasstrasse 22, Basel  
Switzerland  
41-76-407-7104  
rishard.salie@unibas.ch

#### **Personal:**

Birth date: 09/11/1974  
Birthplace: Toronto, Canada  
Nationality: Canadian

Sex: Male  
Marital Status: Single  
Children: None

#### **Education:**

<b>Universities/Colleges Attended:</b>	<b>Degree Obtained</b>	<b>Dates</b>
FMI/University of Basel, Basel, Switzerland	Ph.D. Neurobiology	Nov. 2001-Oct. 2005
University of British Columbia, Vancouver, Canada	M.Sc. Neuroscience	April 1999-Nov. 2001
Queen's University, Kingston, Canada	B.Sc. Biochemistry	Sept. 1993-April 1997

#### **Scholarships:**

**B. C. Neurotrauma Initiative Studentship** July 2000-Nov. 2001  
This is an award for graduate students engaging in promising research in spinal cord injury. Details of the award can be found at:  
<http://www.rickhansen.com/info/research/rhni2000.html>

**Queen's University Trillium Scholarship** Sept. 1993-April 1993  
This was an entrance award for exceptional performance at the high school level.

#### **Projects and Work Experience:**

**Ph.D. Candidate** **University of Basel, Switzerland**  
Nov. 2001-Present  
Exploration of a novel murine family of GPI anchored proteins (RGMs), with activity in neural tube development and iron metabolism.

**M.Sc. Graduate** **University of British Columbia, Canada**  
April 1999-Nov. 2001  
Used tissue culture and immunohistochemical techniques to determine various growth factor effects on brainstem-spinal neurons.

**Research Assistant** **Hoffmann LaRoche, Basel, Switzerland**  
Jan. 1998-Jan. 1999  
Responsible for execution and evaluation of experiments on retinoid precursors. Involved animal handling and radioactive techniques.

## **Teaching Experience:**

**Teaching Assistant**  
Summer Semester 2003

**University of Basel, Basel, Switzerland**  
Assisted a small group (10 students) to comprehend and complete assigned work dealing with basic biology and genetics.

**Student Tutor**  
April 1999-Nov. 2001

**The Tutoring Company, Vancouver, BC, Canada**  
Worked one on one with high school students teaching Biology, Chemistry, Physics and Calculus.

**Student Tutor**  
Sept. 1997-Dec. 1997

**Oxford Learning Center, Oakville, ON, Canada**  
Worked one on one with high school students teaching Biology, Chemistry, Physics and Calculus.

**Student Tutor**  
Sept. 1995-April 1997

**MindFind, Queen's University, Kingston, ON, Canada**  
Worked one on one with undergraduate students teaching Biology, Chemistry, Genetics and Statistics.

## **Skills:**

### **Laboratory:**

Animal Handling and Surgery (Certified)  
Confocal Microscopy  
Cryostat Sectioning  
DNA Cloning  
Immunohistochemistry

In Situ Hybridization  
Northern/Southern/Western Blot  
Radiation Safety (Certified)  
RNA Purification  
Tissue Culture

### **Computer:**

Adobe Acrobat  
Excel  
Image J  
Netscape/Explorer

NIH Image  
Photoshop  
Statistica  
Word

## **Languages:**

English (Native speaker)  
French (Conversational, some written)  
German (Conversational, limited written)

## **References:**

Dr. Silvia Arber, Professor, University of Basel/Senior Group Leader, FMI.  
E-mail: [silvia.arber@unibas.ch](mailto:silvia.arber@unibas.ch)  
Dr. J.D. Steeves, Director of ICORD (International Collaboration on Repair Discoveries), UBC. E-mail: [steeves@icord.org](mailto:steeves@icord.org)  
Dr. W. Tetzlaff, Professor, UBC.  
E-mail: [tetzlaff@icord.org](mailto:tetzlaff@icord.org)  
Reference letters and further contact information available on request

## **Publications:**

Salie, R. and J.D. Steeves. IGF-1 and BDNF Promote Chick Bulbosplinal Neurite Outgrowth *In Vitro*. (In Press, International Journal of Developmental Neuroscience)

Niederkofler, V.\*, Salie, R.\*, and Arber, S. Hemojuvelin Is Essential For Dietary Iron-Sensing and Its Mutation Leads to Severe Iron Overload. ***J. Clin. Invest.*** 115(8): 2180-6, (2005)

Salie, R.\*, Niederkofler, V.\*, and Arber, S. Patterning Molecules: Multitasking in the Nervous System. ***Neuron*** Vol. 45: 1-4, (2005)

Niederkofler, V.\*, Salie, R.\*, Sigrist, M., and Arber, S. Repulsive Guidance Molecule (RGM) Gene Function Is Required for Neural Tube Closure But Not Retinal Topography in the Mouse Visual System. ***J. Neurosci.*** 24: 808 - 818, (2004)

\*Indicates equally contributed authorship

## **Abstracts/Posters:**

Salie, R., Niederkofler, V., Sigrist, M., Müller, B., and Arber, S. *In vivo* Functions of Repulsive Guidance Molecule Family Members in Murine Nervous System Development. Soc. Neurosci. Abstr. Program No. 942.2, (2004) Abstract Viewer/Itinerary Planner. Washington, DC: Society for Neuroscience, 2004. Online.

Salie, R., Niederkofler, V., Sigrist, M., Müller, B., and Arber, S. Identification of a Novel Murine Family of GPI-anchored Proteins Homologous to the Chick Axon Guidance Molecule RGM. Soc. Neurosci. Abstr. Program No. 32.8., (2003) Abstract Viewer/Itinerary Planner. Washington, DC: Society for Neuroscience, 2003. Online.

Salie, R. and Steeves, J.D. The Effect of EGF, IGF-1, and BDNF On Vestibulospinal and Raphespinal Populations in an *In Vitro* Model of Spinal Cord Injury in the Embryonic Chick., Soc. Neurosci. Abstr., Vol. 27, Program No. 473.12, (2001).

I declare that I wrote this thesis: ***Mouse RGMs: A Three Protein Family with Diverse Function and Localization*** with the help indicated and only handed it in to the Faculty of Science of the University of Basel and to no other Faculty and no other University.

Rishard Salie